Irrigation Science

Volume 14
Number 4
1994

J.B. Prendergast, C.W. Rose, W.L. Hogarth
A model for conjunctive use of groundwater and surface waters for control of irrigation salinity *167*

J.B. Prendergast, C.W. Rose, W.L. Hogarth
Sustainability of conjunctive water use for salinity control in irrigation areas: theory and application to the Shepparton region, Australia *177*

V.P. Singh, E.S. Joseph
Kinematic-wave model for soil-moisture movement with plant-root extraction *189*

D.F. Wanjura, J.R. Mahan
Thermal environment of cotton irrigated using canopy temperature *199*

B. Zur, U. Ben-Hanan, A. Rimmer, A. Yardeni
Control of irrigation amounts using velocity and position of wetting front *207*

Indexed in *Current Contents*
IRSCD2 14 (4) 167–212 June 1994
Printed on acid-free paper

Springer International

Irrigation Science will publish original contributions and short communications reporting the results of irrigation research, including relevant contributions from the plant, soil and atmospheric sciences as well as the analysis of field experimentation. Special emphasis will be given to multidisciplinary studies dealing with the problems involved in maintaining the long term productivity of irrigated lands and in increasing the efficiency of agricultural water use.
Aspects of particular interest are:

- Physiology of plant growth and yield response to water status.
- Physical and chemical aspects of water status and movement in the plant-soil-atmosphere system.
- Salinity and alkalinity control by soil and water management.
- Measurement and modification of crop and control of water in plant, soil and atmosphere.
- Water requirements in irrigation practice.
- Ecological aspects of irrigated agriculture.

Manuscripts in triplicate may be submitted to any of the following:

Co-ordinating Editor

G. Stanhill
Institute of Soils and Water,
Agricultural Research Organization,
Volcani Center, P.O. Box 6
Bet Dagan, 50-250, Israel

Co-Editors

G. J. Hoffman
Agricultural Engineering Department
University of Nebraska, 223 L.W. Chase Hall
Lincoln, NE 68583-0726, USA

A. Kassam
88 Gunnersbury Avenue
Ealing, London W54 HA, England

W. S. Meyer
CSIRO Division of Water Resources,
Griffith Laboratory,
PO Griffith, NSW 2680, Australia

Advisory Editors

S. Dasberg, Bet Dagan
J. Doorenbos, Ankara
W. Gardner, Berkeley, California
A. E. Hall, Riverside, California
R. J. Hanks, Logan, Utah
B. Itier, Thiverval-Grignon
R. D. Jackson, Phoenix, Arizona
P. G. Jarvis, Edinburgh
M. E. Jensen, Fort Collins, Colorado
W. D. Kemper, Beltsville, Maryland
J. W. Kijne, Colombo
J. V. Lake, Wageningen
J. L. Monteith, Edinburgh
J. R. Philip, Canberra City
C. W. Rose, Queensland, Australia
V. P. Singh, Baton Rouge, Louisiana
N. C. Turner, Wembley, Western Australia

Copyright. Submission of a manuscript implies: that the work described has not been published before (except in the form of an abstract or as part of a published lecture, review, or thesis); that it is not under consideration for publication elsewhere; that its publication has been approved by all authors, as well as by the responsible authorities at the institute where the work has been carried out; that, if and when the manuscript is accepted for publication, the authors agree to automatic transfer of the copyright to the publisher; and that the manuscript will not be published elsewhere in any language without the consent of the copyright holders.
All articles published in this journal are protected by copyright, which covers the exclusive rights to reproduce and distribute the article (e.g., as offprints), as well as all translation rights. No material published in this journal may be reproduced photographically or stored on microfilm, in electronic data bases, video disks, etc., without first obtaining written permission from the publisher.
The use of general descriptive names, trade names, trademarks, etc., in this publication, even if not specifically identified, does not imply that these names are not protected by the relevant laws and regulations. While the advice and information in this journal is believed to be true and accurate at the date of its going to press, neither the authors, the editors, nor the publisher can accept any legal responsibility for any errors or omissions that may be made. The publisher makes no warranty, express or implied, with respect to the material contained herein.

Special Regulations in the USA: Photocopies may be made for personal or in-house use beyond the limitations stipulated under Section 107 or 108 of U.S. Copyright Law, provided a fee is paid. This fee is US$ 0.20 per page, per copy, plus a basic fee of US$ 2.00 per article. All fees should be paid to the Copyright Clearance Center, Inc., 21 Congress Street, Salem, MA 01970, USA, stating the ISSN 0342-7188, the volume, and the first and last page numbers of each article copied. The copyright owner's consent does not include copying for general distribution, promotion, new works, or resale. In these cases, specific written permission must first be obtained from the publisher.

Subscription Information: ISSN 0342-7188, Volume 15 (4 issues) will appear in 1994.

North America. Annual subscription rate: Approx. US$ 322.00 (single issue price: approx. US$ 95.00) including carriage charges. Subscriptions are entered with prepayment only. Orders should be addressed to: Springer-Verlag New York Inc., Journal Fulfillment Services Dept, 333 Meadowlands Parkway, Secaucus, NJ 07094, USA, Telephone (201) 348-4033, Telex 0023-125994, FAX (201) 348-4505.

All other countries: Recommended annual subscription rate: DM 488.00, plus carriage charges [Federal Republic of Germany: DM 10.80, including value added tax; other countries: DM 15.00. SAL or airmail charges are available upon request. SAL delivery is mandatory to Japan, India, and Australia/New Zealand. Volume price: DM 488.00, single issue price: DM 146.40, plus carriage charges. Subscriptions can either be placed via a bookdealer or sent directly to: Springer-Verlag, Postfach 31 13 40, D-10643 Berlin, Germany, Tel. (0) 30/82 07-0, Telex 1-83 319, FAX (0) 30/82 14 091.

Cancellations must be received by September 30 to take effect at the end of the same year.

Changes of address: Allow six weeks for all changes to become effective. All communications should include both old and new addresses (with postal codes) and should be accompanied by a mailing label from a recent issue.

According to § 4 section 3 of the German Postal Services Data Protection Regulations, the German Federal Post Office can inform the publisher of a subscriber's new address even if the subscriber has not submitted a formal application for mail to be forwarded.
Subscribers not in agreement with this procedure may send a written complaint to Springer-Verlag's Berlin office within 14 days of publication of this issue.

Back Volumes: Prices are available on request.

Microform: Microform editions are available from: University Microfilms International, 300 N. Zeeb Road, Ann Arbor, MI 48106, USA.

Irrig Sci (1994) 14:167–175

Irrigation Science
© Springer-Verlag 1994

A model for conjunctive use of groundwater and surface waters for control of irrigation salinity

J. Bernard Prendergast [1], Calvin W. Rose [2], William L. Hogarth [2]

[1] Institute of Sustainable Irrigated Agriculture, Ferguson Road, Tatura, Vic., 3616, Australia
[2] Faculty of Environmental Sciences, Griffith University, Nathan, Qld., 4111, Australia

Received: 30 May 1992

Abstract. Changes in the hydrologic balance in many irrigation areas, including those in the Murray Basin, Australia, have resulted in high watertables and salinity problems. However, where suitable aquifers exist, groundwater pumping and subsequent irrigation application after mixing with surface waters (referred to as conjunctive water use) can control salinity and watertable depth and improve productivity of degraded land. In order to assess where conjunctive water use will successfully control salinity, it is necessary to estimate the effects of pumped groundwater salinity on rootzone salinity. A simple steady rate model is derived for this purpose from mass conservation of salt and water. The model enables an estimate to be made of rootzone salinity for any particular salinity level of the groundwater being used in conjunction with surface water; this enables calculation of the required crop salt tolerance to prevent yield reductions. The most important input parameters for the model are groundwater salinity, the annual depth of class 'A' pan evaporation, the annual depth of rainfall, the salinity of irrigation water, and a leaching parameter. For model parameters nominated in this paper, where groundwater salinity reaches 5 dS/m a crop threshold salt tolerance greater than 1.6 dS/m is required to avoid yield reductions. Where groundwater salinity approaches 10 dS/m, a crop threshold tolerance of 3 dS/m is required. Whilst the model derived indicates that rootzone salinity is sensitive to groundwater salinity, rootzone salinity is insensitive to leaching for leaching fractions commonly encountered (0.1 to 0.4). The insensitivity to leaching means that it could be expected that similar yields could be attained on heavy or light textured soils. This insensitivity also implies that there is no yield penalty from increasing the mass of pumped salt by pumping to achieve maximum watertable control in addition to leaching. The model developed is also used to estimate yield reductions expected under conjunctive use, for any particular levels of groundwater salinity and crop salt tolerance.

Correspondence to: B. Prendergast

In inland semi-arid areas, irrigation can result in large increases in agricultural productivity. However, if natural groundwater flows are restricted, high watertables and insufficient leaching can prevail. Where unconfined aquifers exist, groundwater pumps can provide effective drainage. Sub-surface drainage problems are often exacerbated if there are no nearby rivers or oceans to provide economic export of saline effluent from groundwater pumps or tile drainage. Although evaporation basins can be used to concentrate drainage effluent, this infrastructure is costly and often produces adverse environmental conditions. Where the salinity of effluent is low there is potential for its irrigation application, after being mixed with surface waters. Conjunctive use of drainage effluent for irrigation has many benefits including:

(a) obviating the immediate need for export of drainage effluent, whilst maintaining effective leaching and therefore agricultural productivity,

(b) reducing salt export requirements to a level necessary only to prevent groundwater degradation,

(c) providing additional irrigation water where groundwater salinity is low and when accelerated groundwater degradation may be acceptable,

(d) better control of rootzone waterlogging without the need for export of groundwater,

(e) having diffuse dispersion of saline effluent on the land surface with reduced environmental problems associated with evaporation basins; problems which can include the hazard of accumulation of toxic elements and unacceptably high levels of soil and groundwater salinity under and near basins.

Conjunctive use, however, also has an impact on rootzone salinity due to applied salt loads. The most important factors affecting rootzone salinity and productivity are:

(a) the salinity of groundwater,
(b) the amount of groundwater applied,
(c) the total amount of applied water,
(d) the amount of water lost below the rootzone including the leaching fraction, and
(e) the salt tolerance of the crop.

Toxic elements and pollutants can also severely restrict the potential for conjunctive use, although this aspect is not considered here.

Prendergast and Heuperman (1988) suggested that the effect of conjunctive water use on rootzone salinity could be modelled through use of a leaching equation with the steady state equations of the salt and water budget. Slavich (1992) used this approach to assess the potential for conjunctive use; however, the groundwater budget equation was not considered, and the analysis was restricted to the salt and water fluxes through the rootzone; this meant that the model could not be applied to field conditions, because under field conditions of groundwater pumping, recharge in addition to leaching fluxes enters the groundwater. In addition, Slavich (1992) uses the somewhat arbitrary criteria of achievement of zero "net recharge" as an indicator of the effectiveness of conjunctive use for controlling waterlogging and salinity, yet it is not clear what the relationship is (if there is one) between net recharge and crop yield.

In this paper the importance to rootzone salinity of the factors (a) to (e) listed above will be assessed using the equations of mass conservation of salt and water in a simple model of a conjunctive use system. The important relationship between groundwater salinity and rootzone salinity is developed as suggested by Prendergast and Heuperman (1988), but extended to include an unconfined aquifer, so that crop salt tolerance required to prevent yield reductions under conjunctive use can be calculated from the model. The model is then used to assess management practices which can increase the effectiveness of conjunctive use in controlling salinity. Additional equations are developed to estimate reduced crop water use under saline conditions, so that crop yield under conjunctive use can also be estimated as a function of groundwater salinity and crop salt tolerance. In a forthcoming paper we will apply the model using experimental data from the Shepparton region.

Steady rate equations have been shown to provide good prediction of water salinity effects on crop yield in lysimeters (Letey et al. 1985), and under field conditions (Prendergast 1993). In this paper the steady rate equations used by Prendergast (1993) are extended to include groundwater mass balance from an unconfined aquifer. The only major assumption additional to those in models developed by Letey et al. (1985) and Prendergast (1993) is that of mass conservation of groundwater, because water salinity in the conjunctive use model is determined by the volume and salinity of pumped groundwater. This additional assumption of mass conservation is used in almost all models without the requirement for field validation. Use of the validated steady rate equations means that the most rigorous testing for the conjunctive use model has already been undertaken. Experimental data to test the model at the scale of the area of influence of a groundwater pump would encompass excessive variability because of extraneous factors that are more likely to affect large scale experiments, and because of practical aspects of sampling (including cost) that limit the amount of experimental data that can be obtained. This greater variability associated with large experiments means that if the model predictions are tested at catchment scale they are much more likely to fall within the range of experimental error. Therefore, because the steady rate equations have already been validated, application of the conjunctive use model is possible once the model parameters have been determined.

Abbreviations

A Salinity threshold (maximum value of rootzone salinity, EC_a, at which no yield reduction is evident) in Eq. (9) of Maas and Hoffman 1977 (dS/m); B percent yield decrease per unit rootzone salinity increase in Eq. (9) of Maas and Hoffman 1977 (%/dS/m); β_0 yield response factor in Eq. (11) of Stewart et al. 1977; C_a average groundwater salinity (dS/m); C_r salinity of rainfall (dS/m); C_s average concentration of salts in the soil solution in the rootzone (dS/m); C_{se} concentration of salts in the soil saturation extract in the rootzone (dS/m) ($\equiv EC_e$); C_i average concentration of salts in total water applied to the crop (dS/m); C_w salinity of surface supply water for irrigation (dS/m); D annual depth of exported drainage groundwater (m/y); EC_e concentration of salts in the soil saturation extract in the rootzone (dS/m) ($\equiv C_{se}$); E_p annual "Class A" pan evaporation (m/y); ET annual crop evapotranspiration (m/y); ET_m annual maximum annual crop evapotranspiration (m/y); F annual equivalent ponded depth of soil water bypass flows (m/y); G annual depth of upward groundwater leakage into the conjunctive use system (m/y); I annual total depth of water applied to the crop as irrigation and rainfall (m/y); J fitted coefficient in equation of Rhoades 1974 (dimensionless); K non-leaching recharge – annual equivalent ponded depth of groundwater recharge which does not contribute to rootzone leaching in the conjunctive use area (equal to $S+F+G$) (m/y); LF the leaching fraction; the fraction of applied water which passes below the crop rootzone (dimensionless); P annual equivalent ponded depth of pumped groundwater (m/y); R annual depth of rainfall infiltrated (m/y); S annual equivalent ponded depth of groundwater recharge from irrigation supply channels or pipe delivery systems (m/y); W annual infiltrated depth of surface water supplied for irrigation (m/y); Y yield under salinity induced water stress relative to maximum yield (dimensionless).

Theoretical development

A conjunctive use system in an unconfined aquifer can be conceptualised as in Fig. 1. The model approach assumes steady rate processes. This assumption is well satisfied if sufficient time is allowed for a dynamic equilibrium to be achieved. It is also assumed initially that pumped groundwater is spread over the whole area of influence of the groundwater pump, because spreading groundwater over a large area reduces the salinity of applied water under conjunctive use, and therefore represents good salinity management. The case when this practice is not followed is examined in a later section of the paper. The model takes no account of the dissolution or precipitation of salts in the profile, or the extraction or excretion of salts by plants, these processes being considered quantitatively negligable compared to other terms. The assessment of the effect of groundwater salinity on yield is made by assuming groundwater salinity can take any constant value. This assumption is appropriate because the rate of groundwater degradation under conjunctive use is low, although the rate is influenced by a number of factors (Prendergast et al. 1994). The level of groundwater salinity at some future time can be estimated as outlined by

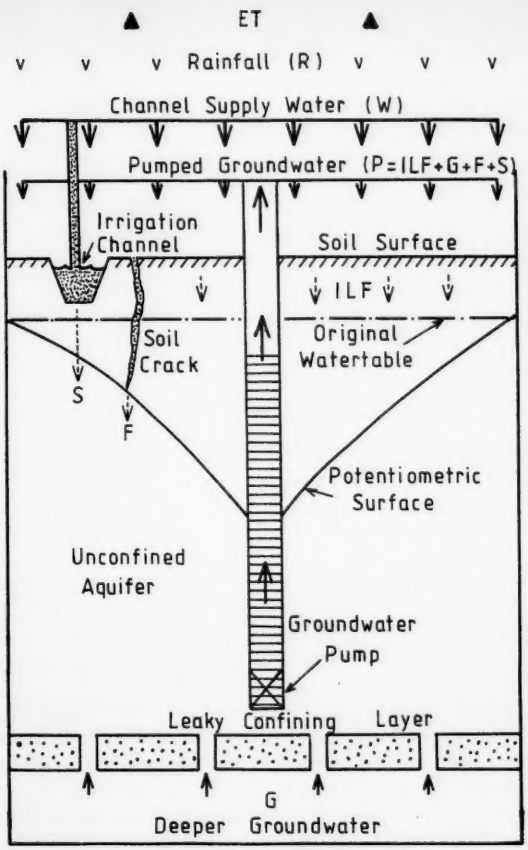

Fig. 1. Conceptual model of irrigation with conjunctive water use. Recharge to the unconfined aquifer occurs from leaching fluxes under crops ($I \cdot LF$), channel seepage (S), upward leakage (G), and soil-water bypass flux (F)

Prendergast et al. (1994). Thus the model presented here can also be used to predict the effects of conjunctive use on crop yield at future times, by using in the model the predicted level of groundwater salinity at any time of interest.

In the analysis presented here conventional units of electrical conductivity are used as a surrogate for salinity concentration. This implies that the relationship between solute concentration and electrical conductivity is assumed constant for all equations, because mass conservation is expressed in terms of conductivity.

In Fig. 1, I is the total depth of applied water, including the depth of irrigation water (W), rainfall (R), and pumped groundwater (P). The volume of groundwater in the system is assumed seasonally constant and is recharged from upward leakage (G), leaching fluxes under irrigated crops ($I \cdot LF$), channel seepage (S), and soil-water bypass fluxes (F), under irrigated crops. The leaching fraction (LF), is defined as the fraction of applied water passing below the rootzone. At very low pumping rates the resulting restricted drainage to the aquifer means the leaching fraction will be principally determined by the pumping rate. At high pumping rates (and resulting free drainage to the aquifer) the leaching fraction will be determined principally by soil type and stratigraphy, though agronomic, water management and climatic factors will also have an influence.

In this paper, based on the assumption of steady rate processes, all rates are expressed as their annual average values.

For analysis of the conceptual model illustrated in Fig. 1, groundwater recharge has been divided into two fractions which have different impacts on rootzone salinity and therefore productivity. These two fractions are:

(a) that portion ($I \cdot LF$) which leaches salts from the crop rootzone in the area of conjunctive use, and

(b) recharge (K) that does not provide leaching in the conjunctive use area, represented by $K = F + S + G$ (see Fig. 1).

The implications of groundwater salinity for crop suitability in an irrigation region

At the steady state achieved under steady rate fluxes, mass conservation of groundwater for the model of Fig. 1 requires that the equivalent ponded depth of pumped groundwater, P, is equal to the inputs to the groundwater system ($I \cdot LF + K$), i.e.:

$$P = I \cdot LF + K . \tag{1}$$

At equilibrium the depth of infiltrated water (I) is the sum of the depths of infiltrated channel water (W), infiltrated rainfall (R), and pumped groundwater (P), so that:

$$I = R + W + P . \tag{2}$$

The equivalent statement for mass conservation of salt is:

$$IC_i = RC_r + WC_r + WC_w + PC_a , \tag{3}$$

where C_i is the average concentration of salts in applied water, C_r is the average concentration of salts in rainfall, C_w is the salt concentration of irrigation channel supply water, and C_a is the groundwater salinity in the aquifer.

Substituting P from Eq. (1) into (3) gives the mass of salt applied at the soil surface to crops, as:

$$IC_i = RC_r + WC_w + C_a(I \cdot LF + K) . \tag{4}$$

Equation (4) indicates that for any particular groundwater salinity (C_a), other values being constant, the mass of salt applied to the crop will depend on the depth of groundwater recharge through leaching. This equation for the conjunctive use system can be used to provide management guidelines where the effect of irrigation water salinity on crop yield is known under local conditions. However, it is believed that crop yield is more functionally related to rootzone salinity than to irrigation water salinity, and crop salt tolerance guidelines are expressed in terms of rootzone salinity (see Maas and Hoffman 1977). Thus a relationship between irrigation water salinity and rootzone salinity is now sought.

Whilst it is generally accepted that crop yield is affected by both the rate of salt application and the rate of salt leaching, there is conflicting evidence as to the relative importance of these two factors. One view is that yield is most closely related to the mean soil salinity in the rootzone (Bower et al. 1969; Shalhevet and Bernstein 1968; Bower et al. 1970; Ingvalson et al. 1976; Rhoades 1974; Ayres and Westcot 1985; Hoffman et al. 1979; Prendergast 1993). Another view is that crop response is more highly correlated with irrigation water salinity, and may be insensitive to high salinity in parts of the soil profile (Bingham and Garber 1970; Lunin and Gallatin 1965); this is implied by use of an equation for the water uptake weighted mean salinity (Dirksen 1985), derived by Bernstein and Francois (1973) and suggested by Smith and Hancock (1986) to be an appropriate yield indicator. Other approaches have also been used as in Ayers and Westcot (1985) and Hoffman and van Genutchen (1983). Prendergast (1993) illustrated that both the equations of Rhoades (1974) and Hoffman and van Genutchen (1983) provided good description of field data.

The semi-empirical leaching equation of Rhoades (1974) will be used for the development of the conjunctive use model, because of its simplicity and its close relationship with mean soil salinity, which appears to be the best yield indicator in many of the studies listed above. The equation is:

$$C_s = 0.5J \cdot C_i[1 + 1/LF], \tag{5}$$

where J is an empirically determined coefficient (and in Eq. (5) replaces K in the original equation of Rhoades (1974) to avoid symbol duplication). Rhoades (1974) suggests $J = 0.8$ approximately. In Eq. (5) C_s can be related to rootzone salinity measured on the soil saturation extract (C_{se}), which is used in salt tolerance guidelines, through $C_s = 2C_{se}$, by assuming the water content of the saturation extract is about twice that at field capacity (Maas and Hoffman 1977; van Schilfgaarde et al. 1974).

In the development of the conjunctive use model the depth of applied water in the mass balance equation (4) can be replaced by a climatic factor to produce a more general expression. Because the volume of groundwater in the system of Fig. 1 is assumed constant, yearly crop evapotranspiration, ET, is the sum of total applied water depth, I, minus the water lost to the groundwater ($I \cdot LF + F$), that is:

$$ET = I(1 - LF) - F. \tag{6}$$

Soil-water bypass flows in the Shepparton region in the Murray Basin, Australia, are estimated to represent up to 8 mm/yr on a major soil type, which is negligibly small compared with other terms in Eq. (6). Equation (6) will therefore be simplified to $ET = I(1 - LF)$. It may not be possible to ignore F in the groundwater budget equation (1), because the magnitude of water fluxes is much smaller than in Eq. (6), and F can be a substantial component in the groundwater budget.

When maximum productivity is achieved, crop evapotranspiration approaches maximum evapotranspiration (ET_m) (Doorenbos and Kassam 1973). Maximum crop evapotranspiration, and therefore maximum yield, is usually aimed for in irrigation areas because of the high cost of irrigation layout. ET_m can be approximated by the evaporation rate (E_p) from a well sited evaporation pan with a pan coefficient of 0.85, and a crop factor of 1 (Doorenbos and Pruitt 1977) as:

$$ET_m = 0.85E_p. \tag{7}$$

Taking $ET = ET_m$ and $F = 0$ in Eq. (6), with $J = 0.8$ and $C_s = 2C_{se}$ in Eq. (5), Eqs. (1), (2), (3), (5), (6) and (7) yield:

$$C_{se} = 0.2\left(1 + \frac{1}{LF}\right) \cdot \left\{C_w + \frac{K(C_a - C_w) - R(C_w - C_r)}{0.85E_p}(1 - LF) + LF(C_a - C_w)\right\}. \tag{8}$$

Equation (8) describes the effect of conjunctive use of groundwater on rootzone salinity for the system in Fig. 1 for full irrigation, LF being dependent on P (Eq. (1)). C_{se} is plotted against the leaching fraction in Fig. 2 for $K = 0.06$ m/yr.

Figure 2 illustrates the mean crop rootzone salinity expected under irrigation incorporating conjunctive water use for certain nominated values of the model parameters. As shown in Fig. 2, C_{se} is very sensitive to restricted leaching ($LF < 0.05$) but is insensitive to leaching fractions commonly encountered (LF from 0.1 to 0.4). Light soils lead to higher LF and therefore higher P. The beneficial effects of higher LF under conjunctive use are offset by the greater depth of pumped groundwater which leads to higher C_i. Rootzone salinity increases only slightly for very high LF (e.g. $LF > 0.3$) because of the greater depth of pumped groundwater (and therefore greater mass of surface applied salt). Figure 2 also indicates that C_{se} is more sensitive to LF at higher values of C_a.

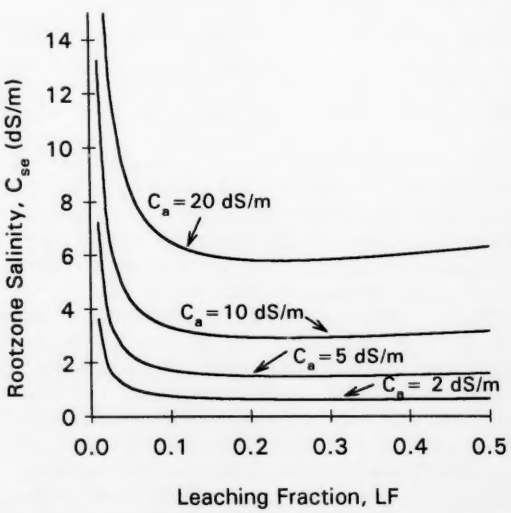

Fig. 2. Rootzone salinity (C_{se}) under conjunctive water use for maximum crop evapotranspiration. Plot of Eq. (8) with $C_w = 0.1$ dS/m, $K = 0.06$ m/y, $R = 0.45$ m/y, $C_r = 0.008$ dS/m, $E_p = 1.4$ m/y

The highest value of rootzone salinity at which no yield reduction occurs is defined as crop threshold salinity (A). For a threshold value of 1.6 dS m^{-1} full yields would be expected to be maintained for C_a below 5 dS m^{-1}, at least for LF between 0.15 and 0.5 (see Fig. 2). A crop threshold salinity of 3.0 dS m^{-1} would be required for C_a up to 10 dS m^{-1}, provided $LF > 0.1$.

The effect of groundwater salinity on crop yield

In many irrigation regions with salinity problems it is likely that some crops will suffer yield reductions and lower water use, but can still be grown economically. In order to assess management strategies under such conditions, the model must include crop water use estimated for rootzone salinities greater than crop threshold values.

Maas and Hoffman (1977), suggest that relative yield, Y (percent of maximum yield, Y_{max}), can be expressed as a function of average rootzone salinity, that is:

$$\%\,\text{Yield} = 100 - B(EC_e - A), \quad EC_e > A\,, \tag{9}$$

where A is the salinity threshold, B the percent yield decrease per unit salinity increase and EC_e is the average salinity of the soil saturation extract in the rootzone. In dimensionless form, after substituting C_{se} for EC_e to eliminate differences in notation, and expressing yield in fractional form (i.e. $Y' = \text{Yield}/Y_{max}$), Eq. (9) becomes:

$$Y' = 1 - 0.01\,B(C_{se} - A), \quad C_{se} > A\,. \tag{10}$$

Decreases in osmotic potential of soil water, associated with high rootzone salinity, reduces crop water use (Bresler et al. 1982; Bernstein 1975), which is highly correlated with crop yield (de Wit 1958; Rasmussen and Hanks 1978; Shalhevet et al. 1976). Crop yield can be expressed as a function of crop evapotranspiration and maximum evapotranspiration (Doorenbos and Kassam 1979; Stewart et al. 1977; Hanks 1983) by:

$$Y = 1 - \beta_0 + \beta_0 \cdot ET/ET_m\,, \tag{11}$$

where β_0 is a yield response factor (Doorenbos and Kassam 1979; Hanks 1983). Solution of Eqs. (7) and (11) yields the expression for evapotranspiration by crops experiencing salinity induced water stress:

$$ET = 0.85\,E_p(Y - 1 + \beta_0)/\beta_0\,. \tag{12}$$

An expression for relative crop yield (Y) can then be found using Eq. (12) instead of (7) for crop water use, and solving Eqs. (1), (2), (3), (5), (6), (10) and (12), with $F = 0$ in Eq. (6) and $J = 0.8$ in Eq. (5), to yield:

$$Y = 1 - 0.01\,B\left\{\left(0.2 + \frac{0.2}{LF}\right)\left[C_w + \frac{K(C_a - C_w) - R(C_w - C_r)}{0.85\,E_p(Y - 1 + \beta_0)} \cdot (1 - LF)\,\beta_0 + LF(C_a - C_w)\right] - A\right\}, \quad C_{se} > A\,. \tag{13}$$

Equation (13) has been illustrated in its simplest form above, by leaving relative yield (Y) on the right hand side as well as the left. The equation is only valid for rootzone salinity (C_{se}) above the threshold (A) (i.e. $Y < 1$).

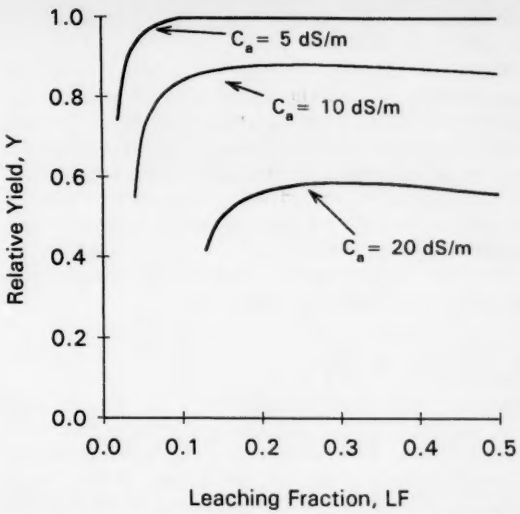

Fig. 3. Yield of fully irrigated perennial pasture suffering salinity impaired water use. Plot of Eq. (13), $C_{se} > A$, with $C_w = 0.1$ dS/m, $R = 0.45$ m/y, $C_r = 0.008$ dS/m, $K = 0.06$ m/y, $E_p = 1.4$ m/y, $A = 1.6$ dS/m, $B = 8.9$ and $\beta_0 = 1$

The quantitative implications of this theory can be illustrated by substituting values for parameters. These values are chosen as representative for perennial pasture grown in the Shepparton region in the Murray Basin, Australia, where channel supply water is generally of high quality, $C_w = 0.1$ dS/m being typical. Using an average regional rainfall $R = 0.45$ m/yr, $C_r = 0.008$ dS/m, $E_p = 1.4$ m/yr and K of 0.06 m/yr, Y is plotted as a function of the leaching fraction and the groundwater salinity in Fig. 3. In this example crop salt tolerance parameters are those measured by Mehanni and Repsys (1986) for perennial pasture, giving $A = 1.6$ and $B = 8.9$ in Eq. (9). Equation (13) is valid for $12.9 > C_{se} > A$. The upper limit for C_{se} is represented by zero yield in Eq. (9). In reality Eq. (9) loses linearity at very high values of rootzone salinity, and these levels are economically unrealistic. A value of 1.0 is assumed for the yield response factor (β_0), although this can be substituted for a more appropriate value, where known. The yield response factor (β_0) often has a value of about 1 (Doorenbos and Kassam 1979) and has a value of about 1.05 for lucerne (Hanks 1983). Equation (13) has been solved iteratively and plotted in Fig. 3 using these values.

From Fig. 3 it can be seen that for $LF > 0.2$ approximately when $C_a = 10$ dS/m, an increase in the leaching fraction results in increased yield. This higher yield with greater leaching becomes more important in absolute magnitude with higher levels of groundwater salinity. At low levels of groundwater salinity, yield is not particularly sensitive to the range of leaching fractions typical of many soils (i.e. 0.1–0.4).

An estimate of crop yields under conjunctive use, for a particular level of groundwater salinity, can be made from Fig. 3. For example where groundwater salinity is 10 dS/m, conjunctive water use will result in 88% of full

yield. Similarly a groundwater salinity of 8 dS/m will result in 92% of maximum yield.

Reduction in leaching to low values of LF causes decreased yield for any particular level of groundwater salinity (Fig. 3). As leaching approaches zero, rootzone salinity increases indefinitely (Fig. 2). In Fig. 3, however, the asymptote of the equation shifts to higher values of LF with increases in C_a, so that exceeding a minimal leaching becomes more critical in comparison with Fig. 2. This occurs because K, assumed constant, represents a greater percentage of the water budget when the crop uses less water whilst under salinity stress.

Salt export for salt balance

Under irrigation with conjunctive water use, groundwater is cycled, so that salt imports in irrigation water and rainfall can cause groundwater degradation. Salt export can maintain a regional salt balance if this export balances surface salt import (Prendergast et al. 1994). The depth of groundwater used conjunctively is then reduced by export of groundwater out of the system, and rootzone salinity is lower. Export in this paper refers to discharge of drainage effluent from the irrigated area through water conveyance infrastructure on the surface.

Mass conservation of salt for the system with salt export means that the annual applied salt (IC_i), is made up of salts in rainfall (RC_r), plus salts in irrigation supply water (WC_w), and pumped groundwater (PC_a), minus the depth of exported groundwater (D) times its salinity (C_a). D must be less than the depth of groundwater recharge, $I \cdot LF + K$ (or P, through Eq. (1)), otherwise a falling watertable results and steady state assumptions used for the derivation of the conjunctive use model are not valid. The equation is therefore:

$$IC_i = RC_r + WC_w + (P - D)\,C_a, \quad P > D. \tag{14}$$

Salt balance maintained through export of some groundwater means that the mass of salt export, DC_a, equals the salt mass applied in rainfall and irrigation water, i.e.:

$$DC_a = RC_r + WC_w. \tag{15}$$

If $D = P$, then by definition there is no conjunctive use. From Eq. (15) the depth of groundwater for export (D) is $(RC_r + WC_w)/C_a$ and this equals P (or $I \cdot LF + K$ from Eq. (1)), when $C_a = (RC_r + WC_w)/(I \cdot LF + K)$. Thus the steady state condition that $P > D$ requires that:

$$C_a > (RC_r + WC_w)/(I \cdot LF + K). \tag{16}$$

The relationship between rootzone salinity, irrigation water salinity and the leaching fraction in Eq. (5) in the presence of groundwater export and with $J = 0.8$ can be solved with (6), (7), (14), (15), and (16), with $F = 0$ in (6), to give:

$$C_{se} = 0.2\,C_a\left(1 + \frac{1}{LF}\right)\left(LF + \frac{K(1 - LF)}{0.85\,E_p}\right),$$

$$C_a > \frac{RC_r + WC_w}{I \cdot LF + K}. \tag{17}$$

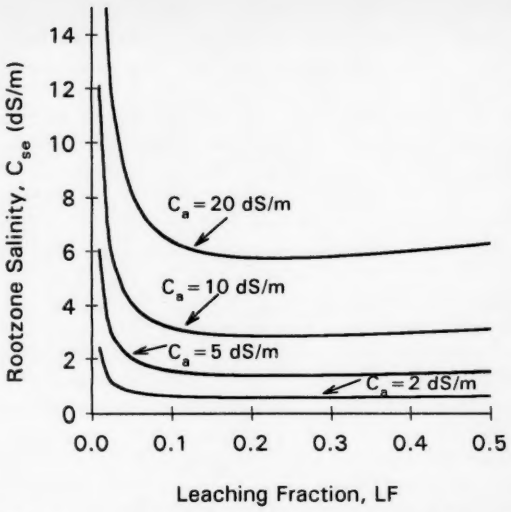

Fig. 4. Rootzone salinity under conjunctive water use for maximum crop evapotranspiration and groundwater export for salt balance. Plot of Eq. (17) with $E_p = 1.4$ m/y and $K = 0.06$ m/y

Equation (17) is plotted in Fig. 4 using the same parameter values typical of the Shepparton Irrigation Region in Australia as were used in Fig. 2. When compared with Fig. 2, Fig. 4 (which also describes crops under no salinity stress) indicates that groundwater export to maintain salt balance, described by Eq. (15), has little effect on rootzone salinity. This is because D (as determined from Eq. (15)) is only a small fraction of P, except at very low levels of groundwater salinity, in which case rootzone salinity is well below threshold in the conjunctive use system.

Discussion

Management to minimise rootzone salinity under conjunctive use

The effect that groundwater recharge from the surface has on the plant rootzone in Fig. 1 is dependent on the path these water fluxes take to the watertable. Water movement through the soil matrix has two opposing effects on rootzone salinity in the conjunctive use system:

(a) this water leaches salts from the crop's rootzone, thus lowering rootzone salinity, but

(b) these leaching fluxes increase groundwater recharge and hence the depth of groundwater that has to be pumped at equilibrium, and therefore indirectly increase rootzone salinity.

Non-leaching recharge (K) affects the plant rootzone only by increasing the depth of pumped groundwater.

Water movement through the soil matrix is generally low when heavy textured soils are irrigated and high when light soils are irrigated. Water application depths, irrigation frequency, and the rate of groundwater pumping also affect water movement through the soil matrix.

However, the above analysis has shown that for the parameter values adopted (at least), changes to water movement below the rootzone through the soil matrix, as indicated by LF, have relatively little impact on rootzone salinity for $LF > 0.1$. Pumps should therefore be operated to achieve free drainage to the aquifer in order to ensure sufficient leaching. Pumping can then also lower the watertable, which will improve crop yields where rootzone waterlogging is a significant problem. Increasing the pumping rate, however, increases well drawdown, which also has the potential to increase G and S and therefore K. If rootzone waterlogging is not a significant problem, pumping at lower rates is therefore desirable to reduce pumping costs. Pump management guidelines, therefore, must be evaluated in the context of local conditions.

The importance of reducing non-leaching recharge for different given aquifer salinities can be assessed by plotting rootzone salinity against K in Eq. (8). Figure 5 presents the results of these calculations. It is notable in Fig. 5 that under the ideal conditions represented by $K = 0$, groundwater of much higher salinity can be utilised without excessively increasing rootzone salinity. For example, with a groundwater salinity of 10 dS/m, $LF = 0.1$ and a crop threshold salt tolerance of 2.3 dS/m there would be little yield reduction (Fig. 5).

Whilst rootzone salinity is relatively insensitive to the leaching fraction over the higher range of LF commonly achieved (as shown in Figs. 2 and 4), C_{se} is linearly sensitive to non-leaching recharge. Thus considerable yield benefits can be obtained from reduction in non-leaching recharge. For example, it can be seen from Fig. 5 that a reduction in non-leaching recharge from 0.25 m/yr to 0.1 m/yr will result in a 35% reduction in rootzone salinity for a groundwater salinity of 5 dS m^{-1} and $LF = 0.1$. The benefit of reducing K is greater at higher levels of groundwater salinity, and greater for small values of LF (Fig. 5). Conversely, the detrimental affect of greater applied salt loads from increased K can be partially offset by greater rootzone leaching. The minimum value of rootzone salinity as a function of LF in the solutions to Eq. (8) plotted in Fig. 2, is also implied in Fig. 5. It can be seen from Fig. 5 that for low values of K, increasing leaching from $LF = 0.01$ to $LF = 0.4$ actually increases rootzone salinity. At high values of K this addional leaching reduces rootzone salinity. Figure 5 shows that the value of K at which higher leaching begins to reduce rootzone salinity is greater with higher levels of C_a.

Management of the conjunctive use system can reduce K in several ways. Reduced channel seepage (S) can be achieved in some regions by piping irrigation water. A reduction in channel supply water salinity can reduce seepage by reducing hydraulic conductivity. Water application with sprinklers is may offer a reduction in bypass flows (F).

If the depth of pumped groundwater used for irrigation exceeds groundwater recharge in a conjunctive use system, the extra irrigation groundwater must have been made up of an equivalent mass of groundwater flowing laterally into the system from outside, if the system is in steady state. Such lateral flows can be considered as

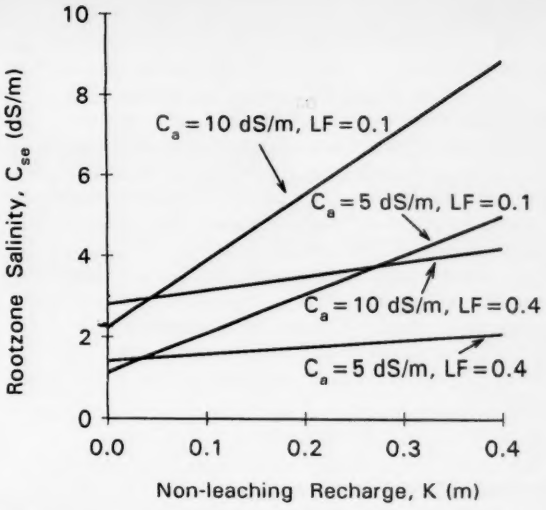

Fig. 5. Rootzone salinity vs. non-leaching recharge for full irrigation with conjunctive water use with no salt export. Plot of Eq. (8) with $C_w = 0.1$ dS/m, $R = 0.45$ m/y, $C_r = 0.008$ dS/m, $E_p = 1.4$ m/y

adding to K, since they do not provide leaching in the conjunctive use system. Although K, as defined earlier, does not describe the situation where groundwater used conjunctively is irrigated over only part of the pump's area of influence, the term K could be readily modified so that this would be included. This situation arises if the area to which conjunctively used groundwater is applied is smaller than the area of influence of the groundwater pump, thus providing a greater depth of groundwater for crops irrigated on that reduced area. However, in order to minimise non-leaching recharge, it is important that conjunctively used groundwater be irrigated over a large percentage of the pump's area of influence. In a conjunctive use system the depth of groundwater recharge is small in comparison with the depth of crop water use. Therefore use of groundwater to provide a large proportion of crop water use implies that much of this groundwater has come from outside the area of conjunctive use. Minimising K and thus rootzone salinity under conjunctive use therefore precludes a large proportion of crop water use being provided by pumped groundwater.

The effectiveness of the conjunctive use system for controlling salinity also depends on management of the groundwater catchment, of which the conjunctive use system is a part. Regional hydrogeological characteristics may result in high values for G (Fetter 1988), so that groundwater pumping in a conjunctive use system may result in beneficial leaching of upstream areas where there are no groundwater pumps. A policy of conjunctive water use can allow crop threshold salt tolerance properties to be exploited to enable control of irrigation salinity without loss of crop yield. The effectiveness of conjunctive use over a catchment is therefore maximised by utilising threshold tolerance over as large an area of the catchment as possible. Irrigated areas which have leaching but not

conjunctive use, and hence little salt application, do not utilise crop threshold salt tolerance. When the groundwater catchment is a closed groundwater system, leached areas without conjunctive use can cause high values of K in conjunctive use areas which overlie groundwaters downstream. Surface redistribution of groundwater back to upstream leached areas which have no installed pumps increases the area over which crop threshold tolerance is utilised for disposal of groundwater. Thus redistribution can improve the effectiveness of conjunctive water use in controlling salinity in the catchment. Surface redistribution of groundwater is most important in groundwater catchments where hydrogeological characteristics result in high values of G in the conjunctive system in parts of the catchment and low or negative values of G in other parts.

Rootzone leaching

As stated earlier, increasing LF has two opposite effects on crop rootzone salinity in a conjunctive use system; firstly, increased LF results in greater salt transport out of the rootzone, which reduces rootzone salinity, but secondly, by resulting in the need for a greater depth of pumped groundwater (Eq. (1)), it increases the applied salt load. This means that in the conjunctive use equations (8), (13) and (17), there is a minimum rootzone salinity which can be achieved. This minimum represents the optimum leaching management of the system, and an expression for this state can be found by evaluating LF where the equation derivative is zero. Thus $LF = LF_{opt}$ when:

$$\frac{\partial C_{se}}{\partial LF} = 0 . \qquad (18)$$

The solution to Eq. (18) is a function of non-leaching recharge, K, and groundwater salinity, C_a, so that optimal management of this system is site specific. As is illustrated in Figs. 2 and 4, to the left of the minimum represented by Eq. (18), decreased leaching will result in increases in rootzone salinity. Especially at low values of C_a, the value of C_{se} is close to the minimum over a range of values of LF. To the right of the minimum, decreasing leaching will have a beneficial effect on rootzone salinity. An example of how LF_{opt} increases with K and C_a is implied in Fig. 5. Increasing leaching from $LF = 0.1$ to 0.4 increases C_{se} when $K = 0$, but decreases C_{se} at high values of K; the value of K where C_{se} is equal for these two leaching fractions and a particular C_a, increases with C_a (see Fig. 5).

From the model describing the conjunctive use system illustrated in Fig. 1, the value of LF_{opt} depends on the importance of leaching in controlling rootzone salinity. In irrigation areas where the parameters used in Figs. 2 and 3 are valid, LF_{opt} occurs at approximately $LF = 0.35$. For areas where leaching is of lesser importance in controlling rootzone salinity and the equation of Bernstein and Francois (1983) is valid, for example, LF_{opt} occurs at low leaching fractions, and reduction in leaching will improve rootzone salinity for values of LF commonly encountered. This highlights the importance of local determination of the leaching parameters before application of the conjunctive use model.

Equation (5) can be fitted to a range of different soils through its empirically determined coefficient, J. Rootzone salinity as described in Eqs. (8) and (17) is proportional to J, so that a higher value of J means greater rootzone salinity in the conjunctive use model. The derivative $\partial C_{se}/\partial(LF)$ for Eqs. (8) and (17) is also directly proportional to J, so that the gradient of the lines in Figs. 2, 3 and 4 increases with increasing J.

Conclusion and comment

Where the leaching equation (5) of Rhoades (1974) is valid, the conjunctive use model developed here suggests that rootzone salinity is insensitive to leaching in the range of leaching fractions commonly encountered (from 0.1 to 0.4). Strategies such as intermittent pumping, which can reduce the pumped water depth and thereby minimise leaching, could result in decreased crop yield if low leaching results (e.g. $LF > 0.05$). The conjunctive use model indicates that high induced leaching rates will be unlikely to increase rootzone salinity. In areas where rootzone waterlogging is a problem, lowering the watertable could therefore be achieved by using high pumping rates or more continuous pumping to increase the pumped water depth, if this does not increase K excessively.

The model indicates that where the nominated parameters are applicable, and the groundwater salinity is 10 dS/m, a threshold crop salt tolerance of 3 dS/m is required to prevent yield reduction under conjunctive water use. Where groundwater salinity is 5 dS/m, a crop threshold salt tolerance of 1.6 dS/m is required to avoid reductions in yield. Export of a mass of salt equal to that applied in irrigation water and rainfall has little effect on rootzone salinity under conjunctive use.

In the analysis of the conjunctive use system, non-leaching recharge is found to be the most important component of the water budget to affect rootzone salinity. There is potential for large additions to this component when groundwater is not irrigated over the whole of the area of influence of the groundwater pump. In some irrigation areas regional hydrogeological characteristics can result in excessive upward leakage (G) into the pumped aquifer and cause large additions to non-leaching recharge. Surface redistribution of pumped groundwater to upstream irrigation areas without groundwater pumps can help counteract the adverse salinity impacts of excessive upward leakage (G) by reducing the volume of groundwater to be applied in the pumped area.

The lumped parameter model developed in this paper has been used to assess management options under conjunctive water use. The model is also likely to have application for providing salinity management guidelines, because of the difficulty, and therefore cost, in obtaining sufficient data for an equivalent distributed parameter model. Applicability of the model will be enhanced by determination of suitable parameters through site investigations in an irrigation region.

References

Ayers RS, Westcot DW (1985) Water quality for agriculture. FAO Irrig Drain Paper 29, Rome 1985

Bernstein L (1975) Effect of salinity and sodicity on plant growth. An Rev Phytopathol 13:295–312

Bernstein L, Francois LE (1973) Leaching requirement studies: sensitivity of alfalfa to salinity of irrigation and drainage waters. Soil Sci Soc Am Proc 37:931–943

Bingham FT, Garber MJ (1970) Zonal salinisation of the root system with NaCl and boron in relation to growth and water uptake of corn plants. Soil Sci Soc Am Proc 34:122

Bower CA, Ogata G, Tucker JM (1969) Rootzone salt profiles and alfalfa growth as influenced by irrigation water salinity and leaching fraction. Agron J 61:783–785

Bower CA, Ogata G, Tucker JM (1970) Growth of Sudan and tall fescue grasses as influenced by irrigation water salinity and leaching fraction. Agron J 61:783–785

Bresler E, McNeal BL, Carter DL (1982) Saline and sodic soils: principles – dynamics – modelling. Springer, Heidelberg

de Wit CT (1958) Transpiration and crop yields. Versl Landbouwk Onderz 64.6 Inst Biol Chem Res Field Crops and Herbage, Wageningen, The Netherlands

Dirksen C (1985) Relationship between root uptake-weighted mean soil water salinity and total leaf water potentials of alfalfa. Irrig Sci 6:39–50

Doorenbos J, Pruit WO (1977) Crop water requirements. FAO Irrig Drain Paper 24, FAO Rome 1984

Doorenbos J, Kassam AH (1979) Yield response to water. FAO Irrig Drain Paper 33, FAO Rome 1986

Fetter CW (1988) Applied Hydrogeology. Merrill Publishing Company, Columbus, Ohio

Hanks RJ (1983) Yield and water use relations. In: Taylor HM, Jordan WR, Sinclair TR (eds) Limitations to efficient water use in crop production. ASA/CSSA/SSSA, Madison, Wis

Hoffman GJ, van Genutchen MTh (1983) Soil properties and efficient water use: water management for salinity control. Chap 2c. In: Taylor HM, Jordan WR, Sinclair TR (eds) Limitation of efficient water use in crop production. ASA/CSSA/SSSA, Madison, Wis

Hoffman GJ, Rawlins SL, Oster JD, Jobes JA, Merrill SD (1979) Leaching requirement for salinity control 1. Wheat, sorghum and lettuce. Agric Water Manag 2:177–192

Ingvalson RD, Rhoades JD, Page AL (1976) Correlation of alfalfa yield with various index of salinity. Soil Sci 122:145–153

Letey J, Dinar A, Knapp KC (1985) Crop-water production function for saline irrigation waters. Soil Sci Soc Am J 49:1005–1009

Lunin J, Gallatin MH (1965) Zonal salinisation of the root system in relation to plant growth. Soil Sci Soc Am Proc 69:608

Maas EV, Hoffman GJ (1977) Crop salt tolerance – current assessment. J Irrig Drain Div ASCE 103 No IR2:115–134

Mehanni AH, Repsys AP (1986) Perennial pasture production after irrigation with saline groundwater in the Goulburn Valley, Victoria. Aust J Exp Agric 26:319–324

Prendergast JB (1993) A model of crop yield response to irrigation water salinity: theory, testing and application. Irrig Sci 13:157–164

Prendergast JB, Heuperman AF (1988) Groundwater pumping/reuse in N. Victoria: recharge processes, aquifer salinisation and farm productivity. BMR J Aust Geol and Geophys, Groundwater 12:149–154

Prendergast JB, Rose CW, Hogarth WL (1994) Sustainability of conjunctive water use for salinity control in irrigation areas: theory and application to the Shepparton region, Australia. Irrig Sci 14:177–187

Rasmussen VP, Hanks RJ (1978) Model for predicting spring wheat yields with limited climatological and soil data. Argon J 70:940–944

Rhoades JD (1974) Drainage for salinity control. In: van Schilfgaarde J (ed) Drainage for agriculture. Agronomy 17:433–461. Am Soc Agron, Madison, Wis., USA

Shalhevet J, Bernstein L (1968) Effects of vertically heterogeneous soil salinity on plant growth and water uptake. Soil Sci 106:85–93

Shalhevet J, Mantell A, Bielorai A, Shimsi D (1976) Irrigation of field and orchard crops under semi-arid conditions. Int Irrig Info Ctr Pub No 1 Bet Dagan, Israel

Slavich PG (1992) Irrigation using groundwater for watertable control: a model of salt and water balance limitations. Aust J Agr Res 43:225–239

Smith RJ, Hancock NH (1986) Leaching requirement of irrigated soils. Agric Water Manag 11:13–22

Stewart LI, Danielson RE, Hanks RJ, Jackson RM, Hagan WO, Pruit WO, Franklin WT, Riley JP (1977) Optimising crop production through control of water and salinity levels in the soil. Utah Water Lab Pub No PRWG 151-1, USA

van Schilfgaarde JL, Bernstein L, Rhoades JD, Rawlins SL (1974) Irrigation management for salt control. J Irrig Drain Div Am Soc Civil Eng 100:321–328

Irrig Sci (1994) 14:177–187

Irrigation Science
© Springer-Verlag 1994

Sustainability of conjunctive water use for salinity control in irrigation areas: theory and application to the Shepparton region, Australia

J. Bernard Prendergast [1], Calvin W. Rose [2], William L. Hogarth [2]

[1] Institute of Sustainable Irrigated Agriculture, Ferguson Road, Tatura, Vic, 3616, Australia
[2] Faculty of Environmental Sciences, Griffith University, Nathan, Qld., 4111, Australia

Received: 2 February 1993

Abstract. The long term sustainability of conjunctive water use for controlling irrigation salinity is affected by increase in groundwater salinity over time. This paper uses mass conservation of salt and water to assess groundwater degradation over long time scales. Management options which affect this rate of degradation are also examined. The groundwater model developed is illustrated using data from the Shepparton Irrigation Region in the Murray Basin, Australia. The model predicts rapid groundwater deterioration when conjunctive use is conducted over only a fraction of the area of influence of a groundwater pump. Where the pumped aquifer is underlain by deeper groundwaters, the rate of groundwater degradation is also affected by leakage into or out of the conjunctive use system. Surface redistribution of groundwater from pumps installed in zones of regional groundwater discharge to areas recharging the regional groundwaters, reduces excessive degradation in the zones of discharge. With optimal surface distribution of groundwater, the rate of degradation is low. The rate of groundwater degradation also depends on salt inputs from irrigation water and rainfall, and the average depth from the soil surface to the base of the aquifer. The rate of degradation resulting from applied salts in surface water and rainfall is typically about 0.01 dSm^{-1} per year for shallow aquifers in the Shepparton region, but the rate is lower where deeper aquifers are pumped. Partial irrigation also reduces the rate of degradation because of the reduced rate of salt inputs. Where poorer quality groundwater lies within the area of influence of the groundwater pump, a greater rate of deterioration in the quality of pumped groundwater can be expected from groundwater mixing. In some irrigation regions limited export of groundwater through surface water conveyance structures to a river is possible, so that a regional surface salt balance could be maintained. However, salt exports made equal to the rate of surface imports into the irrigated area will only significantly impact groundwater salinity in the very long term, or where only shallow aquifers can be pumped. In addition, this export can be costly for downstream water users, or if construction of additional conveyance infrastructure is extensive; export can have a detrimental impact on riverine ecosystems. Other management options such as the depth of pump installation and the spatial distribution of irrigation water and pumped groundwater, which affect the redistribution of salts within the groundwater system, have the potential to have a much greater impact on local groundwater salinity.

Correspondence to: B. Prendergast

Where hydrogeological conditions are such that insufficient leaching for irrigated agriculture occurs, artificial sub-surface drainage is necessary. If suitable aquifers exist, groundwater pumps can provide the most economic means of sub-surface drainage. Application of pumped groundwater in conjunction with surface supplied irrigation water provides the most economic and environmentally acceptable means of dispersing drainage effluent, provided the groundwater is of sufficiently low salinity and toxicity (Salinity Program Advisory Council 1989). However, groundwaters underlying irrigation areas can have annual salt imports from irrigation water of 0.1 to 10 tonnes per year per hectare, and this salt application can cause an increase in groundwater salinity through time. The rate of change of groundwater salinity also depends on whether groundwater flows result in a net addition or loss of salt from the conjunctive use system. Because conjunctive water use results in higher levels of salinity of applied water, sustainability of crop yields can also be affected by salinity and sodicity effects on soil physical properties, although this aspect is not addressed here.

Land and water management have a large impact on groundwater systems, particularly where groundwater is pumped. For example, restricting the area of conjunctive use to less than the area of influence of a groundwater pump (referred to as spatially constricted conjunctive use), or reduction in the depth of irrigation water applica-

tion (referred to as partial irrigation), both affect the rate of salt accumulation under conjunctive use. Therefore the long term implications of conjunctive use of groundwater for salinity control will be dictated by groundwater management, which controls the distribution of groundwater salts above and below the surface, as well as by land and surface water management. Good salinity management aims to minimise rootzone salinity and sustain productivity and groundwater quality. The likely consequences of alternative management options on groundwater quality are examined using a simple steady rate lumped parameter model derived in this paper from mass conservation considerations. Lumped parameter models are usually used where time, but not space, is the important variable (Domenico 1972). Prendergast et al. (1994) used a model of steady rate water fluxes to determine the effect of a particular level of groundwater salinity on crop yield under conjunctive use; however they did not look at the effect of these steady rate fluxes on the change in groundwater salinity over long time scales, which is considered here. Data used in the model are taken as typical of the Shepparton Irrigation Region in the Murray Basin, Australia.

Abbreviations

A_1 Area of influence of a groundwater pump in an unconfined aquifer (m^2); a initial groundwater salinity (C_0) minus final steady state groundwater salinity (c) (dS/m); b ratio of groundwater discharge out of the conjunctive use system to groundwater storage in the system (y^{-1}); C_a average groundwater salinity from the soil surface to the base of an unconfined aquifer (dS/m); C_{a1} average groundwater salinity (dS/m) from the soil surface to the base of an unconfined aquifer within the area of influence of a groundwater pump, but outside the area of conjunctive water use; C_{a2} average groundwater salinity from the soil surface to the base of an unconfined aquifer under irrigation with conjunctive water use (dS/m); C_0 initial average water salinity (dS/m) below the soil surface; C_r salinity of rainfall (dS/m); C_w salinity of surface supply water for irrigation (dS/m); c final steady state groundwater salinity (dS/m); E_p annual "Class A" pan evaporation (m/y); ET_m annual maximum crop evapotranspiration (m/y); G annual equivalent ponded depth of groundwater leakage (positive downwards) below the base of the aquifer to deeper groundwater (m/y); H depth from the soil surface to the base of the aquifer (m); I annual total depth of water applied to the crop as irrigation and rainfall (m/y); K_c crop factor (dimensionless); K_p pan coefficient (dimensionless); LF the leaching fraction; the fraction of applied water passing below the crop rootzone; P annual equivalent ponded depth of pumped groundwater (m/y); R annual depth of rainfall (m/y); S annual equivalent ponded depth groundwater recharge from seepage from irrigation supply channels or pipe delivery systems (m/y); t time in years; U land fraction maintaining conjunctive water use within the area of influence of a groundwater pump; W annual infiltrated depth of surface water supplied for irrigation (m/y); W_1 annual depth of channel (or piped) supply water infiltrating outside the area of conjunctive water use but within the area of influence of the groundwater pump (m/y); W_2 annual depth of channel (or piped) supply water infiltrating within the area of conjunctive water use (m/y); θ average volumetric water content of sediments from the soil surface to the base of the aquifer ($m^3\,m^{-3}$).

Assumptions and background for theoretical development

In deriving this model it will be assumed that groundwater recharge into the conjunctive use system completely mixes with the volume of groundwater under consideration and that there is no lateral flow between the system and its surrounds. Since both the velocity of groundwater recharge and the distances along the groundwater streamlines to the pump screen are highly variable, a high degree of mixing is expected. Even poor mixing of groundwater recharge with groundwater will not affect mass conservation of salts over long time scales, although short term variations in groundwater salinity may occur which are not accounted for in this model.

Diffusion is neglected in the model presented because it is assumed to be of little importance compared to the convective transport of solutes through leaching and pumping. The processes of dissolution and cation exchange are also ignored as the groundwater is considered to be in a state of equilibrium with precipitated and exchangeable ions. The rate of dissolution depends on the chemical nature and rate of mineral decomposition of the stratigraphy. Dissolution is not considered in this paper, although it may need to be incorporated when assessing irrigation regions where substantial mineral decomposition occurs over the very short geologic time scales considered here.

Use of conventional units of electrical conductivity for salinity, in expressing mass conservation of solutes, implies that the relationship between electrical conductivity and solute concentration is assumed constant.

The most important factors that cause changes in groundwater salinity under conjunctive use, which are discussed in this section, are:

(a) salt inputs to the groundwater system from irrigation water and rainfall,

(b) the spatial relationship between the conjunctive use system and the regional groundwater, and the resulting groundwater leakage into or out of the system,

(c) spatial constriction of the area of conjunctive water use,

(d) mixing of groundwaters, and

(e) salt export from the irrigated area; export in this paper refers to groundwater being discharged from the irrigated area through surface conveyance structures.

The lumped parameter groundwater model is developed for conjunctive use in irrigation areas from the conceptual model illustrated in Fig. 1. The model is used to assess factors (a), (b), (c) and (e) above, but not (d), because the model assumptions of perfect mixing render it inappropriate for analysing mixing. All water inputs and outputs are based on the assumption of steady rate processes, with rates expressed as average annual depths.

Crops in Fig. 1 are irrigated with surface water of depth W and concentration C_w, and pumped groundwater, P, to supplement rainfall of depth R and concentration C_r. Recharge to the groundwater occurs from channel seepage (or pipe leakage) (S), and leaching fluxes below the crop rootzone ($I \cdot LF$), where I is the total depth of applied water (equal to $W+P+R$), and LF is the leaching fraction (the fraction of applied water passing below the rootzone). The magnitude of soil-water bypass flows which could enter the groundwater by bypassing the crop rootzone through large cracks and voids is assumed to be zero, which is a reasonable assumption for the soil type prevalent in the Shepparton Region (see Pren-

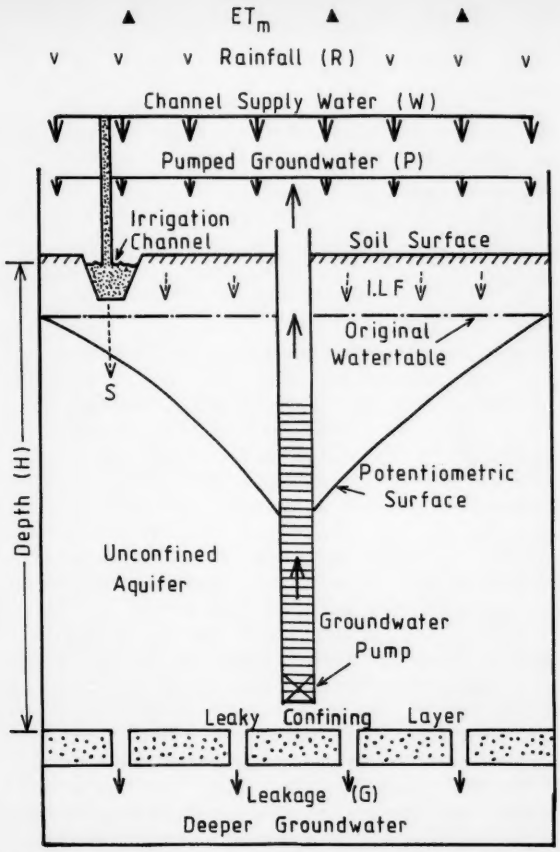

Fig. 1. Conceptual model of a conjunctive use system showing boundary conditions, inputs and outputs, for the development of a groundwater model for an irrigation area with conjunctive use of groundwater

dergast and Noble 1990). Furthermore, bypass flows can be assumed to have little effect on groundwater degradation in the conjunctive use system, because of their low salinity.

Groundwater is pumped from an unconfined (or "watertable") aquifer. Depth H is taken from the soil surface to the permeability layer which forms the lower boundary of the system. No distinction is made between the vadose zone and the saturated zone, so that all layers of the stratigraphy over H are lumped together. The average salinity of water below the surface to depth H can then be C_a (referred to in this paper as groundwater salinity), and the average volumetric water content over depth H is denoted by θ. Some leakage, G, passes through the low permeability layer beneath the conjunctive use system to deeper groundwater (Fig. 1). The area of influence of the groundwater pump is defined as the areal extent of the cone of depression of the watertable (see Todd 1980), as illustrated in Fig. 1. It is initially assumed that conjunctive use of groundwater and surface water for irrigation is maintained over the entire area of influence of the pump. The case where this assumption is not valid is discussed separately in a later section of the paper.

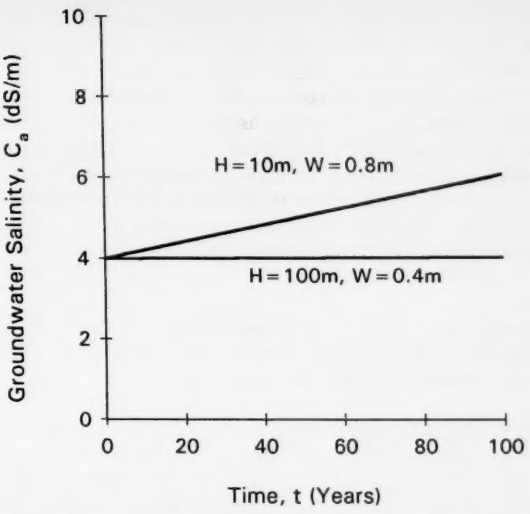

Fig. 2. Changes with time in groundwater salinity caused by salts in irrigation water and rainfall under conjunctive water use with $G=0$. Predictions use Eq. (2) with $R=0.45$ m/y, $C_w=0.1$ dS/m, $C_r=0.008$ dS/m, $\theta=0.4$ and $C_0=4$ dS/m

Irrigation and rainfall salt inputs

For this section the equivalent ponded depth of groundwater leakage beneath the system, G, is considered to be zero, indicating a closed groundwater system. A mass of salt PC_a is extracted through groundwater pumping and applied to the soil surface for conjunctive use; this recycling of groundwater has no net effect on mass conservation of salt within the system. Salt imports into the system, then, are from irrigation water (both surface applied and through channel seepage) and rainfall only.

Conservation of mass of salt requires the rate of change of groundwater salinity (dC_a/dt) to be equal to the annual net salt input rate divided by the volume of water in the conjunctive use system; i.e.

$$\frac{dC_a}{dt}=\frac{(W+S)\,C_w+RC_r}{H\theta} \tag{1}$$

Integrating Eq. (1) with respect to time, and using the initial condition $C_a=C_0$ at $t=0$, gives:

$$C_a=C_0+\left(\frac{(W+S)\,C_w+RC_r}{H\theta}\right)t\,. \tag{2}$$

This linear relationship is plotted for two possible cases in Fig. 2 for parameter values typical of the range of H and W in the Shepparton region. An applied irrigation water depth of 0.8 m represents full irrigation (i.e. sufficient irrigation to supply maximum crop water use) on perennial pastures, which utilise a large percentage of supplied irrigation water. Supply water salinity in the region is normally about 0.1 dS m^{-1}, although salinities up to 0.4 dS/m^{-1} can occur. Unconfined to semi-unconfined aquifers are pumped from depths from 8–150 m (Ife 1988; Nolan and Reid 1989; Brown 1985). More detailed description of

aspects of the groundwater system is given by Brown and Stephenson (1986); Macumber (1991); Prendergast (1989); Lawrence and Abele (1976) and Evans (1988).

Figure 2 also illustrates the effect of partial irrigation, where water available to the crop is half the maximum potential crop water use in the illustrated example. Partial irrigation reduces the mass of applied salts, WC_w. Groundwater degradation then increases with increases in applied irrigation water salts and with decreases in depth to the base of the aquifer (Fig. 2 and Eq. (2)).

Groundwater recharge to and discharge from the conjunctive use system and the influence of the regional groundwater

Whilst it was assumed that $G=0$ for Fig. 1, this is generally not the case on average over a whole region. If indeed $G=0$ on average, then salinity problems would have been severe under pre-farming conditions, and it is unlikely that irrigation would be introduced. Despite the fact that regional net groundwater outflow may occur on average, both zones of discharge from and recharge to the regional groundwater from shallow aquifers will exist, depending on the shape of the region, boundary conditions and heterogeneity in the groundwater flow system (Freeze and Witherspoon 1967). Groundwater flows to or from the conjunctive use system change the mass stored and therefore change groundwater salinity in the system.

The three cases considered in this section which relate to groundwater flows to or from the conjunctive use system in Fig. 1 are:

(1) Groundwater leakage, G, out of the system to deeper groundwaters. These leakage flows are usually small where salinity problems exist, because irrigation salinity problems are caused by restricted groundwater flows. In the Shepparton region, leakage from shallow Shepparton Formation aquifers to deeper aquifers has been estimated to range from 40 mm/y to -3.5 mm/y (Nolan and Reid 1989).

(2) Groundwater leakage from deeper groundwater upwards into the conjunctive use system (i.e. $G<0$).

(3) Export of all pumped groundwater, i.e. there is no conjunctive use. The model developed for this purpose describes the effect on groundwater salinity of export to evaporation basins or oceans. Export may be necessary where groundwaters contain excessive concentrations of toxic elements, or where groundwater salinity is too high for conjunctive use. This model is also used later to describe the situation where subsurface drainage is supplied by a groundwater pump, but where there is no conjunctive use on the soil surface above the drained area.

Leakage out of the conjunctive use system

Mass conservation of salt for the system illustrated in Fig. 1 requires the average annual rate of change in salinity of the groundwater (dC_a/dt) to depend on the salt applied annually in irrigation water and rainfall ($(W+S)C_w+RC_r$), minus that lost through leakage to deeper groundwater (GC_a). Thus:

$$\frac{dC_a}{dt}=\frac{(W+S)C_w+RC_r-GC_a}{H\theta}, \quad G>0. \tag{3}$$

The solution to this first order linear differential equation, using the initial condition $C_a=C_0$ at $t=0$, is:

$$C_a=\left[C_0-\frac{RC_r+(W+S)C_w}{G}\right]\exp\left[-\frac{Gt}{H\theta}\right]+\frac{RC_r+(W+S)C_w}{G}, \quad G>0. \tag{4}$$

This solution (Eq. (4)) is of the form $ae^{-bt}+c$ where a, b and c are constants. The final steady state groundwater salinity, c, is given by the second term on the right hand side of Eq. (4) (i.e. $c=(RC_r+(W+S)C_w)/G$), and so is determined by the ratio of the rate of salt inputs to the system to the rate of groundwater flow out of the system. Thus c is independent of the rate of groundwater recycling (i.e. P). The attainment of a final steady state groundwater salinity implies that c must eventually be in equilibrium with the salinity of recharge fluxes entering the system, i.e. the depth weighted average salinity of channel seepage and salinity at the base of the crop rootzone in Fig. 1. For a given salinity of channel supply water and rainfall, salinity at the base of the rootzone is therefore determined by G in the very long term. The constant a is equal to the initial groundwater salinity, C_0, minus the final steady state groundwater salinity, c, and is therefore positive for groundwater salinity which decreases over time, and negative for groundwater which degrades over time. The parameter b determines the rate of change of salinity to the steady state level and is given by the ratio of the annual depth of groundwater discharge out of the system to the storage in the system (i.e. $G/H\theta$).

Equation (4) is plotted in Fig. 3, with W set to 0.8 m/y to represent full irrigation for the Shepparton region. The depth of groundwater leakage, G, is set to 0.01 m/y, this value being within the range of leakage from -3.5 to 40 mm/y, estimated for the Shepparton region (Nolan and Reid 1989). Other parameter values (typical of the Shepparton region) which are used in the evaluation of Eq. (4) for Fig. 3 are: $R=0.45$ m/y, $C_r=0.008$ dS/m, $C_w=0.1$ dS/m, and $S=0.04$ m/y.

The exponential nature of Eq. (4) is not evident in Fig. 3 because of the short time scale used. For negative a, as illustrated in Fig. 3, the effect of leakage from the groundwater system is to reduce the rate of groundwater degradation from applied salts as described in Fig. 2, and establish a final steady state groundwater salinity, approached only after many centuries. The final steady state groundwater salinity, c, evaluated through Eq. (4) is 8.6 dS/m. The rate of approach of groundwater salinity to the steady state value is determined by $H\theta$ and C_0 for particular values of W, C_w, R, C_r, S and G. For example, for C_0 of 4 dS/m, $H=30$ m and $\theta=0.4$, Eq. (4) predicts that after 500 years groundwater salinity will be 5.5 dS/m and after 1000 years, 6.5 dS/m. The effect of these levels of groundwater salinity on crop yield under conjunctive use can be estimated as outlined by Prendergast et al. (1993).

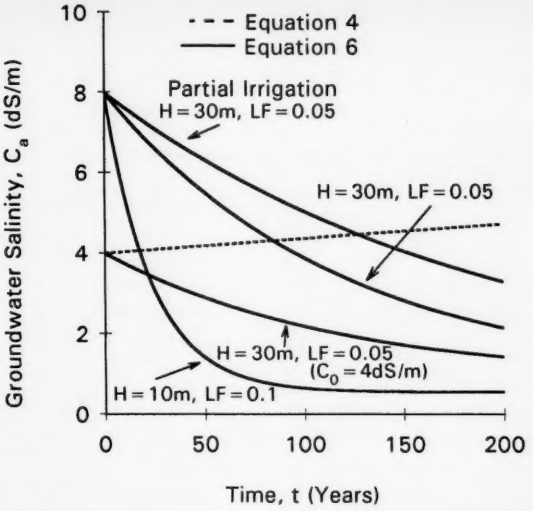

Fig. 3. The impact on groundwater salinity of groundwater discharge out of the conjunctive use system. Plot uses Eq. (4) with $R = 0.45$ m/y, $C_r = 0.008$ dS/m, $S = 0.04$ m, $\theta = 0.4$, $H = 30$ m, $C_w = 0.1$ dS/m, $G = 0.01$ m/y and Eq. (6) after substitution of Eq. (8) with $E_p = 1.4$ m/y. Graphs represent full irrigation unless otherwise indicated

Upward leakage into the conjunctive use system

If G is negative (item (2) above), the rate of groundwater deterioration will be increased. For negative G the rate of salt addition to the conjunctive use system depends on the salinity of deeper groundwater, which is most realistically assumed constant over time, unlike C_a in Eq. (4), so that Eq. (4) does not apply. For constant negative G, then, and constant salinity of deeper groundwater, dC_a/dt is constant and C_a is linear with time. As an example of this case, the rate of degradation can be calculated for the example in Fig. 2 with $H = 10$ m, $C_0 = 4$ dS/m and $W = 0.8$ m, by assuming the deeper groundwater salinity is equal to C_a, or 4 dS/m, and the rate of leakage into the conjunctive use system is -0.02 m/y. This rate will add to the conjunctive use system a salt mass of 4 dS/m × 0.02 m × 10,000 m²/ha × 0.6 (kg/t)/(dS/m) = 480 kg/ha/y (using the generally accepted approximation, 1 dS/m = 600 mg/l = 0.6 kg/t, and assuming a water density of 1 t/m³). This shows that a value of $G = -0.02$ m/y will double the rate of groundwater degradation in comparison to the example for full irrigation given in Fig. 2.

Salt export from the conjunctive use system

When export to evaporation basins or to an ocean is available, there is usually no conjunctive water use. For this case deep drainage out of the system (G) is set to zero for simplicity, and because it is assumed that G is small in comparison to P. Mass conservation of salt in the conjunctive use system is then described by a modified Eq. (3), with G replaced by P, because it is now pumping that discharges salt from the system. For a hydrologic steady state, the annual depth of pumped groundwater (P) must be equal to the groundwater recharge into the system, i.e. channel seepage, S, and the leaching flux under crops ($(W+R)\,LF$), so that:

$$P = (W+R)\,LF + S\,. \tag{5}$$

Substituting P from Eq. (5) for G in Eq. (4) gives:

$$C_a = \left[C_0 - \frac{RC_r + (W+S)\,C_w}{(W+R)\,LF + S}\right] \exp\left[-\frac{(W+R)\,LF + S}{H\theta}\,t\right] + \frac{RC_r + (W+S)\,C_w}{(W+R)\,LF + S}\,. \tag{6}$$

Equation (6), an expression for groundwater salinity under conditions of complete export, is again of the form $ae^{-bt} + c$. Evaluation of C_a using Eq. (6) requires a knowledge of W. The total depth of applied water (I) required, consisting of crop evapotranspiration plus the leaching fraction can be used to evaluate W. Maximum crop water use can be expressed by equating crop evapotranspiration with pan evaporation times a pan coefficient (K_p) of 0.85 and a crop factor (K_c) of 1 (Doorenbos and Pruit 1977). The resulting expression for I is:

$$I = K_c \cdot K_p \cdot E_p + I \cdot LF\,. \tag{7}$$

Since $I = W + R$ where there is no conjunctive use, the depth of channel supply water (W) can be expressed as the difference between I, available from Eq. (7), and rainfall (R). After substitution of values for K_c and K_p the expression becomes:

$$W = \frac{0.85\,E_p}{1 - LF} - R\,. \tag{8}$$

After substituting Eq. (8) for W, predictions using Eq. (6) are also plotted in Fig. 3 for parameter values typical of the Shepparton Irrigation Region.

The effect of partial irrigation illustrated in Fig. 3 is obtained by replacing the crop coefficient of 1 in Eq. (8) with a value of 0.75, and this change results in approximately 50% reduction in W, for $R = 0.45$ m. The effect of partial irrigation on groundwater degradation, using $LF = 0.05$ in Fig. 3, may not be simply compared with full irrigation for the same LF, because a reduction in total applied water would result in a lower value of LF. Because the rate of change of groundwater salinity in Eq. (6) depends on the coefficient of t, which is a function of LF and W, the lower value of LF associated with reduced W would tend to increase the difference between partial and full irrigation.

The final steady state groundwater salinity (c) in Eq. (6) approaches the depth weighted groundwater recharge salinity into the system after a long time period. For $c > C_0$ the groundwater degrades in quality, but for $c < C_0$, the groundwater improves in quality. In most practical cases the depth weighted recharge salinity (c) will be less than the groundwater salinity, as is the case for the evaluations of Eq. (6) illustrated in Fig. 3. If groundwater salinity is low and less than the depth weighted recharge salinity, the groundwater will probably be used for irrigation, in which case export is unnecessary. The

case where $C_0 < c$ has therefore not been illustrated for the export case.

Groundwater degradation from spatially constricted conjunctive use

Conjunctive use of groundwater for salinity control may be maintained over only part of the area of influence of a groundwater pump. This spatially constricted conjunctive use is illustrated for an unconfined aquifer in Fig. 4. For simplicity the model presented here assumes water use by the crop is unaffected by salinity. The area of influence of the groundwater pump is A_1, and the area maintaining conjunctive use UA_1. The area protected from salinity by the groundwater pump, but without conjunctive use, is thus $(1-U)A_1$. Groundwater salinity in the area with conjunctive use is denoted C_{a2} and the depth of channel supply water applied, W_2. In the area without conjunctive use these qualities are denoted by C_{a1} and W_1 respectively.

When the average salinity of recharge fluxes is lower than the groundwater salinity within the area of influence of a groundwater pump, but outside the conjunctive use area (Fig. 4), groundwater quality peripheral to the conjunctive use area in Fig. 4 will improve over time. Mass conservation of salt dictates that the reduction of salt storage in the area without conjunctive use is equal to the increase in salt storage in the land fraction with conjunctive use. This increase in salt storage accelerates groundwater degradation in the area receiving water used conjunctively. Groundwater degradation through spatial constriction of the area of conjunctive use would be expected to become more rapid with increase in initial groundwater salinity, because of the greater mass of salt per unit of groundwater transported into the conjunctive use area. As the groundwater quality improves outside the area of conjunctive use but within the area of influence of the pump (i.e. the area $(1-U)A_1$), the rate of groundwater degradation will slow down in the area with conjunctive use (UA_1).

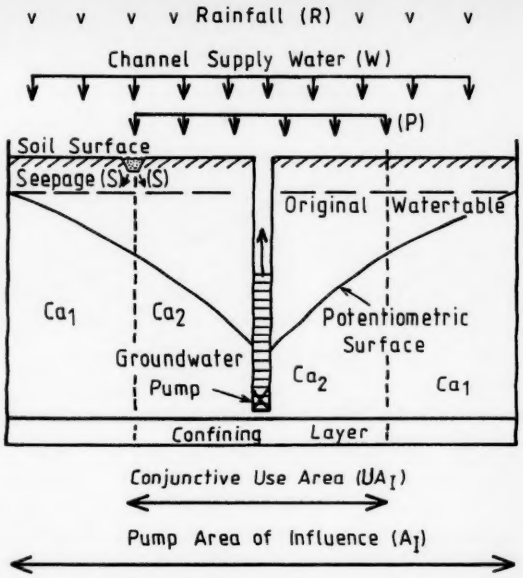

Fig. 4. Conceptual model for spatially constricted conjunctive water use from an unconfined aquifer

The rate of degradation described by Eq. (9) depends on the applied water depth both inside and outside the area of conjunctive use, but within the area of influence of the groundwater pump. In developing the model, the volume of groundwater is assumed constant, so that the depth of groundwater pumped (P) from the area $(1-U)A_1$ outside the conjunctive use area is equal to groundwater recharge in that area as described by Eq. (5). The salinity of groundwater outside the conjunctive use area, C_{a1}, can be described by Eq. (6), which is an expression for groundwater salinity where drainage water is pumped but there is no conjunctive use on the soil surface above. Substituting Eq. (6) for C_{a1}, in the abbreviated form $a e^{-bt} + c$, and Eq. (5) for P into Eq. (9) yields:

$$\frac{dC_{a2}}{dt} = \frac{[a\exp(-b\cdot t)+c](1-U)[(W_1+R)\,LF+S]+U((W_2+S)\,C_w+RC_r)}{H\cdot\theta\cdot U}. \tag{10}$$

Integrating Eq. (10) and using the initial condition $C_{a2} = C_0$ at $t = 0$ yields:

$$C_{a2} = C_0 + \frac{\left\{c\cdot t + \frac{a}{b}[1-\exp(-b\cdot t)]\right\}\frac{(1-U)}{U}[(W_1+R)\,LF+S]+((W_2+S)\,C_w+RC_r)\,t}{H\cdot\theta}. \tag{11}$$

The rate of increase in groundwater salinity in the conjunctive use system in Fig. 4, dC_{a2}/dt, can be expressed by adding the salts entering the area from adjacent pumped groundwater, $(1-U)A_1$, to that from rainfall plus irrigation supply water applied and channel seepage in the area of conjunctive use, and dividing by the volume of groundwater under consideration. That is:

$$\frac{dC_{a2}}{dt} = \frac{PC_{a1}(1-U)A_1+((W_2+S)C_w+RC_r)UA_1}{H\theta UA_1}. \tag{9}$$

Equation (11) is an expression for groundwater salinity as a function of time under spatially constricted conjunctive use.

For full irrigation the depth of irrigation supply water, W_2, applied in the conjunctive use area depends on the volume of groundwater pumped from outside the conjunctive use area. Thus W_2 in Eq. (11) is a function of U. Such an expression for W_2 can be derived from the mass conservation of water and estimated crop water use for this system. For full irrigation, maximum crop evapora-

tion, $ET_m = 0.85\,E_p$, can be expressed as a function of channel supply water (W_2), groundwater pumped from the area of conjunctive use ($I \cdot LF + S$), the depth of water lost to leaching ($I \cdot LF$), in the area of conjunctive use, and the groundwater pumped from outside the area of conjunctive use, as expressed by Eqs. (5) and (8). The depth of water use can then be calculated by summing water volumes and dividing by the area of conjunctive use to yield:

$$ET_m = 0.85\,E_p = \frac{UA_1(W_2 + R + I \cdot LF + S - I \cdot LF) + \left[\frac{0.85\,E_p \cdot LF}{1-LF} + S\right](1-U)A_1}{UA_1}. \quad (12)$$

Rearranging terms to express W_2 in terms of U yields:

$$W_2 = 0.85\,E_p - \frac{(1-U)}{U}\left[\frac{0.85\,E_p \cdot LF}{1-LF} + S\right] - R - S. \quad (13)$$

Equation (13) can be used to calculate the applied depth of channel supply water required to be mixed with groundwater for maximum crop evapotranspiration in the area of conjunctive use in Eq. (11). Equation (8) can be used to estimate W_1 for Eq. (11). Partial irrigation is represented by use of a crop factor of 0.75 instead of 1 for Fig. 2. The predictions of Eq. (11) are then plotted in Fig. 5 with parameter values typical of the Shepparton Irrigation Region in the Murray Basin, Australia. Figure 5 illustrates that very rapid degradation is possible with low values of U, demonstrating the importance of distributing pumped groundwater over the entire area of influence of the groundwater pump.

The rate of groundwater degradation from spatially constricted conjunctive water use is higher with smaller depth of groundwater in the system, and with greater values of the leaching fraction. The rate of degradation is also greater with higher levels of initial groundwater salinity (see Eq. (11) and Fig. 5). Partial irrigation reduces the impact of spatially constricted conjunctive water use (Fig. 5) because of the reduction in leaching fluxes resulting from the reduction in I. Comparison of partial and full irrigation in Eq. (11) and Fig. 5 for the same value of LF underestimates the effect of partial irrigation since a reduction in I could also be expected to reduce LF.

Pumped groundwater salinity may increase excessively after some time due to the effect of spatial constriction of the area of conjunctive use. The increase could be counteracted by installation of another groundwater pump in the area of groundwater outside the area of conjunctive use, where groundwater salinity will be lower. Operation of the pump subsequently installed in the area of low salinity groundwater will then result in groundwater salt transport out of the area of higher salinity groundwater to the area around the pump. Problems with this strategy include the cost of exploration for additional suitable pump sites, the potential lack of available pumpable aquifers for pump relocation, and the lack of on-farm management control if the additional pump site exists beyond the farm boundary. Application of pumped groundwater over the whole of the area of influence of the groundwater pump after some period where there has been spatial constriction of conjunctive water use will also reverse the trend of increasing groundwater salinity caused by spatial constriction of conjunctive use.

Problems introduced by spatial constriction of conjunctive water use are likely to be greatest where groundwater salinity is marginal, or where surface water supplies are inadequate, and there is therefore greater incentive to pump groundwater to augment surface supplies. When groundwater is used over the whole of the area of influence of the groundwater pump, the depth of groundwater for conjunctive use equals the depth of recharge, which is usually a small component of the surface water budget. Conversely, if a substantial proportion of crop water use is supplied by pumped groundwater, a spatial constriction of conjunctive water is implied, and excessive degradation will occur.

Groundwater mixing

The salinity of pumped groundwater varies over time because of spatial variability in groundwater salinity and variations in travel time from the point of recharge to the

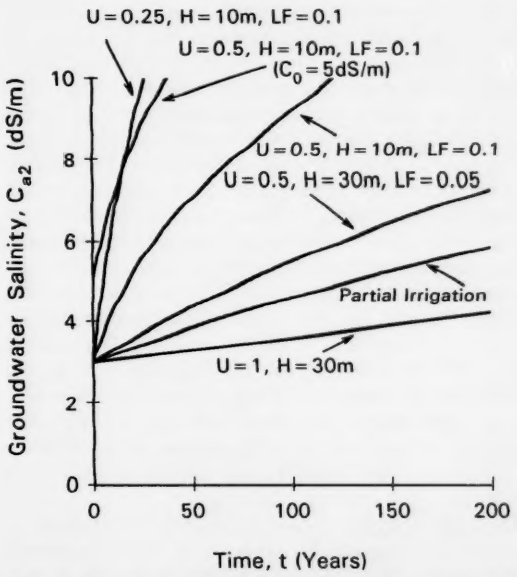

Fig. 5. Groundwater degradation from spatially constricted conjunctive water use. Plot of Eq. (11) with W_1 and W_2 described by Eqs. (8) and (13) respectively. Parameters nominated are: C_w = 0.1 dS/m, R = 0.45 m/y, C_r = 0.008 dS/m, S = 0.04 m/y, θ = 0.4. Plot represent full irrigation (E_p = 1.4 m/y) except where labelled "partial irrigation" (E_p = 0.7 m/y, H = 30 m, LF = 0.05)

pump screen. This variability will reduce over time as groundwaters mix. When a pump is installed in groundwater surrounded by better quality groundwater, pumped groundwater salinity will improve over time through mixing, and vice versa. When groundwater salinity is being assessed for conjunctive use, the total storage within the area of influence of the groundwater pump should be considered, so that the effects of mixing on groundwater degradation can be assessed.

Spatial variations in groundwater salinity will not affect the underlying processes of groundwater degradation already discussed, but it is possible that the resulting temporal variation in pumped groundwater salinity will mask these processes when field data is assessed. In some cases spatial variability in salinity may be so great that specific management strategies may be necessary to achieve optimal salinity control. For example, reduction in the pumped water depth through intermittent pumping, or reduction in recharge through partial irrigation, will increase the time taken for upper groundwaters to reach the pump screen. Such action could be beneficial in areas with higher groundwater salinity in the upper stratigraphy. However, intermittent pumping may result in some loss of leaching and perhaps productivity, as outlined by Prendergast et al. (1994). Where underlying groundwater is of poor quality a reduction in the rate of groundwater deterioration could be achieved by reducing the pumping rate, which reduces well drawdown and therefore the hydraulic gradient from deeper groundwater to the conjunctive use system.

Conjunctive water use incorporating limited export

The effect on groundwater salinity of off-site disposal of all drainage water was described in Fig. 3. Long term sustainability of conjunctive use is also affected if salt export is reduced and made equal to the mass of salt that enters the irrigation area with irrigation water and rainfall; this will be referred to as export for salt balance. Prendergast et al. (1994) suggest that export for salt balance has little effect on crop yield in the conjunctive use system in the short term, because this export usually constitutes only a small fraction of the groundwater pumped.

Equation (2) describes the effect of rainfall and irrigation salt inputs on groundwater salinity under conjunctive use; if export is equal to surface salt inputs for this case groundwater salinity remains constant. The rate of degradation from salt inputs from irrigation and rainfall depends on the depth (H) of the conjunctive use system (Fig. 2). Thus export for salt balance results in greater reduction in groundwater degradation when shallow aquifers are utilised (small H), and has little impact when H is large.

The effect of export for salt balance on the groundwater system described by Eq. (4) and Fig. 3 with positive G (which results in a rate of degradation less than that caused by irrigation water salt inputs) is to reduce groundwater salinity over time. For a negative value of G, referred to in the section "Upward leakage into the conjunctive use system", export for salt balance will reduce the rate of groundwater deterioration.

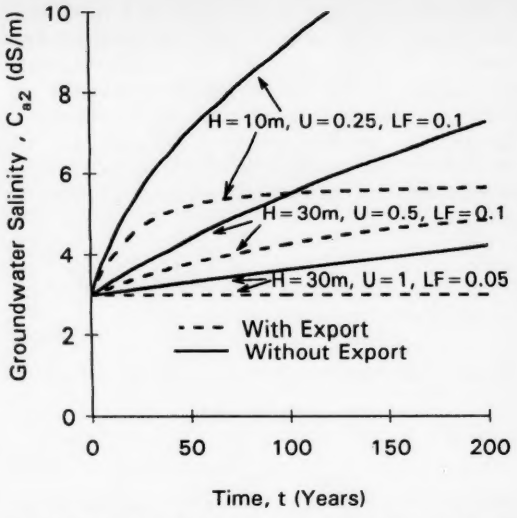

Fig. 6. The impact of salt export (made equal to the rate of surface salt additions) on spatially constricted conjunctive water use. Broken lines represent the conjunctive use system with export

The effect of off-site export for salt balance on the groundwater system described by Eq. (11) (spatially constricted conjunctive water use) can be assessed by subtracting the impact of export; the impact of export on C_{a2} can be quantified as the annual salt inputs from irrigation water and rainfall (i.e. $(W_1C_w+RC_r)(1-U)+(W_2C_w+RC_r)U$) divided by the water depth $H\theta$ and multiplied by t. Equation (11) has been plotted in Fig. 6 as a broken line, after subtraction of this expression for export from the right hand side of Eq. (11).

Export for salt balance has the effect of reducing groundwater degradation caused by spatially constricted conjunctive water use to zero in the long term, after initial rapid degradation. The time to reach this equilibrium depends on the depth (H) of the conjunctive use system. Equilibrium in the conjunctive use area occurs when the groundwater salinity within the area of influence of the groundwater pump, but outside the area of conjunctive use, comes into equilibrium with the salinity of groundwater recharge there (i.e. approaches steady state). Initial degradation from spatial constriction of conjunctive use depends on the difference between the depth weighted groundwater recharge salinity and C_0, and is therefore greater at higher levels of C_0, irrespective of export for salt balance. The difference between the final steady state groundwater salinity and the initial groundwater salinity in Fig. 6 is also greater for higher initial groundwater salinity and smaller values of U.

The rate of groundwater degradation depends on the depth of groundwater in the conjunctive use system (Eqs. (2), (4), (6) and (11)), spatial distribution of irrigation water and groundwater (Eq. (11)), the spatial relationship between the regional groundwater and the conjunctive use system and regional groundwater flows which determine G (Eq. (4)), groundwater mixing, water management (including regional redistribution of groundwater), dis-

posal, and the depth of non-leaching recharge (e.g. S in Eqs. (4), (6) and (11)). If groundwater degradation is to be minimised, management practices which influence these factors must be optimised; disposal for salt balance is insufficient to offset inappropriate groundwater management.

Problems likely to be encountered with export for salt balance include the downstream environmental costs when a river receives the effluent, the cost of drainage infrastructure, and difficulties in accurately calculating the salt mass for export from a groundwater pump, because this mass depends on the pump's area of influence, which may be difficult to determine. Difficulties in determining a pump's area of influence arise because of heterogeneity on local stratigraphy, and temporal variations in pumping and groundwater recharge rates and because of elements of confined aquifer behaviour; in locally confined aquifers, under constant pumping the area of influence expands over time until the recharge zone is reached.

Model testing and groundwater degradation in the Shepparton Irrigation Region

Since the advent of high watertables in the Shepparton region late in the 1970 decade, there has been a steady expansion in the area affected by salinity. A 640 ha project area was established at Tongala in 1981 to monitor the effects of conjunctive use of groundwater on productivity and salinity (Heuperman 1988). In the project area 90% of supplied irrigation water is applied to irrigated perennial pastures that support dairy production, which dominates irrigation water use in the Shepparton region. Conjunctive use of groundwater has been shown to result in considerable reduction in soil salinity in the area (Heuperman 1986).

Average groundwater degradation in the Tongala project area from irrigation water salt inputs and rainfall would be expected to be approximately 0.012 dS m^{-1} per year from Eq. (2), if a lower confining layer at 10 m is considered to be base of the groundwater streamlines. Pumped groundwater salinity has increased by approximately 0.07 dS m^{-1} per year over eight years of measurement (Prendergast and Heuperman 1988). Second order finite element modelling indicated that approximately 40% of the pumped groundwater volume flowed into the project area from outside the project boundary (H. Kleindienst pers. comm.). Difficulties encountered in the modelling included the allocation of appropriate boundary conditions and the obtaining of sufficient descriptive data. Equation (11) can be used to estimate groundwater degradation which could be expected if the lower confining layer is considered to be the base of the streamlines. Suitable parameters are $C_w = 0.1$ dS/m, $C_r = 0.008$ dS/m, $R = 0.45$ m, $\theta = 0.4$, $H = 10$ m, $C_0 = 3$ dS/m, $LF = 0.1$, $W_1 = 0.6$ m, $W_2 = 0.5$ m, $S = 0.04$, and $U = 0.6$. Evaluation of Eq. (11) using these values yields an average groundwater degradation of 0.1 dS/m/yr. It is difficult to assess the accuracy of this prediction given the long time scale of the processes involved, as illustrated in the previous section, and the short time scale of the measured data.

Discussion

Groundwater pump management

Aspects of groundwater pump installation and management can also have a substantial impact on groundwater degradation. The extent of the area of influence of the pump is not always easily determined because of heterogeneity, and many extend across farm boundaries. Farm boundaries can restrict the area of conjunctive use, but not A_1, so that reduced U and increased groundwater degradation can result (Eq. (11)). The depth of groundwater flow per unit area entering the conjunctive use area from outside is likely to be less when a network of pumps operates over a large area. A large area of conjunctive use means that the ratio between the perimeter of the area of influence and the area of influence is less than for an isolated pump.

For isolated pumps, reduction in groundwater flows into the conjunctive use system, and therefore a reduction in groundwater degradation (and an increase in U) could be achieved by intermittent pumping. This reduces the time that lower hydraulic potentials exist in the conjunctive use system and therefore reduces the depth of groundwater entering the system from outside the conjunctive use area. Intermittent pumping will, however, have the effect of restricting leaching which may result in increases in rootzone salinity, despite smaller surface applied salt loads (Prendergast et al. 1994).

Catchment management

Optimal salinity management of conjunctively used water can only be achieved through effective groundwater catchment management. The conjunctive use system is invariably part of a regional groundwater flow system, so that the boundary conditions for the conjunctive use system are affected by regional groundwater. Lateral flow can add or deplete salts from the pumped aquifer and therefore change groundwater salinity. Where regional scale recharge/discharge processes occur (Hubbert 1940; Fetter 1988), surface redistribution of pumped groundwater can enable some groundwater leakage to be maintained in the conjunctive use system over the whole irrigation region, if net groundwater outflows occur on average. In this way redistribution reduces excessive groundwater degradation where discharge from the regional groundwater to shallow aquifers occurs. Groundwater salinity in the conjunctive use system is then described by Eq. (4). Also, conjunctive water use relies on crop threshold salt tolerance to facilitate surface dispersion of groundwater without resulting in crop yield loss; groundwater redistribution can enable utilisation of crop threshold salinity tolerance over as large an area as possible (Prendergast et al. 1994).

Conjunctive use without groundwater export at the surface will probably result in higher regional soil and groundwater salinities which will approach a steady state only after thousands of years. The higher regional equilibrium will result in greater natural discharge of salts from the landscape in comparison to salt discharge at earlier times (as illustrated at a smaller scale by Eq. (4)). Greater

salt discharge will occur through both regional groundwater outflows and surface runoff to rivers. It is impossible to assess what the increases in regional salt storage are likely to be, and whether changes in agricultural practices and salt discharge from the landscape will be sufficient to offset the effects of higher salinity over these long time scales.

The implications of conjunctive water use for the long term could also be evaluated by assuming there is no increase in salt discharge from an irrigation region over time. In the Shepparton region, for example, there is net natural flow out of the groundwater system, although local aquifers can experience either recharge to or discharge from deeper aquifers. There is potential for increases in salt storage within both the shallow and deep aquifer systems. The effect of utilising this storage to reduce salt accumulation on the soil surface, on a regional scale, can be illustrated by a simple example which approximates conditions in the Shepparton region. If the irrigation area comprises 0.5 M ha and has average values of $H = 100$ m, $\theta = 0.4$ and $C_a = 3$ dS/m, the mass of salt storage equals $(0.5 \times 10^6 \times 10^4)$ m$^2 \times 100$ m $\times 0.4 \times (3 \times 0.6/1000) = 3.6 \times 10^8$ t, by using the generally accepted approximation 1 dS/m = 600 mg/l. If the irrigation area has a net salt addition of 50,000 t/y (as is approximately the case with the Shepparton region), the resulting percentage increase in regional salt storage in 100 years is approximately $(5 \times 10^4 \times 100/3.6 \times 10^8) \times 100$, or 1.4%. Conversely, export of 50,000 t/y of salt from the region will reduce regional salt storage by 1.4% after 100 years, in comparison to having no export available. The effectiveness of conjunctive water use in this case will, therefore, ultimately be determined by integrated land and water management, which governs the distribution of salts in the landscape and the groundwater systems, and can prevent excessive salt accumulation in the rootzone.

Conclusions

Under optimal land and water management, salinity at the base of the rootzone in a conjunctive use system will ultimately be determined by net groundwater flows out of an irrigation area, if there is no export of salt (Eq. (4) and Fig. 3). Because irrigation regions usually have some net natural groundwater outflows, groundwater degradation to higher equilibrium salinity occurs slowly over many centuries, if good management of the groundwater catchment is maintained. Good salinity management of the groundwater catchment includes strategies such as:

(a) Distribution of groundwater over the entire area of influence of a groundwater pump. Pumping groundwater to obtain a water depth greater than recharge, to augment irrigation, will induce faster degradation and can be contrary to good salinity management (Fig. 5).

(b) Utilisation of maximum depth of stratigraphy for salt storage through deep installation of groundwater pumps (Fig. 1). Increasing the depth of groundwater for salt storage reduces the detrimental effects of salt inputs from rainfall and irrigation (Fig. 1), discharge from the regional groundwater, groundwater mixing and spatial constriction of conjunctive use (Fig. 5). Deep installation must be weighed up against adverse affects of poorer control of waterlogging and of groundwater mixing if the deeper stratigraphy contains layers of poor quality groundwater.

(c) Reduction of salt inputs from irrigation water, achieved through partial irrigation and reduction in irrigation intensity (Fig. 1). Partial irrigation increases the area which can be irrigated. Partial irrigation also reduces the impact of spatial constriction of conjunctive water use (Fig. 5) by reducing leaching fluxes both through a reduction in total applied water and a probable reduction in the leaching fraction.

(d) Surface redistribution of pumped groundwater to minimise the effects of regional scale groundwater recharge/discharge conditions caused by heterogeneity in topography and hydrogeology. Installed pumps in a conjunctive use area can provide leaching for irrigation in distant areas, which results in high negative G in the conjunctive use area, and therefore excessive degradation, if there is no redistribution.

(e) Development of specific groundwater pump management strategies, such as intermittent pumping, in areas where groundwater mixing is likely to cause excessive degradation, or where only isolated pumps can be installed. These strategies must be developed in the context of local agricultural practices, climate and stratigraphy.

Artificial means of exporting saline groundwater out of the irrigated area also reduces groundwater degradation. However, export from each installed pump, equal to salt additions at the surface, can be costly in terms of infrastructure and downstream environmental impact, and may only significantly affect groundwater degradation where just shallow aquifers can be used to control salinity. Where groundwater salinity is too high for conjunctive use, groundwater export will be necessary if maximum productivity is to be maintained.

Data to adequately describe groundwaters in detail for a specific site are difficult and costly to obtain. This is especially the case where high spatial variability in stratigraphy exists, such as is the case in the fluviolacustrine deposits of the Murray Basin. Because of the long time scale of the processes involved, at least several decades of intensive in-situ measurements will be required for better model validation. Nevertheless, the basic principles of mass conservation of salt and water can be applied as illustrated to provide management guidelines to enable sustainable conjunctive water use.

References

Brown CM (1985) Murray Basin, South Eastern Australia: Stratigraphy and resource potential – a synopis. Bur Mineral Resour, Canberra, Aust, Rep 264

Brown CM, Stephenson AE (1986) Murray Basin subsurface stratigraphic database. Bur Mineral Resour, Canberra, Aust, Rep 262, 60 p

Domenico PA (1972) Concepts and models in groundwater hydrology. McGraw-Hill, 405 p

Doorenbos J, Pruit WO (1977) Crop water requirements. FAO Irrig and Drain Paper 24. FAO Rome 1984

Evans WR (1988) Preliminary shallow groundwater and salinity map of the Murray Basin. Bur Min Resour, Canberra, Australia

Fetter CW (1988) Applied Hydrogeology. Merrill Publishing Company, Columbus, Ohio USA, 43216, 592 p

Freeze RA, Witherspoon PA (1967) Theoretical analysis of groundwater flow. 2. The effect of watertable configuration and subsurface permeability variation. Water Resources Res 3:623–634

Heuperman AF (1986) The Tongala groundwater pumping and reuse project. Res Report No 17, Dept of Agric and Rural Affairs, Melbourne, Aust, pp 1–24

Heuperman AF (1988) The Tongala groundwater pumping and reuse project: a pilot study for groundwater table control in the Shepparton Region in Northern Victoria. Agric Water Manag 14:513–523

Hubbert MK (1940) The theory of groundwater motion. J Geol 48:785–944

Ife D (1988) Hydrogeological mapping of the upper Shepparton Formation, Shepparton Region. Report No 1988/29, Rural Water Commission, Melbourne, Aust, 41 p

Lawrence CR, Abele C (1976) Tertiary Murray Basin. In: Douglas JG, Ferguson JA (eds) Geology of Victoria. Spec Publn Geol Soc Aust 5:191–198

Macumber PG (1991) Interactions between groundwater and surface systems in Northern Victoria. Dept Conservation and Environment, Melbourne, Aust

Murray Darling Basin Ministerial Council (1987) River salinity waterlogging and land salinisation – towards an integrated management strategy. Tech Rep No 87/1, Canberra, Aust, 90 p

Nolan J, Reid M (1989) The role of the deep lead pumping for salinity control and resource development within the Shepparton region. Rural Water Comm Rep No 1989/11, 33 p

Prendergast JB (1989) Mallee groundwater. In: Noble J, Bradstock J (eds) Mediterranean Landscapes in Australia: Mallee Ecosystems and their Management. CSIRO, Melbourne, Aust, pp 54–79

Prendergast JB, Heuperman AF (1988) Groundwater pumping/reuse in N. Victoria: recharge processes, aquifer salinisation and farm productivity. BMR J Aust Geol Geophys, Groundwater 12:149–154

Prendergast JB, Noble CL (1990) The effect of groundwater reuse on infiltration and groundwater recharge under an irrigated perennial pasture. Proc Murray-Darling 1990 Workshop: Groundwater Research and Management. Mildura, 13–15 Nov 1990. NSW Dept Wat Resour Rep 90.038, Sydney, Aust

Prendergast JB, Rose CW, Hogarth WL (1994) A model for conjunctive use of groundwater and surface waters for control of irrigation salinity. Irrig Sci 14:187–197

Salinity Program Advisory Council (1989) Draft Shepparton land and water salinity management plan. Govt of Vic, Melbourne, Aust, 151 p

Todd DK (1980) Groundwater hydrology. J Wiley and Sons, Inc, New York, London, 33 p

Irrig Sci (1994) 14:189–198

Irrigation Science
© Springer-Verlag 1994

Kinematic-wave model for soil-moisture movement with plant-root extraction

V. P. Singh [1], **E. S. Joseph** [2]

[1] Department of Civil and Environmental Engineering, Louisiana State University, Baton Rouge, LA 70803-6405, USA
[2] Department of Civil Engineering, Southern University, Baton Rouge, LA 70813, USA

Received: 23 September 1992

Abstract. A kinematic-wave model is developed for simulating the movement of soil moisture in unsaturated soils with plants. The model involves three free boundaries. Analytical solutions are derived when the plant roots are assumed to extract moisture at a constant rate and the upstream boundary condition is independent of time. Numerical solutions are the only resort when the moisture extraction and the upstream boundary condition both depend on time.

Much of the mathematical treatment of flow in unsaturated porous media has dealt with capillary-induced flow (Smith 1983). However, there exists a multitude of cases where gravity dominates vertical movement of soil moisture. Some examples include: drainage following infiltration, the water percolation deeper into the soil, the vertical movement of moisture in relatively porous soils when rainfall or surface fluxes are typically of the order of, or less than, the soil-saturated hydraulic-conductivity, to name but a few. For treatment in such cases, the kinematic-wave theory is simple yet reasonably accurate.

Although Sisson et al. (1980) applied the kinematic-wave theory to internal drainage, Smith (1983) was probably the first to apply the theory to develop a complete kinematic-wave model for soil moisture movement. Charbeneau (1984) extended Smith's work to solute transport, and Charbeneau et al. (1989) to multiple solute transport. In a series of papers, Germann and coworkers (Germann 1985; Germann and Beven 1985, 1986; German et al. 1987) extended the application of the theory to infiltration and drainage into and from soil macropores, as well as to microbial transport. Yamada and Kobayashi (1988) discussed the kinematic wave characteristics of vertical infiltration and soil moisture, with the aid of field observations on tracers. They concluded that the vertical infiltration of soil moisture had the characteristics of kinematic waves.

Correspondence to: V. P. Singh

In this study, a kinematic-wave model is formulated for soil-moisture movement with plant-root extraction. Analytical solutions are derived under the condition that the moisture extraction by plants and the surface flux are both constant in time. This condition is severe, but leads to intriguing and useful results. For more realistic conditions numerical solutions are the only resort, these together with field verification, will be reported in the near future.

Kinematic-wave model

Formulation

For vertical unsaturated flow with plant-root extraction and with the neglect of the flow of air, the governing equations are the law of conservation of mass and a flux law. The one-dimensional conservation of mass equation or the continuity equation can be expressed as

$$\frac{\partial \theta}{\partial t} + \frac{\partial q}{\partial z} = -e(z, \tau) \tag{1}$$

where θ is the volumetric moisture content (dimensionless, volume of water/volume of soil), q is the vertical flux of soil moisture (L/T), $e(z, \tau)$ is the rate of soil moisture loss due to plant-root extraction at time t ($1/T$), z is the depth (L) measured downward from the ground surface, τ is the time (T) that water has stayed at location $\tau = t - w(z)$, $w(z)$ is the time history of the moisture advance front, and t is time (T). At a fixed τ, $e(\tau)$ is essentially the rate of plant-root extraction of soil moisture on a unit depth basis defined as

$$\frac{r(z, \tau)}{n} = e(z, \tau) \tag{2}$$

where n is the soil porosity, and $r(t)$ is the soil-moisture extraction rate per unit depth at time t ($1/T$). It may, however, be reasonable to assume $e(z, \tau) = e(\tau)$. This assumption implies spatially uniform extraction, that may be true if the plant roots are uniformly developed in the soil.

The flux law for a kinematic-wave model can be expressed as

$$q(\theta) = K(\theta) \tag{3}$$

where $K(\theta)$ is the unsaturated hydraulic conductivity (L/T) as a function of the soil-moisture content. A variety of expressions have been proposed for $K(\theta)$ (Hsu and Liu 1990). Of all the expressions, the best-known perhaps is the Brooks-Corey relation (Brooks and Corey 1964) which can be written as

$$K(\theta) = K_s\left(\frac{\theta - \theta_0}{\theta_s - \theta_0}\right)^a \tag{4}$$

where K_s is the saturated hydraulic conductivity (L/T), θ_0 is the residual value of θ below which water cannot be extracted (or moved) by capillary forces, θ_s is the saturated water content = porosity = n, and a is a parameter typically between 3 and 4, and is related to the pore-size distribution index.

In Eq. (1), τ is unknown and a relation is needed whereby τ can be determined. With such a relation, the formulation of the kinematic-wave model will be complete. To that end, when water is applied to the soil at its surface, it infiltrates into the soil and advances vertically downward, increasing the moisture content. If the soil is initially dry, the advance front, also called the shock front, will define the interface between moist and dry parts of the soil matrix. Let $z = s(t)$ or $t = w(z)$ be the time history of that advancing front; this time history gives the space-time coordinates of the shock front. The front is a free boundary and has to be determined along with the solution. An equation for $z = s(t)$ or $t = w(z)$, therefore, has to be formulated. This can be accomplished by observing that

$$u(\theta) = u(z, t) = \frac{q(\theta)}{\theta} = \frac{K(\theta)}{\theta} \tag{5}$$

where $u(\theta)$ is the average velocity with which θ moves. Thus, the free-boundary equation is obtained by replacing z by $s(t)$ or t by $w(z)$ in $u(z, t)$ as

$$\frac{ds(t)}{dt} = u(s(t), t) = \frac{K(\theta(s(t), t))}{\theta(s(t), t)}, \quad s(0) = 0 \tag{6}$$

or

$$\frac{dw(z)}{dz} = [u(z, w(z))]^{-1} = \frac{\theta(z, w(z))}{K(\theta(z, w(z)))}, \quad w(0) = 0\,. \tag{7}$$

Equation (6) is valid for $\theta(z, t) > 0$. Equations (6) and (7) require the advance front to move with the speed immediately behind the front.

The kinematic-wave model formulation consists of a partial differential Eq. (1), an algebraic Eq. (3), and an ordinary differential Eq. (6) or (7) with two unknowns $\theta(z, t)$ and $s(t)$ or $w(t)$. In order to derive solutions of these equations, the following can be assumed:

$$\theta(z, 0) = f(z), \quad z \geq 0\,, \tag{8}$$

$$\theta(0, t) = g(t), \quad 0 \leq t < T \tag{9}$$

$$= \theta_0, \quad t \geq T$$

where T is the duration for which moisture is applied at the upstream boundary. Note that $g(0) = f(0) = \theta_0$.

Equations (1) and (3) can be combined to produce

$$\frac{\partial\theta}{\partial t} + \frac{dK(\theta)}{d\theta}\frac{\partial\theta}{\partial z} = -e(z, \tau)\,. \tag{10}$$

For notational simplicity, let

$$M(\theta) = \frac{\mathrm{d}K(\theta)}{d\theta} = \frac{\partial\theta/\partial t}{\partial\theta/\partial z} = \left.\frac{\partial z}{\partial t}\right|_{\theta = \text{constant}} \tag{11}$$

which is referred to as the mobility of water in soil by Irmay (1956); this is analogous to celerity, commonly used in open channel flows.

Solution

Equation (10) is satisfied in the domain bounded by the positive t axis and the curve $t = w(z)$ or $z = s(t)$. Solution of Eqs. (10) and (6) can be derived by using the method of characteristics. Accordingly, one can choose σ as the parameter on the t-axis and t as the parameter along the characteristics. The characteristics originate from the t-axis on the segment $0 \leq t \leq T$. The solution domain can be divided into two subdomains D_1 and D_2, with the characteristics $z(t, T)$ serving as the dividing line (called the bounding characteristic), as shown in Fig. 1. The characteristic curves $z(t, \sigma)$, $\theta(t, \sigma)$ passing through the points $(0, \sigma, g(\sigma))$ in the (z, t, θ) space, satisfy

$$\frac{d\theta(t, \sigma)}{dt} = -\sigma(\tau), \quad \theta(\sigma, \sigma) = g(\sigma)\,, \tag{12}$$

$$\frac{dz(t, \sigma)}{dt} = M(t, \sigma), \quad z(\sigma, \sigma) = 0\,. \tag{13}$$

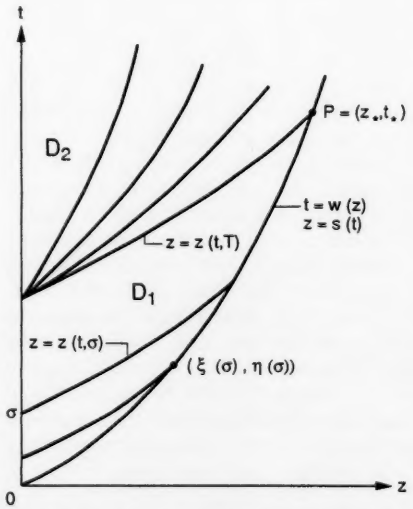

Fig. 1. Characteristic solution domain for unsaturated flow with plant-root extraction

$z(t, \sigma)$ is the position at time t of the soil-moisture content θ which was at $z = 0$ and at $t = \sigma$; $\theta(t, \sigma)$ is the soil-moisture content at time t. The plant-root extraction rate depends upon the nature of vegetation and availability of soil moisture. If $e(\tau)$ is constant, which is not entirely unreasonable, especially when the soii-moisture is not limiting plant root extraction, then $e(\tau) = e$.

Depending upon the nature of the function $g(t)$, three cases can be distinguished: (1) $g(t)$ = constant, (2) $dg(t)/dt < 0$, and (3) $dg(t)/dt > 0$. To describe the variation of soil moisture in time at a fixed z or in space at a fixed t, one may determine $\partial\theta/\partial z$ and $\partial\theta/\partial t$.

Solution for domain D_1

This domain is bounded by $0 \le t \le T$, $z(t, T)$, and $z = s(t)$. Solution of Eq. (12) is

$$\theta(t, \theta) = g(\sigma) - (t - \sigma)\, e\,. \tag{14}$$

Substitution of Eq. (14) in Eq. (13), and then integration yields

$$z(t, \sigma) = \int_{\sigma}^{t} M(g(\sigma) - (t - \sigma)\, e)\, dt\,. \tag{15}$$

With the use of Eq. (4),

$$M(\theta) = \frac{K_s a}{(\theta_s - \theta_0)} \left(\frac{\theta - \theta_0}{\theta_s - \theta_0}\right)^{a-1}. \tag{16}$$

Substitution of Eq. (14) in Eq. (16) yields

$$M(\theta, \sigma) = \frac{a K_s}{(\theta_s - \theta_0)} \left[\frac{g(\sigma) - (t - \sigma)\, e - \theta_0}{\theta_s - \theta_0}\right]^{a-1}. \tag{17}$$

With the use of Eq. (17), Eq. (15) leads to

$$z(t, \sigma) = \frac{K_s}{e} \left\{\left[\frac{g(\sigma) - \theta_0}{\theta_s - \theta_0}\right]^{a} - \left[\frac{g(\sigma) - (t - \sigma)\, e - \theta_0}{\theta_s - \theta_0}\right]^{a}\right\}. \tag{18}$$

Equations (14) and (18) constitute the characteristic solution for domain D_1. By eliminating σ between these equations, θ can be expressed as a function of z and t. To do that, $z(t, \sigma)$ must be, for fixed t, either an increasing function of σ or a decreasing function of σ. Differentiating Eq. (18) with respect to σ yields

$$z_\sigma(t, \sigma) = \frac{\partial z(t, \sigma)}{\partial \sigma} = \frac{a K_s}{e(\theta_s - \theta_0)} \left\{g'(\sigma) \left\{\left[\frac{g(\sigma) - \theta_0}{\theta_s - \theta_0}\right]^{a-1} - \left[\left(\frac{g(\sigma) - \theta_0}{\theta_s - \theta_0}\right)^{a} - \frac{e z}{K_s}\right]^{(a-1)/a}\right\} - e\left[\left(\frac{g(\sigma) - \theta_0}{\theta_s - \theta_0}\right)^{a} - \frac{e z}{K_s}\right]^{(a-1)/a}\right\} \tag{19}$$

or

$$z_\sigma(t, \sigma) = \frac{a K_s}{(\theta_s - \theta_0)^a} \{g'(\sigma)[(g(\sigma) - \theta_0)^{a-1} - (\theta(t, \sigma) - \theta_0)^{a-1}] - e(\theta(t, \sigma) - \theta_0)^{a-1}\}. \tag{20}$$

It is seen from Eq. (20) or (19) that $g'(\sigma) = dg/d\sigma \le 0$ is a sufficient condition for $z_\sigma(t, \sigma) < 0$. The condition $g'(\sigma) \le 0$ includes the case of principal interest to us, namely, $g(\sigma)$ = constant.

Case 1. $g(t)$ = constant: If $g(\sigma) = \theta_u$, then Eq. (18) becomes

$$z(t, \sigma) = \frac{K_s}{e} \left\{\left[\frac{\theta_u - \theta_0}{\theta_s - \theta_0}\right]^{a} - \left[\frac{\theta_u - (t - \sigma)\, e - \theta_0}{\theta_s - \theta_0}\right]^{a}\right\}. \tag{21}$$

By coupling Eqs. (41) and (21), θ can be expressed as a function of z and t as

$$\theta(z) = \theta_0 + (\theta_s - \theta_0) \left\{\left[\frac{\theta_u - \theta_0}{\theta_s - \theta_0}\right]^{a} - \frac{e z}{K_s}\right\}^{1/a}. \tag{22a}$$

It is seen that in domain D_1, θ is a function of z and does not depend on t. The soil moisture profile is nonuniform but steady-state. In Eq. (22a), there are two terms within braces. The second term is due to water uptake and the first term is due to the boundary flux. If $e = 0$, then $\theta(z) = \theta_u$. The nonuniformity of soil moisture is a direct consequence of the plant-root extraction. If e were zero, then θ would be independent of z. Thus, the alteration of the soil moisture profile is caused by plant roots. Of course, the degree of alteration depends on the value of e. On a short-time scale, the value of e is relatively small in field. Equation (22a) can be written with use of Eq. (4) as

$$\theta(z) = \theta_0 + (\theta_s - \theta_0) \left(\frac{K(\theta_u)}{K_s}\right)^{1/a} \left\{1 - \frac{e z}{K(\theta_u)}\right\}^{1/a}. \tag{22b}$$

In many practical cases, $e z / K(\theta_u)$ is much less than 1, and attenuation of the θ-profile, as a result, will be small. When Eq. (22a) is inserted into Eq. (4), the soil-moisture flux, with the aid of Eq. (3), is obtained:

$$K(\theta) = q(z) = K_s \left\{\left[\frac{\theta_u - \theta_0}{\theta_s - \theta_0}\right]^{a} - \frac{e z}{K_s}\right\}. \tag{23}$$

Similarly, the average velocity of the soil-moisture movement is obtained by substituting Eq. (22) in Eq. (5),

$$u(z) = \frac{K_s \left\{\left[\frac{\theta_u - \theta_0}{\theta_s - \theta_0}\right]^{a} - \frac{e z}{K_s}\right\}}{\theta_0 + (\theta_s - \theta_0) \left\{\left[\frac{\theta_u - \theta_0}{\theta_s - \theta_0}\right]^{a} - \frac{e z}{K_s}\right\}^{1/a}}. \tag{24}$$

Similarly, substitution of Eq. (22) in Eq. (16) yields the mobility of water:

$$M(\theta) = \frac{a K_s}{(\theta_s - \theta_0)} \left\{\left[\frac{\theta_u - \theta_0}{\theta_s - \theta_0}\right]^{a} - \frac{e z}{K_s}\right\}^{(a-1)/a}. \tag{25}$$

The behavior of the soil moisture in this case can be fully described. From Eq. (22) at a fixed z, $z \ge 0$,

$$\frac{\partial \theta}{\partial t} = 0 \tag{26}$$

and at any t, $0 \le t < T$,

$$\frac{\partial \theta}{\partial z} = -\frac{e}{a K_s} (\theta_s - \theta_0) \left\{\left[\frac{\theta_u - \theta_0}{\theta_s - \theta_0}\right]^{a} - \frac{e z}{K_s}\right\}^{(1-a)/a}. \tag{27}$$

Equation (27) shows that at any depth within D_1, θ remains constant in time and at any time it decreases with increasing z from the ground surface. The gradient of θ increases with increasing z. This corresponds to the case of a wetting event.

Case 2. $dg(t)/dt < 0$: In this case, $\partial\theta/\partial z$ and $\partial\theta/\partial t$ are obtained from Eqs. (14) and (18) by noting that

$$\frac{\partial\theta}{\partial z} = \frac{\partial\theta/\partial\sigma}{\partial z/\partial\sigma}, \quad \frac{\partial\theta}{\partial t} = \frac{\partial\theta/\partial\sigma}{\partial t/\partial\sigma}. \tag{28}$$

To that end, with $g' = g'(\sigma) = \partial g(\sigma)/\partial\sigma$,

$$\frac{\partial\theta}{\partial\sigma} = g' + e, \tag{29}$$

$$\frac{\partial z}{\partial\sigma} = \frac{K_s}{e}\frac{a}{(\theta_s-\theta_0)}\left\{\left[\frac{g-\theta_0}{\theta_s-\theta_0}\right]^{a-1} g' - \left[\left(\frac{g-\theta_0}{\theta_s-\theta_0}\right)^a - \frac{ez}{K_s}\right]^{(a-1)/a}(g'+e)\right\}, \tag{30}$$

$$\frac{\partial t}{\partial\sigma} = 1 + \frac{g'}{e}\left\{1 - \left[\frac{g-\theta_0}{\theta_s-\theta_0}\right]^{a-1}\left[\left(\frac{g-\theta_0}{\theta_s-\theta_0}\right)^a - \frac{ez}{K_s}\right]^{(1-a)/a}\right\}. \tag{31}$$

Therefore, by dividing Eq. (29) by Eq. (30),

$$\frac{\partial\theta}{\partial z} = \frac{e(g'+e)(\theta_s-\theta_0)}{aK_s\left\{\left[\frac{g-\theta_0}{\theta_s-\theta_0}\right]^{a-1} g' - (g'+e)\left[\left(\frac{g-\theta_0}{\theta_s-\theta_0}\right)^a - \frac{ez}{K_s}\right]^{(a-1)/a}\right\}}. \tag{32}$$

It should be noted that in this characteristic method of solution, t was chosen as the parameter along characteristics. Therefore, in Eq. (18), z is the dependent variable, and σ is the independent variable. In order to obtain $\partial\theta/\partial t$, one can choose t as the dependent variable and z as the parameter along characteristics. The procedure, however, remains the same in both cases. Employment of t as the dependent variable results in

$$\frac{\partial\theta}{\partial\sigma} = g'(g-\theta_0)^{a-1}\left[(g-\theta_0)^a - \frac{ez}{K_s}(\theta_s-\theta_0)^a\right]^{(1-a)/a} \tag{32a}$$

and

$$\frac{\partial t}{\partial\sigma} = 1 - \frac{g'}{e}(g-\theta_0)^{a-1}\left[(g-\theta_0)^a - \frac{ez}{K_s}(\theta_s-\theta_0)^a\right]^{(1-a)/a}. \tag{32b}$$

By dividing Eq. (32a) by Eq. (32b),

$$\frac{\partial\theta}{\partial t} = \frac{eg'(g-\theta_0)^{a-1}\left[(g-\theta_0)^a - \frac{ez}{K_s}(\theta_s-\theta_0)^a\right]^{(1-a)/a}}{e - g'(g-\theta_0)^{a-1}\left[(g-\theta_0)^a - \frac{ez}{K_s}(\theta_s-\theta_0)^a\right]^{(1-a)/a}}. \tag{33}$$

The variation of θ with z for a fixed t can be analyzed from Eq. (32). If $e < g'(\sigma)$ then $\partial\theta/\partial z > 0$; that means that θ increases with increasing z. On the other hand, if $e = g'(\sigma)$, then θ is independent of z. This is also the case when $z \geq K_s/e\{(g-\theta_0)/(\theta_s-\theta_0)\}^a$. If $e > g'(\sigma)$ then θ decreases with z but can also have a complex variation. At a fixed z, the variation of σ can be analyzed with the aid of Eq. (33). If $g'(\sigma) = 0$, then θ is independent of t. If $g'(\sigma) < 0$, then θ decreases with time. If $e = g'(\sigma)$, then θ is a decreasing function. At $z = K_s((g-\theta_0)/(\theta_s-\theta_0))^a/e$, then

$$\frac{\partial\theta}{\partial t} = 0 \quad \text{and} \tag{34}$$

$$\frac{\partial\theta}{\partial z} = \frac{e(g'+e)(\theta_s-\theta_0)^a}{aK_s g'(g-\theta_0)^{a-1}}. \tag{35}$$

Equation (34) shows that θ becomes independent of t whereas Eq. (35) shows that as a function of z, θ decreases with z.

Case 3. $dg(t)/dt > 0$: This can be analyzed from Eqs. (32) to (35). However, Eq. (20) reveals that when $g'(\sigma) > 0$, $z_\sigma(t,\sigma) > 0$ and this case may entail shock formation. In that case, the analytical treatment becomes unwieldly and is not discussed in this paper.

Determination of advance front (free boundary of domain D_1)

In order to determine the shock front $t = w(z)$, it is convenient to express it in terms of the parameter σ introduced above. If one considers the characteristic curve $z(t,\sigma)$ in the (z,t) plane, then it will intersect the free boundary at the point denoted by $(\xi(\sigma), \eta(\sigma))$ as shown in Fig. 1. Therefore, $z = \xi(\sigma)$, $t = \eta(\sigma)$ is the parametric representation of the free boundary in terms of the parameter σ. For the case $g(t) = \theta_u = \text{constant}$, and $e(\tau) = e = \text{constant}$, determination of the free boundary is relatively simple. From Eq. (22), with t replaced by $\eta(\sigma)$,

$$z(\eta(\sigma),\sigma) = \xi(\sigma) = \frac{K_s}{e}\left[\left(\frac{\theta_u-\theta_0}{\theta_s-\theta_0}\right)^a - \left(\frac{\theta_u-(\eta(\sigma)-\sigma)e-\theta_0}{\theta_s-\theta_0}\right)^a\right]. \tag{36}$$

From Eqs. (6), (14) and (4), and noting that θ does not fall below θ_0,

$$\frac{ds(t)}{dt} = \frac{\xi'(\sigma)}{\eta'(\sigma)} = \frac{K(\theta(\xi(\sigma),\eta(\sigma)))}{\theta(\xi(\sigma),\eta(\sigma))} = \frac{K_s}{(\theta_s-\theta_0)}\left[\frac{\theta_u-(\eta(\sigma)-\sigma)e-\theta_0}{\theta_s-\theta_0}\right]^{a-1}. \tag{37}$$

Equations (36) and (37) can be solved for $\xi(\sigma)$ and $\eta(\sigma)$. To that end, Eq. (36) can be differentiated to yield

$$\xi'(\sigma) = \frac{aK_s}{(\theta_s-\theta_0)}\left[\frac{\theta_u-(\eta(\sigma)-\sigma)e-\theta_0}{\theta_s-\theta_0}\right]^{a-1}(\eta'(\sigma)-1). \tag{38}$$

On eliminating $\xi'(\sigma)$ between Eqs. (24) and (25),

$$\eta'(\sigma) = \frac{a}{a-1}, \quad \eta(0) = 0 \tag{39}$$

which gives

$$\eta(\sigma) = \frac{a}{a-1}\sigma. \tag{40}$$

Similarly, eliminating $\eta'(\sigma)$ between Eqs. (37) and (38) leads to

$$\xi'(\sigma) = \frac{K_s}{(\theta_s - \theta_0)} \frac{a}{(a-1)} \left[\left(\frac{\theta_u - \theta_0}{\theta_s - \theta_0} \right)^a - \frac{\xi e}{K_s} \right]^{(a-1)/a} \tag{41}$$

which gives

$$\xi(\sigma) = \frac{K_s}{e} \left\{ \left(\frac{\theta_u - \theta_0}{\theta_s - \theta_0} \right)^a - \left[\left(\frac{\theta_u - \theta_0}{\theta_s - \theta_0} \right) - \frac{e\sigma}{(\theta_s - \theta_0)(a-1)} \right]^a \right\}. \tag{42}$$

Equations (40) and (42) constitute the parametric representation of the free boundary. By eliminating σ between Eqs. (46) and (42), and noting that ξ corresponds to z and η to t. In terms of q,

$$z = \frac{K_s}{e} \left\{ \left(\frac{\theta_u - \theta_0}{\theta_s - \theta_0} \right)^a - \left[\left(\frac{\theta_u - \theta_0}{\theta_s - \theta_0} \right) - \frac{et}{a(\theta_s - \theta_0)} \right]^a \right\}, \tag{43}$$

$$z = \frac{q_0}{e} - \frac{K_s}{e} \left[\left(\frac{q_0}{K_s} \right)^{1/a} - \frac{et}{a(\theta_s - \theta_0)} \right]^a \tag{44}$$

where $q_0 = q(\theta_u)$. Equation (43) or (44) expresses the advance front. It is seen from Eq. (43) that the coordinates of the point to which the free boundary can extend is given by

$$t = \frac{a}{e}(\theta_u - \theta_0), \quad z = \frac{K_s}{e} \left(\frac{\theta_u - \theta_0}{\theta_s - \theta_0} \right)^a. \tag{45}$$

To complete the solution for domain D_1, the intersection of the bounding characteristic $z(t, T)$ and the free boundary $z = s(t)$ is to be determined. Let that point be $P = (z_*, t_*)$. This point can be determined explicitly by equating Eq. (21) with $\sigma = T$, $t = t_*$ and $z = z_*$ to Eq. (43) with $z = z_*$ and $t = t_*$; that results in

$$t_* = \frac{a}{a-1} T, \tag{46}$$

$$z_* = \frac{K_s}{e} \left\{ \left(\frac{\theta_u - \theta_0}{\theta_s - \theta_0} \right)^a - \left[\frac{(\theta_u - \theta_0)}{(\theta_s - \theta_0)} - \frac{eT}{(a-1)(\theta_s - \theta_0)} \right]^a \right\}. \tag{47}$$

For the case when $g(t)$ is not constant, we use the same parametric representation as before. Therefore, analogous to Eq. (36),

$$\xi(\sigma) = \frac{K_s}{e(\theta_s - \theta_0)^a} \{ [g(\sigma) - \theta_0]^a - [g(\sigma) - (\eta(\sigma) - \sigma)\, e - \theta_0]^a \} \tag{48}$$

and analogous to Eq. (37),

$$\frac{\xi'(\sigma)}{\eta'(\sigma)} = \frac{K_s}{(\theta_s - \theta_0)^a} [g(\sigma) - (\eta(\sigma) - \sigma)\, e - \theta_0]^{a-1}. \tag{49}$$

Differentiating Eq. (48) and then substituting the differential in Eq. (49) yield

$$\frac{d\eta}{d\sigma} + \frac{a}{e(a-1)} \frac{g'(\sigma)[g(\sigma) - \theta_0]^{a-1}}{[g(\sigma) - (\eta(\sigma) - \sigma)\, e - \theta_0]^{a-1}} = \frac{a}{e(a-1)} (g'(\sigma) + e), \quad \eta(0) = 0. \tag{50}$$

Equation (50) cannot, in general, be solved in terms of simple forms of $g(t)$, an analytical solution for $\eta(\sigma)$ is tractable. With substitution of this solution in Eq. (48), $\xi(\sigma)$ is obtained. If, however, $g'(\sigma) = 0$, Eq. (50) reduces to Eq. (39).

Another method to determine the advance front

The velocity of the front can be expressed as

$$\frac{ds(t)}{dt} = u(s(t), t) = \frac{q(\theta_2) - q(\theta_1)}{\theta_2 - \theta_1}. \tag{51}$$

Representing θ_1 by θ_0 and θ_2 by θ, and taking advantage of Eqs. (22) and (23), Eq. (46) can be written for the case $g(t) =$ constant, as

$$\frac{ds(t)}{dt} = \frac{K_s^{1/a}}{\theta_s - \theta_0} (q - ez)^{(a-1)/a} \tag{52}$$

which, when integrated, leads to

$$z = s(t) = \frac{q}{e} - \frac{K_s}{e} \left[\left(\frac{q}{K_s} \right)^{1/a} - \frac{te}{a(\theta_s - \theta_0)} \right]^a \tag{53}$$

which is the same as Eq. (44).

Solution for domain D_2

Domain D_2 is bounded by $T \le t$, $z = z(t, T)$, $z = s(t)$ beyond the point $p = (z_*, t_*)$. In this case, $\theta(0, t) = \theta_0$ for $t \ge T$; $\theta_0 < \theta_u$. Let $g(t, \varepsilon)$ be a continuous function of t coinciding with $g(t)$ on $0 \le t < T$, $g(t, \varepsilon) = \theta_0$ on $t \ge T + \varepsilon$, as shown in Fig. 2. Then, it is seen from Eqs. (14) and (18) that the characteristics $z = z(t, \sigma, \varepsilon)$, $T \le \sigma \le T + \varepsilon$, cover the region above $z = z(t, T)$ completely.

$$z(t, \sigma, \varepsilon) = \frac{K_s}{e} \left\{ \left[\frac{\theta(t, \sigma, \varepsilon) + (t - \sigma)\, e - \theta_0}{\theta_s - \theta_0} \right]^a - \left[\frac{\theta(t, \sigma, \varepsilon) - \theta_0}{\theta_s - \theta_0} \right]^a \right\}. \tag{54a}$$

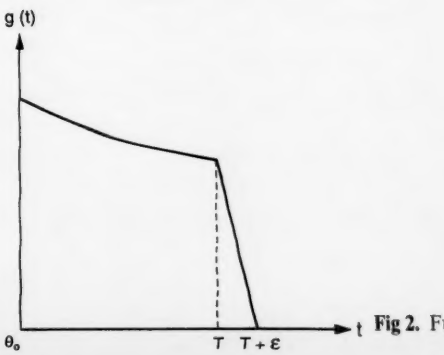

Fig 2. Function $g(t, \varepsilon)$

By letting $\varepsilon \to 0$ and $\sigma \to T$, one obtains

$$z(\theta, t) = \frac{K_s}{e}\left[\left(\frac{\theta + e(t-T) - \theta_0}{(\theta_s - \theta_0)}\right)^a - \left(\frac{\theta - \theta_0}{\theta_s - \theta_0}\right)^a\right]. \quad (54\,b)$$

This equation expresses the soil-moisture θ as a function of z and t in domain D_2; θ varies from θ_u to θ_0. The reduction in θ is caused by the plant-root extraction, and hence the water uptake is the dominant factor for variation of water content. This can be easily shown for a special case when a is an integer. To that end, Eq. (54b) can be written as

$$z(\theta, t) = \frac{K_s}{e}\left(\frac{\theta - \theta_0}{\theta_s - \theta_0}\right)^a \left\{\left[\frac{e(t-T)}{\theta - \theta_0} + 1\right]^a - 1\right\}. \quad (55\,a)$$

With use of the bionomial theorem, this can be written as

$$z(\theta, t) = \frac{K_s}{e}\left(\frac{\theta - \theta_0}{\theta_s - \theta_0}\right)^a \left\{\sum_{i=0}^{a-1}\binom{a}{i}\left(\frac{e(t-T)}{\theta - \theta_0}\right)^{a-i}\right\} \quad (55\,b)$$

$$= K_s\left(\frac{\theta - \theta_0}{\theta_s - \theta_0}\right)^a \left\{\sum_{i=0}^{a-1}\binom{a}{i}(e)^{a-i-1}\left(\frac{(t-T)}{\theta - \theta_0}\right)^{a-i}\right\}.$$

It is seen that each term in the series is affected by the plant-root extraction e raised to the power $(a-i-1)$. Assume that only the first term of the series is most significant. Then,

$$z(\theta, t) = K_s\left(\frac{\theta - \theta_0}{\theta_s - \theta_0}\right)^a a\, e^{a-1}\left(\frac{t-T}{\theta - \theta_0}\right)^a. \quad (55\,c)$$

Thus, the reduction in θ is primarily caused by water uptake.

The characteristics in domain D_2 are given by

$$z = \frac{K_s}{e}\left[\left(\frac{\theta_i - \theta_0}{\theta_s - \theta_0}\right)^a - \left(\frac{\theta_i - e(t-T) - \theta_0}{\theta_s - \theta_0}\right)^a\right] \quad (56)$$

where θ_i is the initial soil-moisture $\theta_0 < \theta_i < \theta_u$, that is carried out by the i-th characteristic.

Determination of free boundaries for domain D_2

Domain D_2 has two free boundaries FB2 and FB3 as shown in Fig. 3. Along FB3 that starts at $t = T$ and $x = 0$, $\theta(z, t) = \theta_0$; thus, this is the locus defined by θ_0. This is the time history of the drying front as it advances from $x = 0$. From Eq. (14), we have

$$\theta_0 = g(\sigma) - (t - \sigma)\, e, \quad T \le \sigma \le T + \varepsilon. \quad (57)$$

Thus, from Eq. (18), we obtain

$$z(t, \sigma, \varepsilon) = \frac{K_s}{e}\left[\frac{(t-\sigma)\, e}{\theta_s - \theta_0}\right]^a. \quad (58)$$

Letting $\varepsilon \to 0$, $\sigma \to T$, we get the free boundary FB3

$$z(t) = \frac{K_s}{e}\left[\frac{e(t-T)}{\theta_s - \theta_0}\right]^a. \quad (59)$$

Between $z = 0$ and Eq. (59), $\theta(z, t) = \theta_0$.

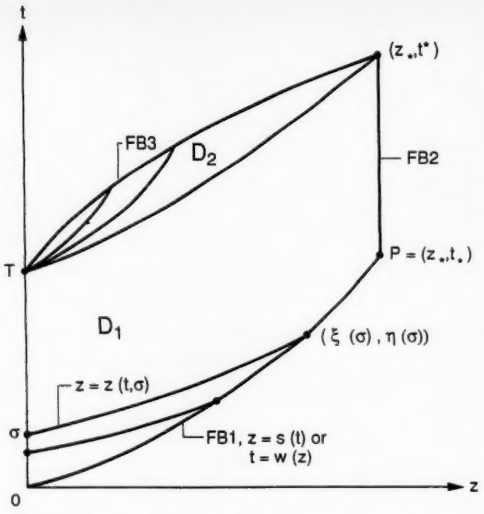

Fig. 3. Characteristic solution domain for the case $g'(t) = 0$, $0 \le t \le T$

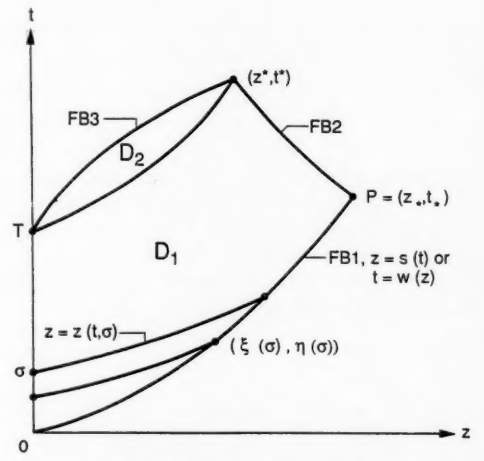

Fig. 4. Characteristic solution domain for the case when $e = \text{constant} > 0$, $-e < g'(t) < 0$, $0 \le t \le T$

It is seen from Eq. (56) that the maximum distance that the characteristics will travel is given by

$$z^* = \frac{K_s}{e}\left(\frac{\theta_u - \theta_0}{\theta_s - \theta_0}\right)^a \quad (60)$$

which is the same as given by Eq. (45). This shows that FB2 (the locus $\theta(z, t) = \theta_0$) is a vertical wall with lower end given by Eq. (45) and the upper end by Eq. (56) and

$$t^* = T + \frac{1}{e}(\theta_u - \theta_0). \quad (61)$$

In the case when $g(t)$ is not constant, we get the parametric representation of FB2:

$$z_{FB2} = \frac{K_s}{e}\left[\frac{g(\sigma) - \theta_0}{\theta_s - \theta_0}\right]^a, \quad (62)$$

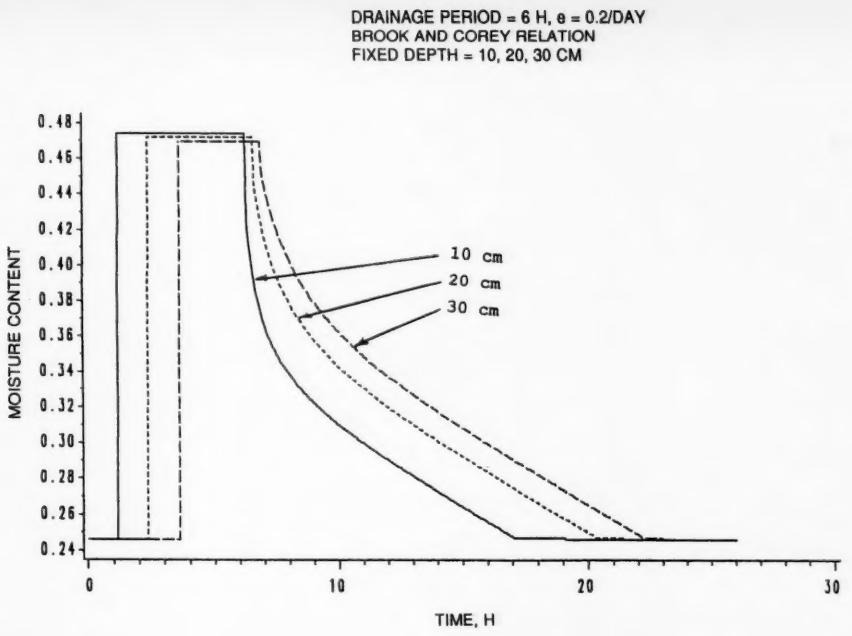

Fig. 5. Moisture content as a function of time for fixed values of depth

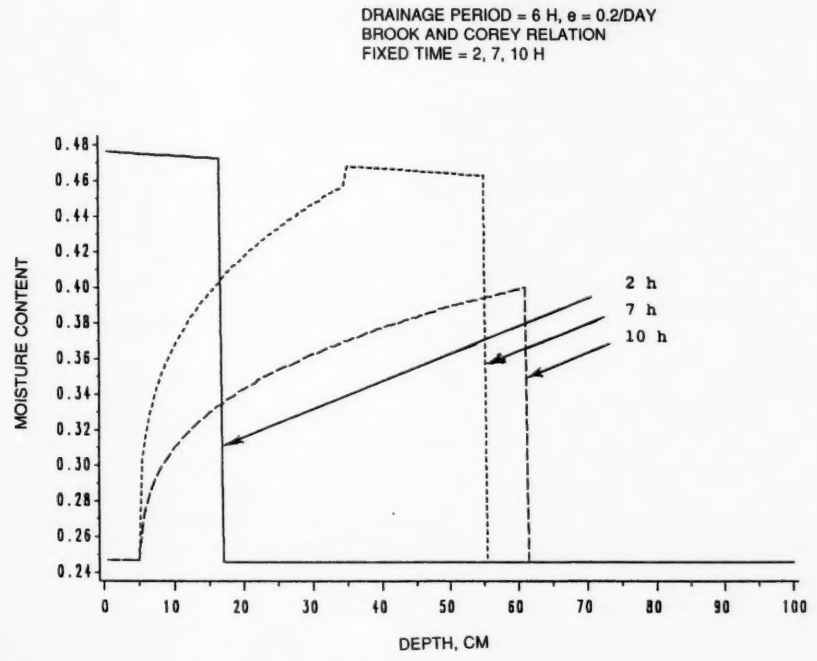

Fig. 6. Moisture content as a function of depth for fixed values of time

$$t_{FB2} = \sigma + \frac{g(\sigma) - \theta_0}{e}. \tag{63}$$

Thus

$$\frac{dz}{dt} = \frac{z'(\sigma)}{t'(\sigma)} = \frac{a K_s g'(\sigma)(g(\sigma) - \theta_0)^a}{(\theta_s - \theta_0)^a (e + g'(\sigma))}. \tag{64}$$

Since $g'(\sigma) \leq 0$, we have for FB2, $-e \leq g'(\sigma) \leq 0 \rightarrow dz/dt \leq 0$, and $g'(\sigma) < -e \rightarrow dz/dt > 0$. Under the condition $-e < g'(\sigma) < 0, 0 < \sigma < T$, the front wall of water recedes $(dz/dt < 0)$ when its moisture content is θ_0. In this case, the appearance of FB2 is as shown in Fig. 4. If $g'(\sigma) = 0$, $0 \leq \sigma \leq T$, the front wall of water is stationary $(dz/dt = 0)$, as shown in Fig. 3, when it has moisture content θ_0.

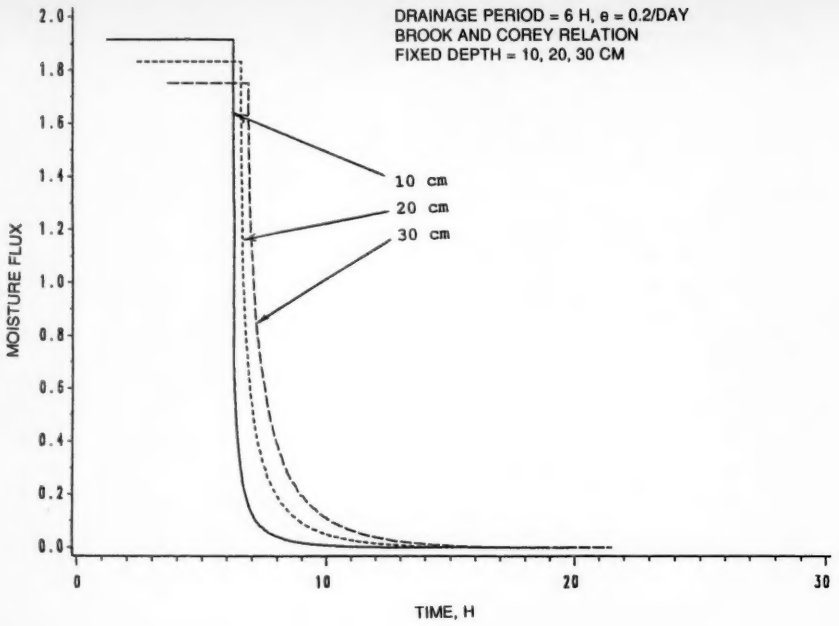

Fig. 7. Moisture flux as a function of time for fixed values of depth

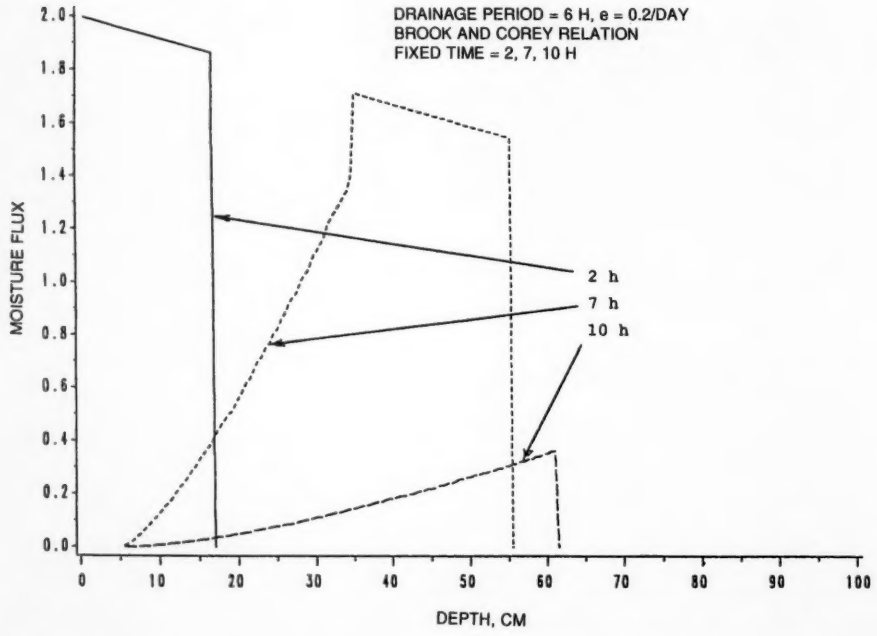

Fig. 8. Moisture flux as a function of depth for fixed values of time

Total moisture content

The total moisture content W varies within the region, and can be determined by integrating the moisture profile from $z = 0$ to a particular depth $z = L$. Let $L < z^*$. Referring to Fig. 1, at $t = 0$, the initial total moisture content $W_i = \theta_0 L$. For $0 < t < T$, say, $t = t_1$, when $g(t) =$ constant,

$$W = \theta_u z_1 + \theta_0 (L - z_1) \tag{65}$$

where z_1 is the point of intersection of $t = t_1$ and $z = s(t)$. For $t > t^*$,

$$W(t, L) = \int_0^L \theta(x, t)\, dz \tag{66}$$

where $\theta(z, t)$ is prescribed by Eq. (55). An explicit solution of this integral is, however, not tractable.

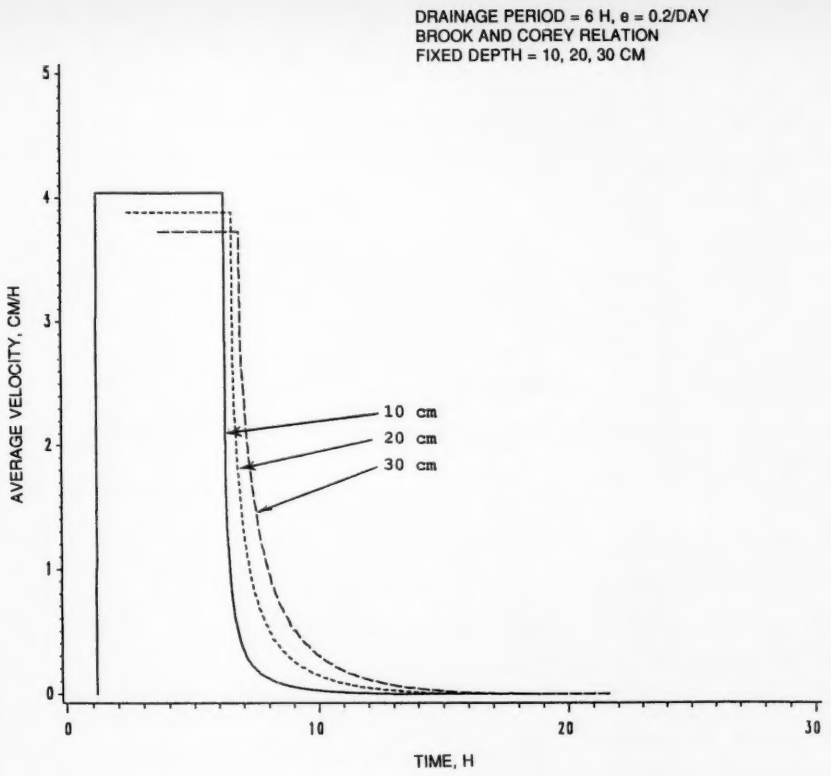

Fig. 9. Average velocity as a function of time for fixed values of depth

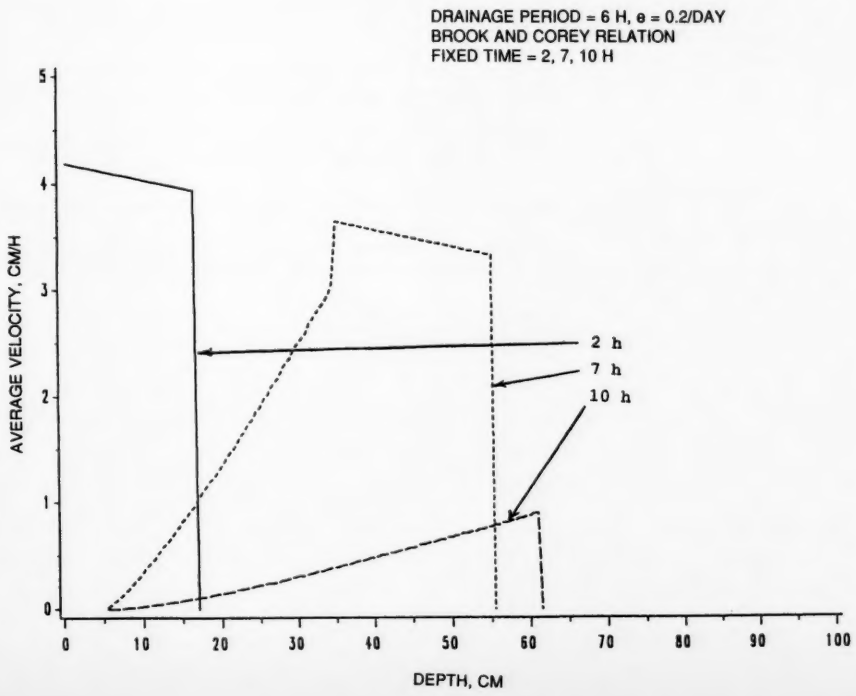

Fig. 10. Average velocity as a function of depth for fixed values of time

An example of application

A wetting event with moisture applied at the ground surface was considered, with $K(\theta)$ given by Eq. (4). The soil was Glendale clay loam, investigated by Sisson et al. (1980), with the following properties: $\theta_s = 0.52$, $\theta_0 = 0.246$, $K_s = 1$ m/day, and $a = 4.25$. The moisture was applied at the rate of 2 cm/h for 6 hours. These values were used by Charbeneau (1984). The plant-root extraction $e(t)$ was considered constant but values of $e = 0.1$, 0.2, 0.3, 0.4, and 0.5/day were considered. It should be emphasized that these values were used to illustrate the procedure presented in the paper. If $n = 0.52$, then $e = 0.1$/day would correspond to $r(t) = 0.052$/day. For one meter of soil column, this would translate into 5.2 mm of plant-root extraction for a day. Likewise, $e = 0.5$/day would yield $r(t) = 0.25$/day or 25 mm/day. This rate is clearly high but the objective here was to intentionally show the modulation of soil moisture profile by the plant-root extraction.

The kinematic wave model was applied to compute $\theta(z, t)$, $q(z, t)$, and $u(z, t)$. Then $\theta(t)$, $u(t)$ and $q(t)$ were obtained at selected values of z. Likewise, $\theta(z)$ and $q(z)$ were computed at selected values of t. For a sample case of $e = 0.2$/day, computations are illustrated. Figure 5 shows $\theta(t)$ at $z = 10$, 20, and 30 cm, and Fig. 6 shows $\theta(z)$ at $t = 2$, 7 and 10 h. The moisture profile has realistic appearance. The moisture flux is plotted as a function of t in Fig. 7, and as a function of z in Fig. 8. The average velocity is plotted as a function of t in Fig. 9, and as function of z in Fig. 10. Both q and u appear to be realistic in their variation. The effect of increasing e was to compress domain D_2. In other words, after the moisture flux was ended at the ground surface, the moisture profile returned to its initial state more quickly where the moisture extraction rate was higher. For higher e, the characteristics in domain D_1 were more curved.

Conclusions

The kinematic wave model for soil moisture movement has been formulated, and its solution domain involves three free boundaries. Analytical solutions are tractable for the case when the upstream boundary condition is independent of time. For a time-dependent boundary condition, numerical solutions are the only resort. In this model, the advancing front of water or wetting front is necessarily an advancing shock wave. It is plausible to assume that the moisture content at the wetting front is θ_0. Since the kinematic wave theory cannot account for this assumption, the diffusion wave model has to be employed in that case.

Acknowledgements. This study was supported in part by Army Research Office under the project "A Continuum Model for Streamflow Synthesis", Grant No. DAALO3-89-G-0116.

References

Brooks RH, Corey AT (1964) Hydraulic properties of porous media. Hydrology Paper 3, Colorado State University, Fort Collins, Colorado

Charbeneau RJ (1984) Kinematic models for soil moisture and solute transport. Water Resour Res 20:699–706

Charbeneau RJ, Weaver JW, Smith VA (1989) Kinematic modeling of multiphase solute transport in the vadose zone. EPA Report EPA/600/2-89/035, RS Kerr Environmental Research Laboratory, U.S. Environmental Protection Agency, Ada, Oklahoma

Germann P (1985) Kinematic wave approach to infiltration and drainage into and from soil macropores. Trans ASAE 28:745–749

Germann P, Beven K (1985) Kinematic wave approximation to infiltration into soils with sorbing macropores. Water Resour Res 21:990–996.

Germann PF, Beven K (1986) A distribution function approach to waterflow in soil macropores based on kinematic wave theory. J Hydrol 83:173–183

Germann PF, Smith MS, Thomas GW (1987) Kinematic wave approximation to the transport of Escherichia coli in the vadose zone. Water Resour Res 23:1281–1287

Hsu R, Liu CL (1990) Use of parameter estimation in determining soil hydraulic properties from unsaturated flow. Water Resour Manag 4:1–19

Irmay SE (1956) Extension of Darcy law to unsaturated flow through porous media. Proc Darcy Symposium, IASH-IUGG, Dijon, France

Sisson JB, Ferguson AH, van Genuchten MTh (1980) Simple method for predicting drainage from field plots. Soil Sci Soc Am J 44:1147–1152

Smith RE (1983) Approximate soil water movement by kinematic characteristics. Soil Sc Am J 47:3–8

Yamada T, Kobayashi M (1988) Kinematic wave characteristics and new equations of unsaturated infiltration. J Hydrol 102:257–266

Irrig Sci (1994) 14:199–205

Irrigation Science
© Springer-Verlag 1994

Thermal environment of cotton irrigated using canopy temperature

D. F. Wanjura, J. R. Mahan

USDA-Agricultural Research Service, Cropping Systems Research Laboratory, Lubbock, TX 79401, USA

Received: 5 February 1993

Abstract. The threshold canopy temperature method for controlling a drip irrigation system includes a physiologically based threshold temperature and irrigation application rate that responds to the environment. Energy input from the environment causes canopy temperature to exceed the threshold value and irrigation is then applied. This study evaluated temperature distributions, amount of optimum time, and the amount of irrigation control time for cotton where irrigation scheduling was controlled by different threshold temperatures during the years 1988 to 1991. Optimum time for cotton growth was defined as the accumulated time that canopy temperatures were between 25 and 31 °C and the time accumulated above different threshold temperatures was designated as irrigation control time. Threshold temperatures over a 26 to 32 °C range altered the frequency distribution of temperature within the optimum temperature range (25–31 °C) by reducing temperatures above the threshold. Frequency of canopy temperatures of a 28 °C threshold temperature treatment decreased in the 28 to 29 °C increment and then remained below air temperature. Irrigation control time was more sensitive than optimum time to changes in threshold temperature between 26 and 31 °C. Optimum time and irrigation control time of the 28 °C threshold temperature varied by 37% and 29%, respectively. Lint yields in 1988 and 1990 were high while those in 1989 and 1991 were low because of unfavorable weather. Irrigation amounts applied during DOY 198-273 that were above 20 cm in high yield years or 12 cm in low yield years did not increase yield.

Temperature significantly influences plant vegetative growth and phenological development. The metabolism of plants is affected by temperature in such a manner that there is an optimal thermal range for their growth and development (Burke et al. 1988). The existence of an optimal thermal range implies that some plant temperatures are more conducive to plant growth than others and that an increase in the amount of time that the plant is within the optimal range will result in increased plant growth.

Continuous measurement of canopy temperature and application of irrigation for 15-minute periods when a threshold temperature was exceeded has been demonstrated as an automated irrigation scheduling procedure for cotton using a drip irrigation system (Wanjura et al. 1992). Plant temperature is influenced by its water status (Idso et al. 1982; Grimes et al. 1987) which can be altered through irrigation. Two assumptions that are made in using canopy temperature for irrigation management are that, first, canopy temperatures above the threshold indicate inadequate plant water status and second plant growth or productivity are positively correlated with the amount of time that the plant's temperature is within its optimal thermal range.

Optimum time for crop production is a concept that recognizes there is a specific temperature where growth is maximized. A field grown crop does not grow under a constant temperature regime but rather in a fluctuating thermal environment. Burke et al. 1988 defined the thermal kinetic window for cotton as 23.5–32 °C. Earlier research by Arndt (1945) found that the optimum temperature for cotton growth was 27 °C after germinating for three days. An analysis of the thermal dependence of reaction velocity of the enzyme glutathione reductase from cotton showed that velocity was highest at 28 °C. In this paper an optimal thermal range of 25–31 °C was selected where reaction velocity is predicted to be within 33% of its maximum value. Thus the *optimum time* (OPT) for cotton is the time that the canopy temperature is within a range from 25–31 °C, Fig. 1. Mathematically, OPT = Σ time, when 31 °C < T_c > 25 °C. Optimum time can be determined from measured canopy temperatures or specified by values of environmental factors that allow the plant canopy to maintain its optimal thermal range. Since plant canopy temperature depends on both the atmospheric environment and the water status of the plant, a well-watered plant was used as a reference.

In temperature-controlled-irrigation scheduling (TCIS) using a drip irrigation system the threshold temperature

Correspondence to: D. F. Wanjura

determines when and how much water is applied. The cumulative time that the threshold temperature is exceeded represents the maximum available time for irrigation and is termed *irrigation control time* (ICT), Fig. 1. Expressed mathematically as ICT = Σ time, when $T_c > T_t$, where T_c is canopy temperature and T_t is the threshold canopy temperature level. Irrigation control time depends on the threshold canopy temperature level and the environment. The overall result is that the threshold temperature level determines irrigation control time which controls the amount of water applied. Applied water affects the range and distribution of canopy temperature.

The TCIS method assumes that plant canopy temperature is a sufficient indicator of plant water stress, see Fig. 1. Canopy temperature is a direct indicator of crop water status and atmospheric energy dynamics. Canopy temperature is used to control irrigation by automatically applying irrigation through a drip system whenever a threshold canopy temperature is exceeded. The use of TCIS requires that the energy input from the environment be large enough to raise the crop canopy temperature above the threshold temperature.

In order to assess the effect of canopy temperature changes that result from TCIS, an estimate of the maximum amount of time that the canopy temperature could be within a specific thermal range is required. Drip irrigated cotton where water application was controlled by a threshold temperature of 28 °C produced the highest average yield during a four-year study (Wanjura et al. 1992). The thermal environment of cotton where irrigation was controlled by a 28 °C threshold is used as a reference because yield was maximum and presumably water status was optimized. The primary motivation for analyzing the thermal environment of the canopy is to determine whether the accumulation of temperature above a threshold limits the use of threshold canopy temperature to control irrigation scheduling.

The purpose of this paper is to examine the temperature environment of drip irrigated cotton where scheduling was controlled by threshold temperature. The specific objective was to evaluate temperature distributions, amount of time within the optimum temperature range, and irrigation control time.

Materials and methods

The analysis was conducted using data from a cotton production area where irrigation supplements rainfall and the length of the growing season is often limited by low temperature. The period of the growing season that was used in the analysis was the middle portion of the crop production cycle (DOY 198–273) when fruit are initiated and matured, and most irrigation is applied. Plant canopies were the maximum size during this period which was optimum for measuring canopy temperature with infrared thermometers.

The data was collected from TCIS studies conducted on the Texas Agricultural Experiment Station located at Lubbock, Texas between 1988–1991. The experimental plots were flat-broken with a moldboard plow each year prior to planting and herbicide broadcast and incorporated. Fertilizer application, based on soil samples, was applied before planting. A preplant furrow irrigation was applied when needed to ensure adequate moisture for seed germination and to refill the top 2 m of soil to field capacity.

Cotton was planted in rows oriented east-west spaced 0.76 m (30 inches) apart. Plot size was 18 rows wide by 30.5 m long. Temik [1] was applied in the seed furrow at planting for the control of thrips. Irrigation was applied through 16 mm diameter polyethylene dripline emitter hose with 61 cm spacing between emitters. The dripline hose was placed on the soil surface in each row. Nitrogen was applied to the plots through the irrigation system at the rate of 0.221 kg(N)/ha-mm.

All plots were instrumented as follows: Infrared thermometers (IRTs) were placed on each side of a row to view the upper one-third of the canopy, and net radiation was measured above the canopy. One anemometer and pyranometer were positioned 2 m above the

[1] The use of trade names does not imply endorsement by the U.S. Department of Agriculture

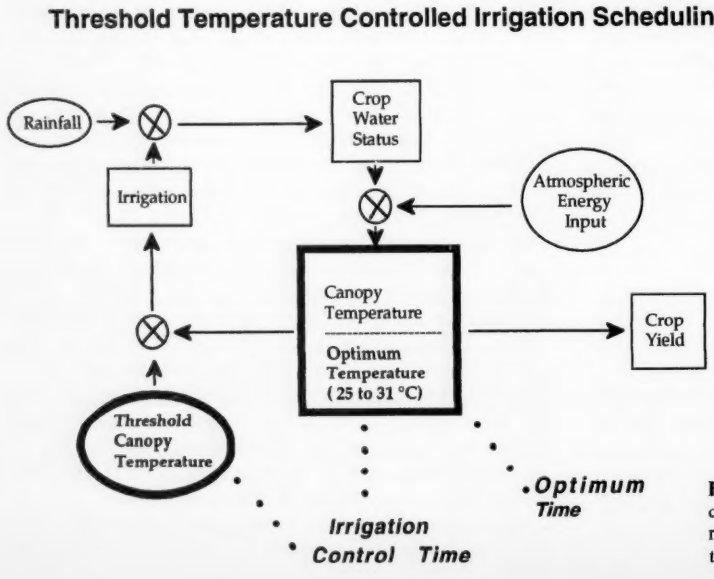

Fig. 1. Representation of threshold temperature controlled irrigation scheduling which depicts the relationship of optimum time and irrigation control time with specific parameters

soil surface in a well-watered treatment to measure ambient conditions. Dry bulb air temperature (AT) and wet bulb air temperature were also measured at a 2 m height in the study area. Instruments were located in the north-east quadrant of each plot to provide maximum fetch for a prevailing south-west wind direction.

Irrigation scheduling of threshold canopy temperature controlled treatments was controlled by two 4° field-of-view IRTs viewing the canopy perpendicularly from a 45° angle from the north and south sides. Additional information on temperature measurement and data recording are reported in Wanjura et al. (1992).

The following threshold canopy temperatures were used: 28, 30, and 32 °C in 1988; 28 °C in 1989; 26, 28, and 30 °C in 1990; and 28 °C in 1991. The treatment whose irrigation was scheduled by a 28 °C threshold temperature (T 28 C) in each year was used as the reference "well-watered" treatment.

Amount of irrigation control time for different canopy temperature thresholds were calculated. Optimum time was the amount of time that temperatures were between 25–31 °C. Irrigation-control-time was the amount of time that canopy temperature exceeded different thresholds.

Results and discussion

Air and canopy temperatures

Frequency distributions of dry bulb air temperature at 2 m (AT) and canopy temperatures of the 28 °C treatment (T 28 C) measured during 24-hour periods are compared in Fig. 2. The most frequently occurring temperatures in all years were 19 °C and 18 °C, respectively, for AT and T 28 C over the period of day-of-year (DOY) 198–273. Above 19 °C, AT frequencies declined linearly to an upper limit temperature of 33 °C. Canopy temperature frequencies declined from 18 °C to 20 °C, stabilized between 20 and 28 °C, and declined again between 28 °C and 32 °C. Presumably transpiration cooled the canopy and maintained uniform temperatures in the 20 to 28 °C range. The steep decline above 28 °C coincides with the threshold canopy temperature of 28 °C which caused irrigation to be applied and reduced the occurrence of temperatures above the threshold value.

The frequency distribution of AT and T 28 C was also compared in the optimum temperature range between 25–31 °C. The daily period for making the comparison was restricted to those times when AT was 25 °C or higher and total solar radiation was above 200 W/m^2. These restrictions represent atmospheric conditions when well-watered plants were transpiring in response to evaporation demand. The amount of time that AT and T 28 C were in the optimum range was lowest in 1989, Fig. 3. Air temperatures between 25 and 31 °C were more uniformly distributed than T 28 C. The difference (T 28 C – AT) in daily time that temperatures were within 1 °C increments between 25 °C and 31 °C were statistically compared using a *T*-test (analysis not shown). These comparisons were significant, except when designated as "ns" in Fig. 3.

The effect of using the 28 °C threshold canopy temperature to apply irrigation is shown by comparing the cumulative times that T 28 C and AT were between 25–29 °C and 29–31 °C, Table 1. Cumulative time at temperatures from 25 through 28 °C for T 28 C was always greater than for AT; however, from 29 to 31 °C AT was always greater than T 28 C. Irrigating when canopy temperature exceeded 28 °C reduced the amount of time that the cotton canopy exceeded 28 °C compared to that for AT. Among years both AT and T 28 C were lowest in 1989. The only year effect on AT and T 28 C was a lower amount of time that these temperatures were in the range from 25–31 °C in 1989.

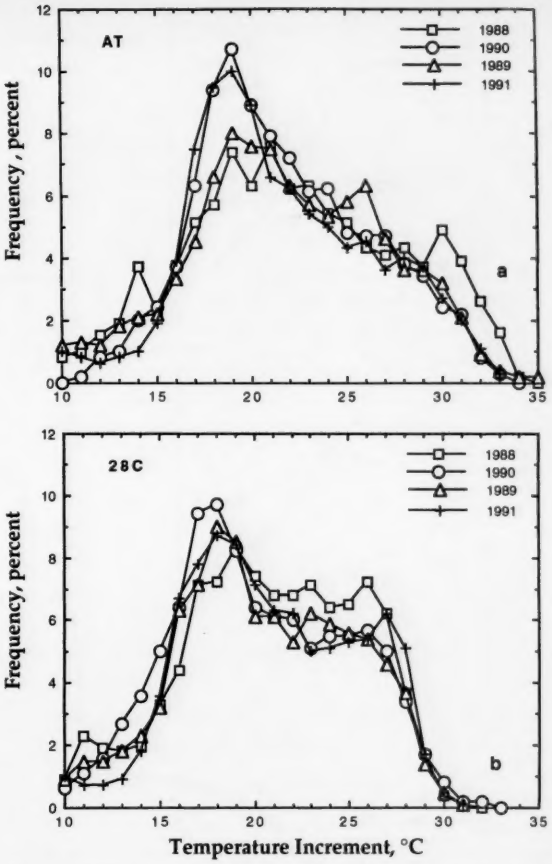

Fig. 2. Frequency distribution of air temperatures (AT) and canopy temperatures of the 28 °C threshold treatment (T 28 C) during 24-h periods for the interval DOY 198–273, 1988–1991

Optimum temperature

Optimum time was calculated using the time that either T 28 C or AT was within the range of 25–31 °C during the entire 24-hour period without filtering for any environmental condition. The distributions of AT and T 28 C within the optimum temperature range were different in all years, Fig. 4. The linear relationships between cumulative frequency with increasing temperature show that within the optimum temperature interval AT temperatures are uniformly distributed. Cumulative frequency of T 28 C increased most rapidly through the 27–28 °C increment but then decreased in comparison to AT. Times

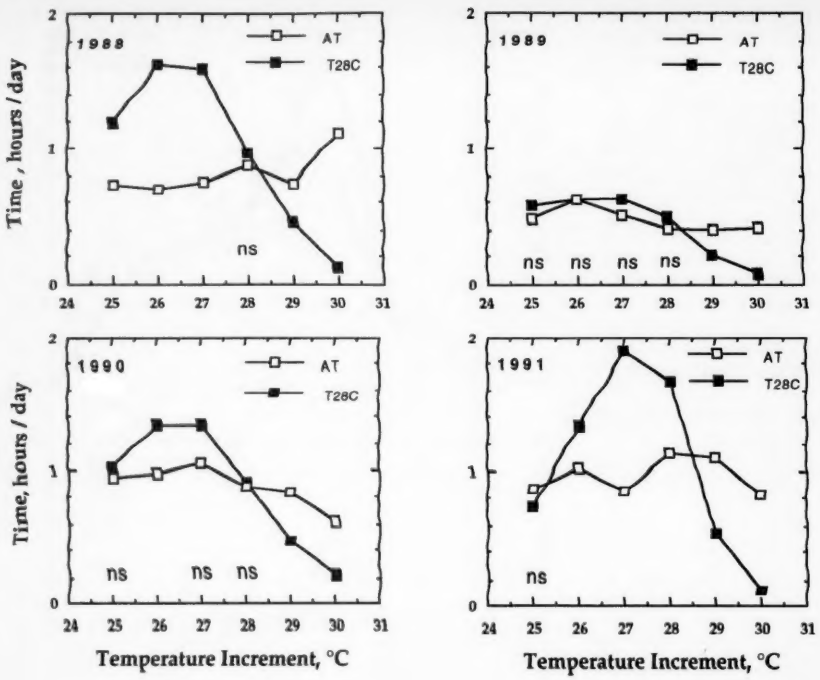

Fig. 3. Average daily time that air *temperature (AT) and canopy* temperature of the 28 °C threshold treatment (T28C) were within 1 °C intervals in the optimum temperature range (25–31 °C) for the interval DOY 198–273, 1988–1991. The daily periods were restricted to conditions when AT exceeds 25 °C and total radiation exceeds 200 W/m². Time per day is not statistically different where "ns" appears for the temperature increment

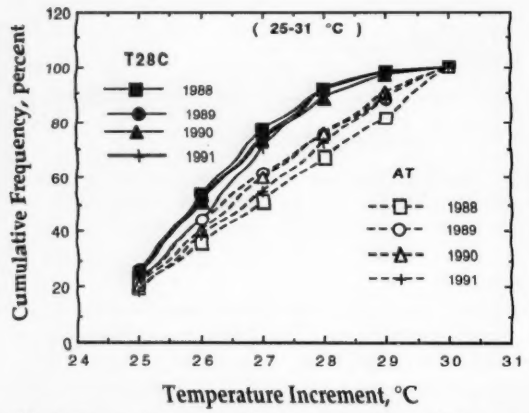

Fig. 4. Comparison of cumulative frequencies of air temperature (AT) and canopy temperature of the 28 °C threshold treatment *(T28C) within the optimum temperature range for the conditions* described in Fig. 3

Table 1. Cumulative time that canopy temperature of well-watered *cotton (T28C) and air temperature measured at two meters (AT)* were in the temperature range 25–31 °C while total radiation exceeded 200 W/m² and AT was equal to or greater then 25 °C during the period DOY 198–273

Year	Days	Total Time[a]	25–29 °C		29–31 °C	
			T28C	AT	T28C	AT
		Hours[b]				
1988	66	461	354	203	38	123
1989	60	200	14	121	17	49
1990	62	384	286	239	43	90
1991	55	378	311	214	37	106

[a] Total number of hours when AT exceeded 25 °C and total radiation was above 200 W/m²

[b] Cumulative times for T28C and AT within each temperature range were significantly different except in 1989

at optimum temperature were similar for AT and T28C in each year except 1989 during DOY 198–273, Table 2. The largest difference in optimum time between AT and the T28C occurred in 1989 when AT was 109 h higher than T28C. The large difference in 1989 contrasts with all other years when differences were 30 h or less.

Irrigation control time

Irrigation control time was analyzed by comparing the different threshold temperature levels used to schedule irrigation. The year effect on irrigation control time for well-watered conditions was estimated by comparing values for T28C, Table 3. Irrigation control time had a range of 35 h (37%) compared with a range of 107 h (29%) in optimum time. The 37% range in irrigation control time would result in the same proportional range of application for a drip system with a constant irrigation rate.

The influence of threshold canopy temperature level on irrigation control time was estimated by comparing the different temperature thresholds used in 1988 and 1990, Fig. 5. Variations in irrigation control time among

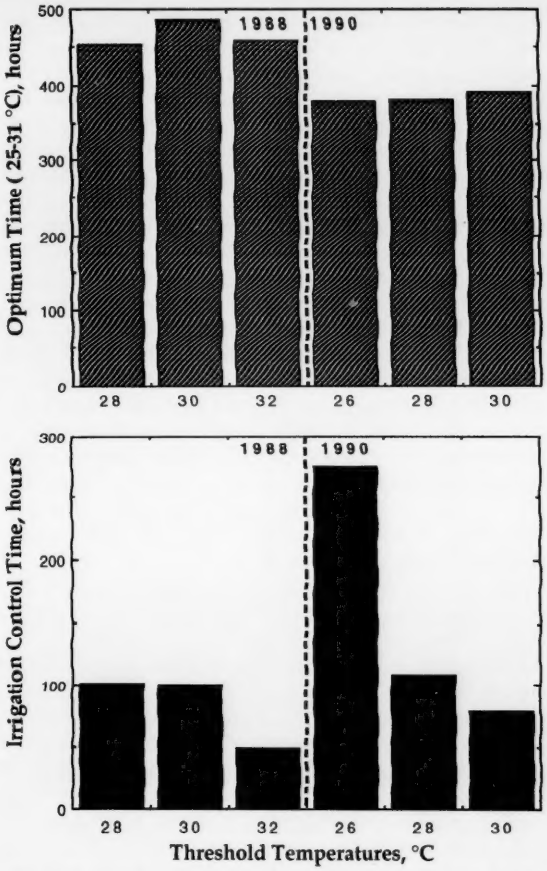

Fig. 5. Comparison of total optimum time and irrigation control time for threshold canopy temperature levels in 1988 and 1990 for the period DOY 198–273

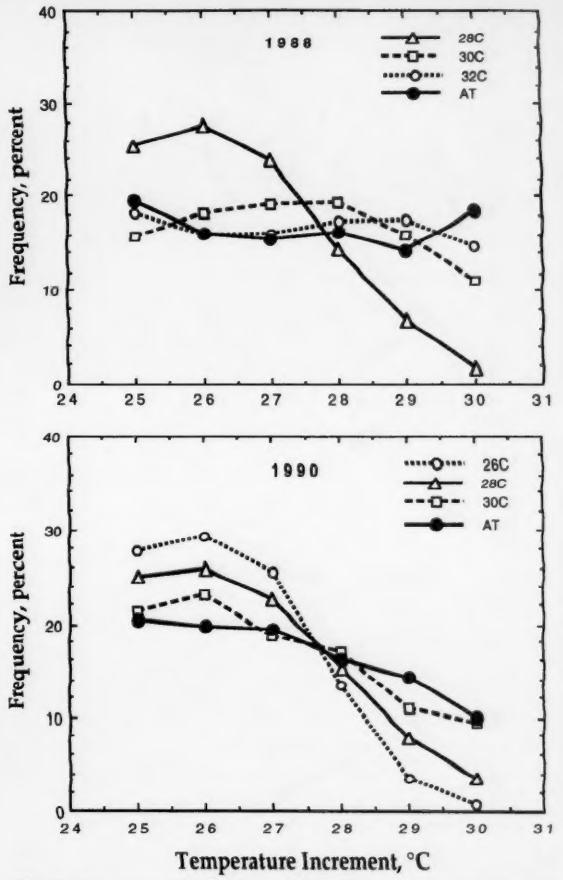

Fig. 6. Frequency distributions within the optimum temperature range (25–31 °C) for different threshold temperature levels and air temperature (AT) for the period DOY 198–273, 1988 and 1990

Table 2. Optimum time (25–31 °C) for canopy temperature of well-watered cotton (T28C) and for air temperature measured at two meters (AT) for the period DOY 198–273, 1988–1991

Year	T28C	AT	T28C	AT
	Hours		Percent of total time[a]	
1988	453	471	25	26
1989	366	475	20	26
1990	378	408	21	22
1991	437	414	24	23
Average	409	442	22	24

[a] Percentages were calculated based on 1824 total hours (76 days × 24-hours per day) during DOY 198 and 273

Table 3. Irrigation control time and optimum time for a 28 °C threshold canopy temperature controlled irrigation treatment (T28C) for the period DOY 198–273, 1988–1991

Year	Irrigation (Hours)	
	control time[a]	optimum time[b]
1988	102	453
1989	95	366
1990	109	378
1991	130	437

[a] Time above a threshold canopy temperature of 28 °C
[b] Time within the temperature range from 25–31 °C

threshold temperature levels were larger than their corresponding optimum times. In 1988 threshold temperatures of 28, 30, and 32 °C had a range of 54 h in irrigation control time which corresponded with a range of 32 h for optimum time. In 1990 irrigation control time of threshold temperatures 26, 28, 30 °C had a range of 196 h while optimum time had a range of only 14 h. Threshold temperatures between 26 and 32 °C were inversely related to irrigation control time. Higher threshold temperatures results in significantly less irrigation control time than lower temperatures but their optimum time was not reduced. Since optimum time was similar among different

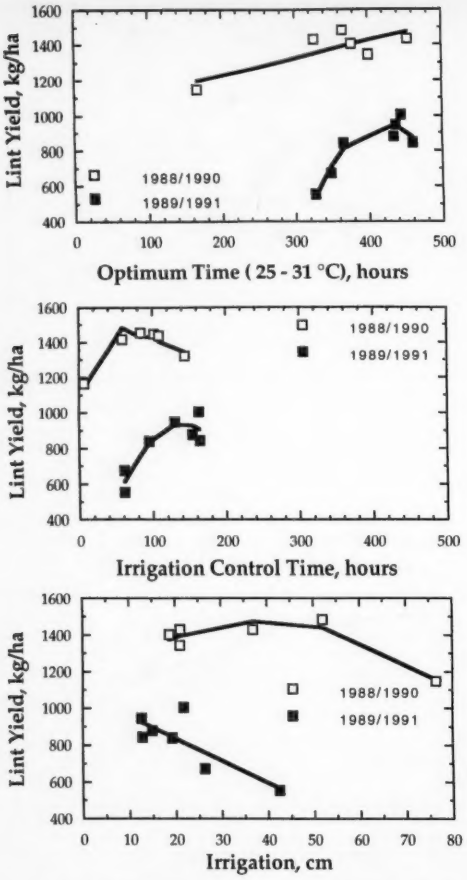

Fig. 7. Relationship of lint yield with optimum time, irrigation control time, and amount of irrigation during the period DOY 198–273 for high yield years (1988/1990) and low yield years (1989/1991)

threshold temperature levels but canopy temperatures were modified above the threshold temperature used for irrigation control it follows that the distribution of canopy temperatures within the optimum interval should be different among threshold temperatures, Fig. 6. In 1988 and 1990 threshold temperatures above 28 °C had few temperatures below 28 °C and more temperatures at or above 28 °C than did the lower threshold temperatures. The distributions of AT were more uniform than for any threshold canopy temperatures.

Lint yield

Well-watered irrigation treatments were used to minimize water stress effects on yield, Fig. 7. In this comparison, well-watered included threshold temperatures of 26 °C and 28 °C and a treatment that fully replaced soil water used on a weekly interval as measured by a neutron scattering technique. An obvious difference in years is apparent where 1988 and 1990 yields were higher than those in 1989 and 1991. Optimum time and irrigation control time had similar ranges in both the high and low yield years which suggests that they were not the causes for these large yield differences. The year effect on yield occurred outside the period, DOY 198–273, for which optimum time and irrigation control time were accumulated. The yield reduction in 1989 and 1991 resulted from plant damage caused by cool temperatures or thunder storms, (prior to DOY 198) that reduced plant vigor and population and late season cool temperatures that delayed maturity. The linear and second-order curves were computed using regression analysis. Criterion for choosing the best fit curve was that all regression model coefficients be statistically significant. Optimum time was linearly related to lint yield in high yield years (1988 and 1990) and nonlinearly in low yield years (1989 and 1991). Optimum time had the greatest effect on yield in the low yield years because low temperatures in 1989 and 1991 after DOY 243 did not allow the crop to fully mature. Irrigation control time was linearly related to yield in the low yield years and nonlinearly in the high yield years. Again, the effect of irrigation control time was greater in the low yield years because low temperatures after DOY 243 did not permit full crop maturity.

Total irrigation applied to the well-watered treatments, in direct proportion to differences in irrigation control time, during the period DOY 198–273, had a neutral effect on lint yield in the high yield years and a negative effect in the low yield years, Fig. 7. In the high yield years well-watered treatments received adequate irrigation during DOY 198–273 with some treatments being excessively irrigated. In low yield years irrigation amounts that showed a neutral effect in the high yield years decreased yield. Since one of the differences between high and low yield years was a shortened growing season, it is a reasonable assumption that the higher irrigation amounts applied in low yield years slowed crop maturity and reduced yield.

Conclusions

Correct application of threshold temperature controlled irrigation scheduling requires the crop to be thermally adapted to its growing environment and the threshold temperature must be appropriately selected to result in an amount of irrigation (water stress level) that is compatible with efficient production. The 28 °C threshold canopy temperature which results in a well-watered crop condition had maximum daily irrigations that ranged from 10–12 mm during the four years of this study. These irrigations were applied through a drip irrigation system where the average application rate varied from 1.5 to 2.1 mm/h. Daily potential evapotranspiration estimated by the Penman-Monteith combination method for a well watered short grass surface described in Jensen et al. 1990 averaged 7 mm/day during the period DOY 198–273. Thus, the irrigation system and scheduling procedure had the capability of completely supplying the full evapotranspiration demand. The irrigation scheduling method used in this study resulted in frequent irrigations. Small frequently applied irrigations are an effective and efficient method of irrigation (Bordovsky et al. 1992; Radin et al. 1989).

Different threshold canopy temperature levels did not significantly change the amount of optimum time when canopy temperature was within the optimum temperature range from 25–31 °C, but the frequency distribution of canopy temperatures within the optimum range was altered. Controlling irrigation scheduling with different threshold temperature levels changed the amount of irrigation control time and quantity of irrigation. Irrigation control time and optimum time were positively related to cotton lint yield.

References

Arndt CH (1945) Temperature-growth relations of the roots and hypocotyls of cotton seedlings. Plant Physiol 20:200–220

Burke JJ, Mahan JR, Hatfield JL (1988) Crop specific thermal kinetic windows in relation to wheat and cotton biomass production. Agron J 80:553–556

Bordovsky JP, Lyle WM, Lascano RJ, Upchurch DR (1992) Cotton irrigation management with LEPA systems. Trans ASAE 35:879–884

Grimes DW, Yamada H, Hughs SW (1987) Climate-normalized cotton leaf water potentials for irrigation scheduling. Agric Water Mgt 12:293–304

Idso SB, Reginato RJ, Reicosky DC, Hatfield JL (1982) Determining soil-induced plant water potential depressions in Alfalfa by means of infrared thermometry. Agron J 73:826–830

Jensen ME, Burman RD, Allen RG (1990) Evapotranspiration and irrigation water requirements, ASCE Manuals and Reports on Engineering Practice No. 70, American Society of Civil Engineers, New York, NY, 332 pp

Radin JW, Mauney JR, Kerridge PC (1989) Water uptake by cotton roots during fruit filling in relation to irrigation frequency. Crop Sci 29:1000–1005

Wanjura DF, Upchurch DR, Mahan JR (1992) Automated irrigation based on threshold canopy temperature. Trans ASAE 35:153–159

Irrig Sci (1994) 14:207–212

Irrigation Science
© Springer-Verlag 1994

Control of irrigation amounts using velocity and position of wetting front

B. Zur [1], U. Ben-Hanan [2], A. Rimmer [1], A. Yardeni [3]

[1] Agricultural Engineering Department, Technion, Haifa, Israel, 32000
[2] Mechanical Engineering Section, Ort-Braude College, Carmiel, Israel
[3] Agroteam Consultants Ltd., Migdal HaEmeck, Israel

Received: 29 May 1993

Abstract. A new approach for the estimation and control of the quantity of water applied in an irrigation is presented in which irrigation is stopped when the wetting front reaches a critical depth, Z_L. An expression for calculating the critical depth Z_L was developed. A major parameter in this expression is the velocity of advance of the wetting front, V, which was shown to be directly related to the application rate, IR, and inversely related to the initial soil water content, θ_i. A depth probe (patent pending) was designed, constructed and tested for the purpose of monitoring the position of the wetting front during infiltration and redistribution and for computing the value of V. Equations developed for relating the velocity of advance of the wetting front to θ_i as well as for estimating the value of the critical depth Z_L were successfully tested under conditions of uniform distribution of the initial soil water content. An iterative learning process which utilizes the real time output from the depth probe during each irrigation and is therefore capable of handling realistic field conditions where nonuniformity is the rule is presented. The acquired information is used to estimate a critical depth of the wetting front, Z_L, for a planned final wetted depth, Z_F, during each irrigation. This process is incorporated in the depth probe and is used to stop irrigation and thus control the quantity of water applied.

Ideally the net amount of water applied during an irrigation, Q_I is defined as:

$$Q_I = \int_{Z=0}^{Z_F} (\theta_f - \theta_i)\, dz \qquad (1)$$

where θ_f is the volumetric soil water content at field capacity, θ_i is the volumetric soil water content prior to irrigation and Z_F is the desired depth of soil to be wetted to field capacity. The value of Z_F is estimated using the current rooting depth of the crop as well as the leaching requirements.

Correspondence to: B. Zur

An accurate estimate of Q_I is a basic requirement for optimal irrigation management. Applying the correct amount of water is important both for efficient water use as well as to reduce groundwater contamination resulting from deep percolation. The use of Eq. (1) requires a dependable estimate of θ_i at a range of soil depths, whereas the values of θ_f at these depths should be known as part of the general information representing the soil. Taking soil samples to estimate θ_i is seldom practiced because it is cumbersome and labor consuming. Instead, physical and empirical relationships employing meteorological parameters and crop coefficients are generally employed to estimate water use by the crops. Current procedures for estimating Q_I are incapable of identifying the depths from which soil water was extracted by the crop and lack the means to insure that the estimated Q_I is sufficient to wet the desired soil depth.

In the present paper we propose a new way to estimate the value of Q_I and to monitor is distribution in the soil profile. In principle, the value of Q_I applied in the field is determined by the duration of the irrigation. We propose to stop an irrigation, and thus control Q_I, when the wetting front reaches a critical depth, Z_L. The critical depth Z_L is defined as the position of the wetting front at the end of an irrigation from which sufficient water would be redistributed to bring the soil profile down to the depth Z_F to its field capacity.

The specific objectives of the present paper are:

1. Develop equations for estimating the critical depth Z_L.
2. Present a system for tracking the position of the wetting front during an irrigation.
3. Test objectives 1 and 2.
4. Discuss irrigation control algorithms under realistic field conditions.

Theory

The process of wetting a soil profile goes through two stages.

At the end of the first, infiltration stage, a soil depth, Z_L, is wetted in excess to a water content, θ_L, which is a function of the application rate and is constant with depth, Fig. 1. During the second, redistribution stage, excess water from the initially wetted soil depth drains downward to wet an additional depth of soil. The resulting wetted soil profile down to the depth Z_F is characterized by a relatively stable soil water content of field capacity, θ_f, Fig. 1. Duration of the redistribution stage varies depending on soil texture, soil structure and depth of wetted profile. For medium textured soils the duration of this stage is about 24 h.

Ideally, the arrival of the irrigation water to the depth Z_F could be used as a signal to stop an irrigation. However, since the irrigation water reaches the depth Z_F after a period of redistribution this possibility is not practical. An alternative approach is to define a critical depth Z_L as the position of the wetting front at the termination of irrigation which would bring the soil profile down to the planned wetting depth Z_F to its water content of field capacity at the end of a redistribution period. The arrival of wetting front to the depth Z_L could be used as a signal to stop the irrigation. The relationship between the planned depth, Z_F, and the critical depth, Z_L, is expected to depend on soil type, initial soil water content distribution and the application rate, IR.

Values of Z_L which would yield desired depths Z_F following redistribution could be computed using a numerical procedure where the Richards equation is solved for the infiltration and redistribution processes (Van Genuchten, 1978, 1980). However, this procedure requires initial conditions which include knowledge of the initial distribution of volumetric soil water content, θ_i, which is usually not available. In addition, hysteresis plays a significant role in water flow during redistribution and numerical solutions are not properly equipped to take this phenomenon into consideration (Van Genuchten, 1978, 1980). Therefore, this possibility is of limited value when applied to field conditions.

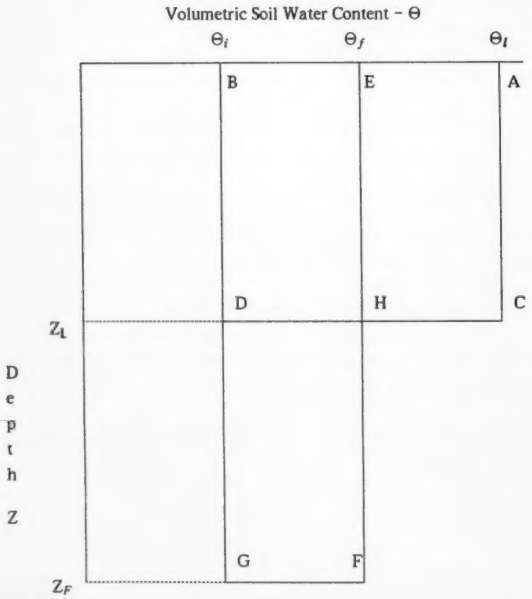

Fig. 1. Schematic presentation of water balance during irrigation and redistribution

In the present paper a simple relationship between Z_L and Z_F is developed based on the equality of the mass balance of soil water at the end of an irrigation and after 24 h of redistribution. For the conservation of mass the areas ABDC and EBGF, Fig. 1, must be equal. The area ABDC which represents the amount of water added to the soil during an irrigation is estimated as:

$$Q_I = (\theta_L - \theta_i) \cdot Z_L. \tag{2}$$

The arrival of the wetting front to the depth Z_L is indicated in the proposed approach by the response of a sensor positioned at that depth. The value of θ_L is estimated by taking soil samples down the wetted profile immediately following an irrigation.

The area EBGF represents the distribution of the added water at the end of redistribution, therefore:

$$Q_I = (\theta_f - \theta_i) \cdot Z_F. \tag{3}$$

The arrival of the redistribution front to the depth Z_F is indicated in the proposed system by a sensor positioned at that depth which had just sensed the arrival of the redistribution front about 24 to 48 hours after an irrigation. Equating Eq. (2) and (3) we obtain:

$$(\theta_L - \theta_i) \cdot Z_L = (\theta_f - \theta_i) \cdot Z_F. \tag{4}$$

Similarly, from Fig. 1, the areas AEHC and HDGF are equal and we can write:

$$(\theta_L - \theta_f) \cdot Z_L = (\theta_f - \theta_i) \cdot \Delta Z \tag{5}$$

where the left side of Eq. (5) represents the amount of water drained from the initially wetted profile and the right side of Eq. (5) represents the additional depth ΔZ, wetted to field capacity.

Based on Eq. (4) and (5) we can now write:

$$\frac{(\theta_L - \theta_f) \cdot Z_L}{(\theta_L - \theta_i) \cdot Z_L} = \frac{(\theta_f - \theta_i) \cdot \Delta Z}{(\theta_f - \theta_i) \cdot Z_F}. \tag{6}$$

For ideal systems where θ_i, θ_f and θ_L are uniform for depths larger than Z_F, Eq. (6) becomes:

$$\frac{\Delta Z}{Z_F} = \frac{(\theta_L - \theta_f)}{(\theta_L - \theta_i)} \tag{7}$$

and since $\Delta Z = Z_F - Z_L$:

$$\frac{Z_L}{Z_F} = 1 - \frac{(\theta_L - \theta_f)}{(\theta_L - \theta_i)}. \tag{8}$$

The expression $(\theta_L - \theta_f)$ represents the volume fraction of water in the wetted soil depth which will drain to depths below Z_L during redistribution. Generally this quantity is characteristic of a soil, depends on soil texture and tends to increase with sand content. The expression on the right side of Eqs. (7) and (8) is the ratio between the volume fraction of water drained from the wetted profile during

redistribution to the volume fraction of water taken up by the same depth during irrigation.

Equations (4–8) are valid for conditions where θ_i is uniform with depth, for infiltration times longer than a critical value after which θ_L is constant with depth, and for a piston type advance of the wetting front. An expression for the velocity of advance of the wetting front, V, for the above conditions was proposed by Phillip (1957) and later modified by Rubin and Steinhardt (1963) as follows:

$$V = \frac{IR - K(\theta_i)}{(\theta_L - \theta_i)} \tag{9}$$

where IR, the application rate, is smaller than the stable infiltration rate of the soil.

The value of $K(\theta_i)$ in Eq. (9) is normally much less than IR and therefore can be neglected. Values of IR and θ_L are interrelated and are constant for a given irrigation system-soil combination.

Thus, the velocity of advance of the wetting front, V, is expected to be inversely related to the value of $(\theta_L - \theta_i)$ and therefore to the value of θ_i. Velocity of advance of the wetting front, V, is a major parameter in the present scheme for estimating the critical depth Z_L and for controlling the value of Q_I.

Introducing Eq. (9) into Eq. (8) we obtain:

$$\frac{Z_L}{Z_F} = 1 - \frac{(\theta_L - \theta_f)}{IR} \cdot V. \tag{10}$$

By definition, the velocity of advance of the wetting front is the change with time in the position of the wetting front during irrigation. Thus, the measurement of V must involve a system capable of monitoring the position of the wetting front during irrigation. The same system could signal the arrival of the wetting front to the critical depth Z_L, for stopping the irrigation, as well as for indicating the arrival of the redistribution front to the depth Z_F, to determine whether Q_I was sufficient.

Materials and methods

Description of system

Velocity of advance of the wetting front, V, is estimated by noting the times at which the wetting front reaches predetermined soil depths during an irrigation. This is achieved by using a wetting depth probe (patent pending), Fig. 2. Sensors which respond to the arrival of the wetting front are imbedded at 5 cm intervals along the probe. Each sensor consists of a hollow cylinder of a hydrophilic porous material with thin annular stainless steel electrodes tightly fitted at the lower and upper ends. The spacing between adjacent sensors is taken up by a hollow plastic cylinder of the same outside dimensions. The upper annular electrode is connected to a central metal rod which acts both as an electrical common and as a pole which holds all the parts together. The lower annular electrode is connected to a separate wire led through the hollow inside of the probe to an external device. The electrical resistance between the two annular electrodes changes immediately following a change in the amount of water absorbed by the hydrophilic porous cylinder.

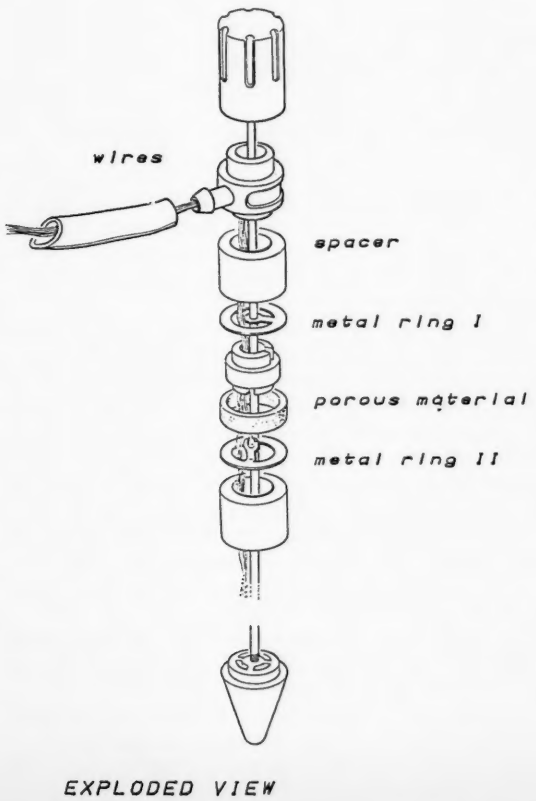

Fig. 2. Schematic presentation of the wetting depth probe

The electrical resistance or current flow across each sensor along the wetting depth probe is measured at frequent time intervals during irrigation and redistribution. A microprocessor circuit positioned at the top of the wetting depth is programmed to scan the current flow across each sensor at predetermined time intervals, record the time at which a predetermined change in the meter reading of each sensor takes place and log and store the data.

Experimental studies

In 1986, a preliminary study using metal oil drums 56 cm in diameter and 86 cm high were packed with a Hamra loam soil was conducted. Prior to packing the soil was moistened to initial water contents of 10, 12 and 15% by weight. In addition, the air dry soil with a water content of 5% was also used. Four drums packed with soils at the above θ_i values were irrigated by minisprinklers at IR values in the range of 7–8 mm/h. An additional group of tests with similar θ_i values were subjected to IR values in the range of 26–32 mm/h. The velocity of advance of the wetting front as well as the values of θ_f, θ_L, Z_L and Z_F were measured using an older version of the wetting depth probe.

In later experiments, plastic drums with a diameter of 54 cm and height of 96 cm were packed with soil of known initial water content θ_i, to a predetermined dry bulk density. Two or three wetting depth probes were placed in each drum during packing. Precautions were taken to assure good contact between soil and sensors during packing of the drums. Prior to irrigation soil samples were taken at 10 cm depth intervals to estimate the value of θ_i in the drum. The sampling holes were than refilled with the same soil. Mini-sprinklers, with application rates calibrated on site, were used to apply controlled amounts of water at known application rates to the soil in the drums. Scanning of the sensors on each probe at five minutes intervals started 20 minutes before an irrigation and continued at this rate during water application. Time intervals for scanning were reduced to once every hour when irrigation was terminated. Soil samples for water content determination were taken at 10 cm depth intervals immediately following an irrigation to estimate the value of θ_L, and after 24 h to estimate θ_f.

The time the wetting front reached a sensor at a given depth was obtained from reviewing printouts of the scanning results and noting the times when the current flow across each sensor changed by more than 5% of the original reading. Velocity of advance of the wetting front, V, was obtained from linear regression of the relationship between the time of arrival of the wetting front and depth. Values of Z_L and Z_F were estimated from the same printouts during irrigation and redistribution and were compared with estimates from the results of the gravimetric soil sampling.

Three soils were used in the present trials, a sand, a sandy loam and a kaolinitic clay. Table 1 summarizes the dry bulk densities, initial soil water contents, θ_i, application rates, IR, maximal soil water content at the end of an irrigation, θ_L, and soil water content after 24 h of redistribution, θ_f, for the three test soils.

Results and discussion

Results of scanning the depth probe every five minutes during infiltration into a Hamra sandy loam soil at an initial volumetric water content of 3% are plotted in Fig. 3. Based on the time when a detectable change in the meter readings was observed, it is clear that the wetting front passed by the sensor positioned at the 5 cm depth 115 min after the start of the irrigation. Similarly, the wetting front passed by the sensor at 10 cm depth after 195 min, by the sensor at 15 cm after 280 min, by the sensor at 20 cm after 370 min and by the sensor at 25 cm after 460 min. Irrigation was terminated after 505 min. The response of the sensors to the arrival of the wetting front was instantaneous and the changes in the meter readings were considerable. The meter readings for each sensor reached a new stable value 15 to 25 min after the initial change. The average velocity of advance of the wetting front, V, in this trial was computed to be 3.0 cm/h with a R^2 value of 0.98.

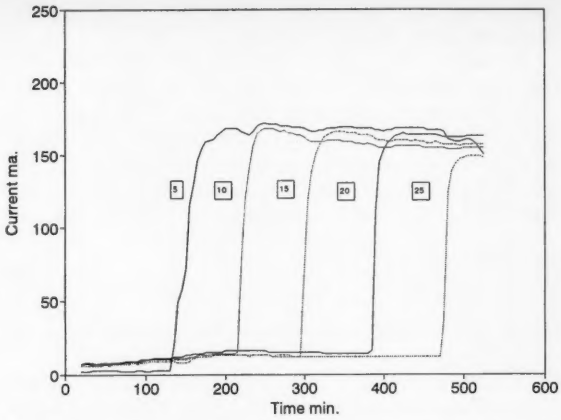

Fig. 3. Response of individual sensors during infiltration into Hamra sandy loam soil. Number in box indicates depth in cm

Table 1. Basic parameters of test soils

Soil type	ϱ_d gm/cm^3	θ_i (%)	IR mm/h	θ_L (%)	θ_f (%)
Sand	1.5	0.5	10.0	20	9
		6	10.0	20	9
		7	10.5	20	9
Sandy loam	1.3	3	7.7	21	14*
		4	7.0	21	14
		10	9.1	21	14
		14	10	21	14*
Bukata clay (kaolinitic)	1.2	15	10.0	47	41
		34	0.77	47	41*
		36	0.95	47	41

* Water drained to bottom of drum during redistribution

The time required for the wetting front to reach specified depths during infiltration into a Bukata Kaolinitic clay soil with initial volumetric soil water contents of 15 and 36% are presented in Fig. 4. Three depth probes were used in the drum with 15% volumetric water content and only two probes in the drum with soil at 36% water content. Computed average velocities of advance of the wetting front from the reading of the three probes were 2.6, 2.7 and 2.7 cm/h for the 15% initial volumetric soil water content. The two probes placed in the drum with soil at volumetric water content of 36% resulted in average velocities of 7.6 and 7.7 cm/h.

Similar results for a Hamra sandy loam soil with initial volumetric water contents of 3 and 10% are presented in Fig. 5. For the soil with an initial volumetric water content of 3% velocities of 4.5, 4.2 and 4.6 cm/h were computed using linear regression. For an initial volumetric water content of 10% velocities of advance of the wetting front of 10.8, 10.8 and 9.8 cm/h were computed.

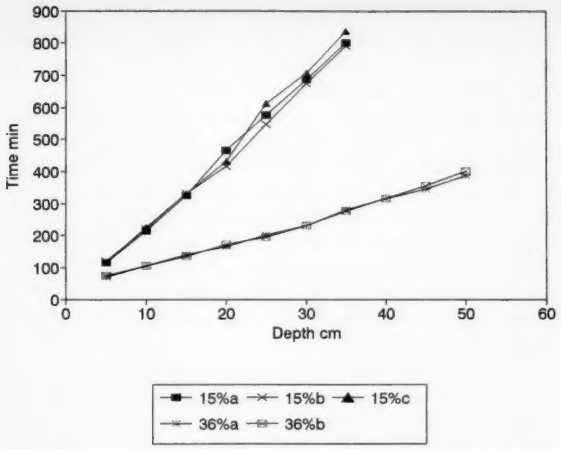

Fig. 4. Time of arrival of the wetting front as a function of depth under two initial volumetric water contents during infiltration. Bukata clay soil

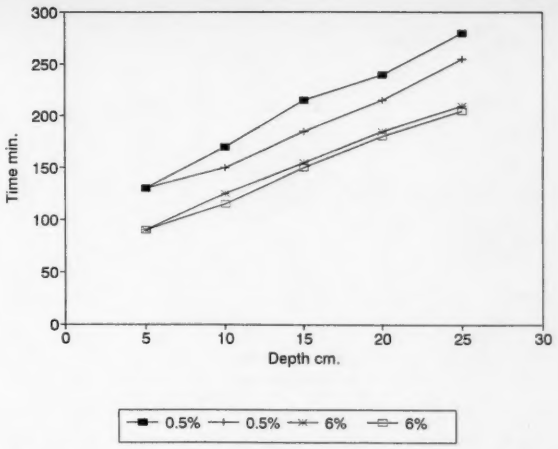

Fig. 6. Time of arrival of the wetting front as a function of depth under two initial volumetric water contents during infiltration. Sandy soil

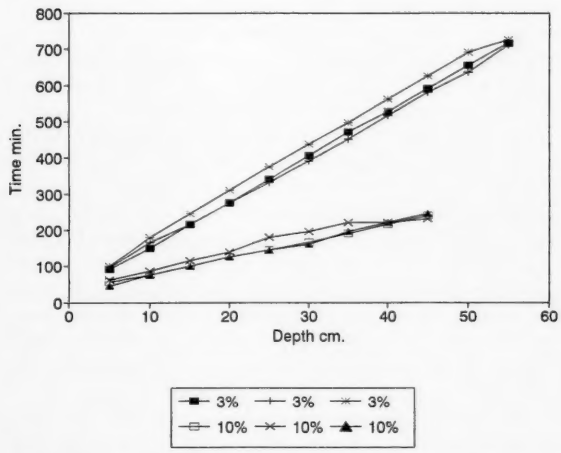

Fig. 5. Time of arrival of the wetting front as a function of depth under two initial volumetric water contents during infiltration. Hamra sandy loam soil

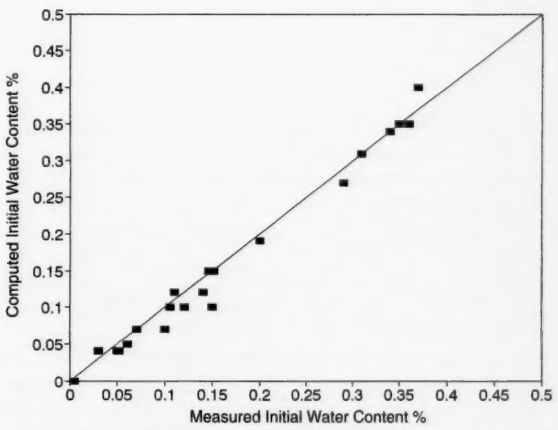

Fig. 7. Relationship between measured and computed values of the initial soil water content

Results of tests with a sand at initial volumetric water contents of 0.5 and 6% are presented in Fig. 6. Velocities of advance of the wetting front of 4.7 and 5.3 cm/h were computed for the sand soil at an initial volumetric water content of 0.5%. Under an initial volumetric water content of 6% velocities of 6.5 and 6.6 cm/h were computed.

Results presented in Table 1, in Figs. 4, 5, 6 and from additional measurements are used to test the applicability of Eq. (9) for estimating the value of θ_i from measured values of V, IR and θ_L. Computed values of θ_i, using Eq. (9) are plotted against measured values in Fig. 7. The points in this figure represent a range of soils, application rates and initial soil water contents. A linear regression analysis of the data yielded an R^2 value of 0.98 and a slope of 0.98.

The assumption of a piston type advance of the wetting front can be evaluated from the response of individual sensors to the passage of the wetting front during infiltration. The response of sensors to a change in the water content of the surrounding soil was instantaneous. Thus the thickness of the wetting zone can be estimated from the product of the time interval between the first response of a sensor and when its reading became stable, and the average value of V. Based on such an analysis and under the present test conditions the thickness of the wetting zone for the Bukata kaolinitic clay soil ranged from 2 cm when θ_i was that of an air dry soil to 4 cm when θ_i was 36%. For the sand and Hamra sandy loam soils the thickness of the wetting zone was in the range of 2–4 cm under all test conditions.

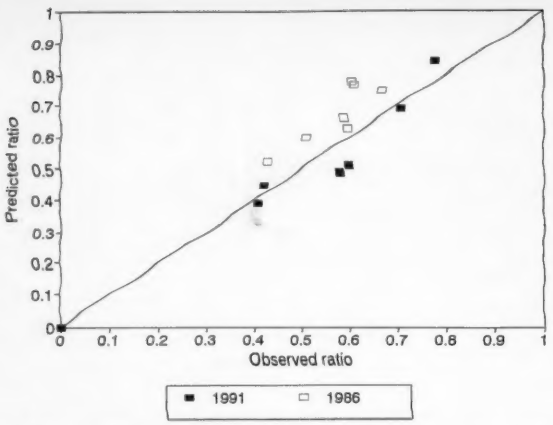

Fig. 8. Relationship between observed and predicted ratio of relative depth of wetting, Z_L/Z_F

Table 2. *Coefficients from linear regression analysis*

	Intercept	R^2	Slope
1991 data	−0.063	0.87	1.06
1986 data	0.055	0.74	1.08
All data	0.025	0.64	1.03

The relationship between measured and predicted Z_L/Z_F ratios from both the plastic container and metal oil drum experiments representing a range of soil types, initial water contents and application rates are presented in Fig. 8. Estimated values of the ratio Z_L/Z_F were computed Eq. (10). The ability of Eq. (10) to predict the ratio Z_L/Z_F was evaluated by subjecting the data presented in Fig. 8 to linear regression analysis. Three linear regressions tests were performed. In the first test only the 1991 data was used, in the second test only the 1986 results were analyzed and in the third test all the data was pooled together. The resulting coefficients of the linear regression analysis are presented in Table 2. In all three linear regression tests the slope of the regression lines was between 3 to 8% higher than 1.0. The R^2 value of 0.87 for the 1991 data suggests a good agreement between computed ratio of Z_L/Z_F using Eq. (10) with the improved wetting depth probe and measured values. An R^2 value of 0.74 was obtained for the 1986 data and 0.644 for the pooled data. In all three tests the computed intercepts were close to zero. Since the sensors were spaced at 5 cm intervals the uncertainty in determining the position of the wetting front was ± 2.5 cm.

When the initial soil water content distribution is uniform down to depths below Z_F, the use of Eq. (10) to estimate the critical depth of the wetting front Z_L was shown to be successful. However, under field conditions the distribution of θ_i prior to an irrigation is far from being uniform. Under these conditions the distribution of θ_i below the critical depth, Z_L, can not be estimated from measurements of the velocity of advance of the wetting front during an irrigation. Without this information the resulting final wetted depth, Z_F, cannot be computed.

Thus, under realistic field conditions Eq. (10) cannot be used to estimate the critical depth Z_L. Instead, an iterative learning process for estimating the value of Z_L was developed. The learning process is built on the following statements which were based on our laboratory and field experience. The velocity of advance of the wetting front during irrigation is essentially constant and is responsive to an average value of the initial soil water content distribution and to soil texture. Following termination of irrigation the velocity of advance of the wetting front gradually slows down and approaches zero at the final wetting depth, Z_F. The redistribution depth $(Z_F - Z_L)$, is related to the velocity of the advance of the wetting front during irrigation.

The iterative learning process starts during the first irrigation of the season. A desired final wetting depth, Z_F, is introduced and a critical depth Z_L is estimated by multiplying the value of Z_F by a reasonable coefficient in the range of 0.4 to 0.7 depending on soil type. Irrigation is then initiated and the time of arrival of the wetting front to each of the sensors spaced along the depth probe is recorded and the average velocity of advance of the wetting front computed. Irrigation is stopped when the wetting front reaches the sensor closest to the estimated depth Z_L. The time of arrival of the wetting front during redistribution to the deeper sensors and the depth of the wetting front 24 and 48 h after stopping the irrigation are recorded. Coefficients are than computed and introduced into relationships based on the above statements. At the start of the next irrigation the probe is activated and the average velocity of advance of the wetting front is computed based on measurements in real time. A new value for the critical depth Z_L is than computed based on the present velocity of advance of the wetting front, on the site calibrated empirical relationships and on the planned value of Z_F. Irrigation is stopped when the wetting front reaches the depth Z_L. The position of the wetting front during redistribution and the depth of the wetted profile 24 and 48 h after irrigation are recorded. In case there is a significant difference between the planned and measured values of Z_F, a new value of Z_L is calculated and tested during the next irrigation. This iterative learning process is repeated during each irrigation and changes are made in the value of Z_L whenever necessary. The described system does not require initial calibration of any kind, the sensors respond to relative change rather than to quantities or potentials and the decision when to stop an irrigation is based on real time measurements. The manufactured system is presently under going field tests.

References

Phillip JR (1957) The theory of infiltration. 2. The profile at infinity. Soil Sci 83: 435–448

Rubin J, Steinhardt R (1963) Soil water relations during rain infiltration. I. Theory. Soil Sci Soc Am Proc 27: 246–251

Van Genuchten MTh (1980) A closed-form equation for predicting the hydraulic conductivity of saturated soils. Soil Sci Soc Am J 44: 892–898

Van Genuchten MTh (1978) Numerical solution of the one-dimensional saturated-unsaturated flow equation. Resarch Report 78-WR-9, Water resources Program, Department of Civil Engineering, Princeton University, Princeton, New Jersey

Irrigation Science

Volume 14 1993/94

Co-ordinating Editor

G. Stanhill
Institute of Soils and Water, Agricultural Research Organization,
Volcani Center, P.O. Box 6, Bet Dagan, 50-250, Israel

Co-Editors

G. J. Hoffman
Agricultural Engineering Department
University of Nebraska
223 L.W. Chase Hall
Lincoln, NE 68583-0726, USA

A. Kassam
88 Gunnersbury Avenue
Ealing, London W54 HA, England

W. S. Meyer
CSIRO Division of Water Resources
Griffith Laboratory
PO Griffith, NSW 2680, Australia

Advisory Editors

S. Dasberg, Bet Dagan
J. Doorenbos, Ankara
W. Gardner, Berkeley, California
A. E. Hall, Riverside, California
R. J. Hanks, Logan, Utah
B. Itier, Thiverval-Grignon
R. D. Jackson, Phoenix, Arizona
P. G. Jarvis, Edinburgh
M. E. Jensen, Fort Collins, Colorado
W. D. Kemper, Beltsville, Maryland
J. W. Kijne, Colombo
J. V. Lake, Wageningen
J. L. Monteith, Edinburgh
J. R. Philip, Canberra City
C. W. Rose, Queensland, Australia
V. P. Singh, Baton Rouge, Louisiana
N. C. Turner, Wembley, Western Australia

Springer International

Copyright

Submission of a manuscript implies: that the work described has not been published before (except in the form of an abstract or as part of a published lecture, review, or thesis); that it is not under consideration for publication elsewhere; that its publication has been approved by all coauthors, if any, as well as by the responsible authorities at the institute where the work has been carried out; that, if and when the manuscript is accepted for publication, the authors agree to automatic transfer of the copyright to the publisher; and that the manuscript will not be published elsewhere in any language without the consent of the copyright holders.

All articles published in this journal are protected by copyright, which covers the exclusive rights to reproduce and distribute the article (e.g., as offprints), as well as all translation rights. No material published in this journal may be reproduced photographically or stored on microfilm, in electronic data bases, video disks, etc., without first obtaining written permission from the publisher.

The use of general descriptive names, trade names, trademarks, etc., in this publication, even if not specifically identified, does not imply that these names are not protected by the relevant laws and regulations.

While the advice and information in this journal is believed to be true and accurate at the date of its going to press, neither the authors, the editors, nor the publisher can accept any legal responsibility for any errors or omissions that may be made. The publisher makes no warranty, express or implied, with respect to the material contained herein.

Special regulations for photocopies in the USA

Photocopies may be made for personal or in-house use beyond the limitations stipulated under Section 107 or 108 of U.S. Copyright Law, provided a fee is paid. This fee is US$ 0.20 per page, per copy, plus a basic fee of US$ 2.00 per article. All fees should be paid to the Copyright Clearance Center, Inc., 21 Congress Street, Salem, MA 01970, USA, stating the ISSN 0302-8933, the volume, and the first and last page numbers of each article copied. The copyright owner's consent does not include copying for general distribution, promotion, new works, or resale. In these cases, specific written permission must first be obtained from the publisher.

Printers: Graphischer Betrieb Konrad Triltsch, Würzburg

© Springer-Verlag Berlin Heidelberg 1994

Springer-Verlag GmbH & Co KG, D-14197 Berlin, Germany

Printed in Germany

Contents

Abo-Ghobar HM: Influence of irrigation water quality on soil infiltration 15
Allison BA → Gerdes G
Al-Omary SS → Yasseen BT
Aragüés R → Grattan SR
Ayars JE, Hutmacher RB, Schoneman RA, Vail SS, Pflaum T: Long term use of saline water for irrigation 27

Bajwa MS, Josan AS, Choudhary OP: Effect of frequency of sodic and saline-sodic irrigations and gypsum on the buildup of sodium in soil and crop yields 21
Bay D → Bertuzzi P
Bertuzzi P, Bruckler L, Bay D, Chanzy A: Sampling strategies for soil water content to estimate evapotranspiration 105
Biggar JW → Hutmacher RB
Bruckler L → Bertuzzi P

Chanzy A → Bertuzzi P
Chartzoulakis K, Noitsakis B, Therios I: Photosynthesis, plant growth and dry matter distribution in kiwifruit as influenced by water deficits 1
Choudhary OP → Bajwa MS
Condon AG → Richards RA

Dale F → Hutmacher RB
De Lorenzi F → Stanghellini C
Dinar A: Economic factors and opportunities as determinants of water use efficiency in agriculture 47

El-Haddad HM → El-Sayed HM
El-Sayed HM, El-Haddad HM, O'Leary JW: Effect of salinity and K/Na ratio of irrigation water on growth and solute content of *Atriplex amnicola* and *Sorghum bicolor* 127

Gerdes G, Allison BA, Pereira LS: Overestimation of soybean crop transpiration by sap flow measurements under field conditions in Central Portugal 135
Gomez-Macpherson H → Richards RA
Grattan SR, Royo A, Aragüés R: Chloride accumulation and partitioning in Barley as affected by differential root and foliar salt absorption under saline sprinkler irrigation 147

Hoffman GJ, Martin DL: Engineering systems to enhance irrigation performance 53
Hutmacher RB → Ayars JE
Hutmacher RB, Nightingale HI, Rolston DE, Biggar JW, Dale F, Vail SS, Peters D: Growth and yield responses of almond (*Prunus amygdalus*) to trickle irrigation 177

Josan AS → Bajwa MS

Kanber R, Yazar A, Önder S, Köksal H: Irrigation response of Pistachio (*Pistacia vera* L.) 7
Kemper WD: Effects of soil properties on precipitation use efficiency 65
Köksal H → Kanber R

Lamm FR → Sweeney DW
Letey J: Relationship between salinity and efficient water use 75
López-Castañeda C → Richards RA

Martin DL → Hoffman GJ
Monteith JL: The exchange of water and carbon by crops in a mediterranean climate 85

Nightingale HI → Hutmacher RB
Noitsakis B → Chartzoulakis K

O'Leary JW → El-Sayed HM
Önder S → Kanber R

Pereira LS → Gerdes G
Peters D → Hutmacher RB
Pflaum T → Ayars JE

Richards RA, López-Castañeda C, Gomez-Macpherson H, Condon AG: Improving the efficiency of water use by plant breeding and molecular biology 93
Rolston DE → Hutmacher RB
Royo A → Grattan SR

Schoneman RA → Ayars JE
Stanghellini C, De Lorenzi F: A comparison of soil- and canopy temperature-based methods for the early detection of water stress in a simulated patch of pasture 141
Sweeney DW, Lamm FR: Timing of limited irrigation and N-injection for grain sorghum 35

Therios I → Chartzoulakis K

Vail SS → Ayars JE
Vail SS → Hutmacher RB

Yasseen BT, Al-Omary SS: An analysis of the effects of water stress on leaf growth and yield of three barley cultivars 157
Yazar A → Kanber R

Book Reviews 41, 163

Editorial 45

Keep up to date in an active field

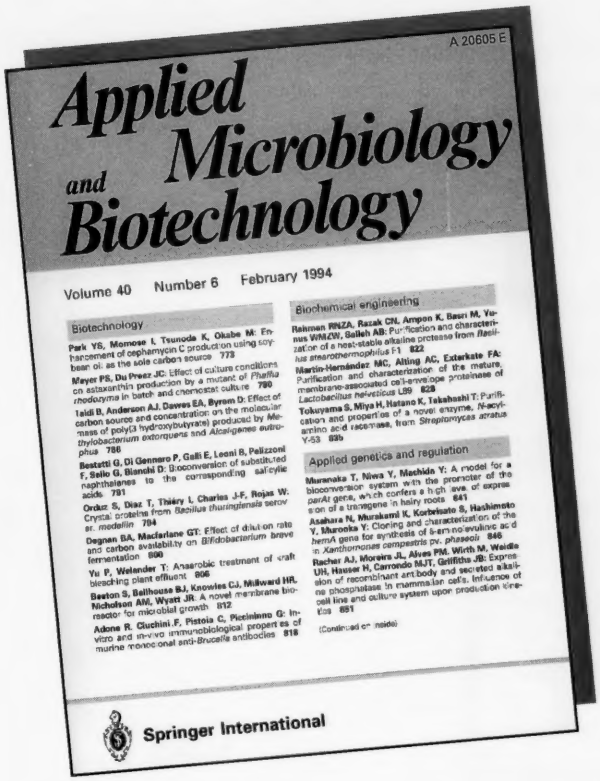
A 20605 E
Applied Microbiology and Biotechnology
Volume 40 Number 6 February 1994
Biotechnology
Park YS, Momose I, Tsunoda K, Okabe M: Enhancement of cephamycin C production using soybean oil as the sole carbon source 773
Meyer PS, Du Preez JC: Effect of culture conditions on astaxanthin production by a mutant of Phaffia rhodozyma in batch and chemostat culture 780
Teldi B, Anderson AJ, Dawes EA, Byrom D: Effect of carbon source and concentration on the molecular mass of poly(3 hydroxybutyrate) produced by Methylobacterium extorquens and Alcaligenes eutrophus 786
Bestetti G, Di Gennaro P, Galli E, Leoni S, Pelizzoni F, Sello G, Bianchi D: Bioconversion of substituted naphthalenes to the corresponding salicylic acids 791
Ordaz S, Diaz T, Thiéry I, Charles J-F, Rojas W: Crystal proteins from Bacillus thuringiensis serovar. medellin 794
Degnan BA, Macfarlane GT: Effect of dilution rate and carbon availability on Bifidobacterium breve fermentation 800
Yu P, Welander T: Anaerobic treatment of kraft bleaching plant effluent 806
Beston S, Bellhouse BJ, Knowles CJ, Millward HR, Nicholson AM, Wyatt JR: A novel membrane bioreactor for microbial growth 812
Adone R, Ciuchini F, Pistoia C, Piccininno G: In-vitro and in-vivo immunobiological properties of murine monoclonal anti-Brucella antibodies 818
Biochemical engineering
Rahman RNZA, Razak CN, Ampon K, Basri M, Yunus WMZN, Salleh AB: Purification and characterization of a neat-stable alkaline protease from Bacillus stearothermophilus F1 822
Martin-Hernández MC, Alting AC, Exterkate FA: Purification and characterization of the mature membrane-associated cell-envelope proteinase of Lactobacillus helveticus L89 828
Tokuyama S, Miya H, Hatano K, Takahashi T: Purification and properties of a novel enzyme, N-acylamino acid racemase, from Streptomyces aratus Y-53 835
Applied genetics and regulation
Murawaka T, Niwa Y, Machida Y: A model for a bioconversion system with the promoter of the parAt gene, which confers a high level of expression of a transgene in hairy roots 841
Asahara N, Murakami K, Korbinato S, Hashimoto Y, Marooka Y: Cloning and characterization of the hemA gene for synthesis of δ-aminolevulinic acid in Xanthomonas campestris pv. phaseoli 846
Racher AJ, Moreira JL, Alves PM, Wirth M, Weidle UH, Hauser H, Carrondo MJT, Griffiths JB: Expression of recombinant antibody and secreted alkaline phosphatase in mammalian cells. Influence of cell line and culture system upon production kinetics 851
(Continued on inside)
Springer International

Fields of interest

- Biotechnology
- Biochemical engineering
- Applied genetics and regulation
- Applied microbial and cell physiology
- Food biotechnology
- Environmental biotechnology

Covered in Springer Journals Preview Service

International Editors:

For Europe, Africa, Australia, New Zealand, The Near East, India: H.-J. Rehm, Münster; K. Esser, Bochum

For the Americas: A. L. Demain, Massachusetts

For Japan, The Far East: A. Kimura, Kyoto

Springer

Tm.1747/MNTZ/N/1

ORDER FORM

Applied Microbiology & Biotechnology ISSN 0175-7598 Title No. 253

❒ Please enter my subscription beginning with 1994: Vol. 40+41 (12 issues) DM 2596.– (suggested list price) plus carriage charges: FRG DM 43,80; other countries DM 57,–

❒ Please send me a free sample copy

❒ Please bill me

❒ Please charge my credit card
- ❒ Eurocard/Access/MasterCard
- ❒ American Express
- ❒ Visa/Barclaycard/BankAmericard
- ❒ Diners Club

Number

Valid until:

Name / Address

Date: Signature:

Please note: I realize that I may cancel this order within ten days by writing to the address on the order form, whereby the postmark date will suffice as proof that the cancellation was made within the deadline. I confirm my understanding of this with my second signature.

2nd Signature

In EC countries the local VAT is effective. Customers in EC countries, please state your VAT-Identification-Number if applicable

Please hand this order form to your bookseller or return to:
Springer-Verlag, Marketing Communication,
Postfach 10 52 80, D-69042 Heidelberg, FRG

The classics for your library!

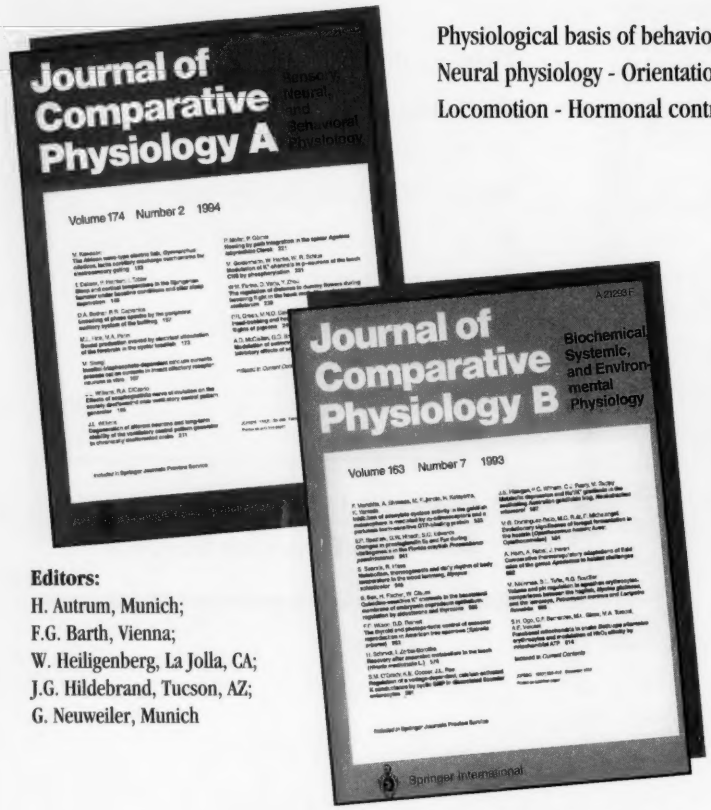
Journal of Comparative Physiology A
Sensory, Neural, and Behavioral Physiology
Volume 174 Number 2 1994
Journal of Comparative Physiology B
Biochemical, Systemic, and Environmental Physiology
Volume 163 Number 7 1993
Springer International

Physiological basis of behaviour - Sensory physiology - Neural physiology - Orientation, communication - Locomotion - Hormonal control of behaviour

Editors:
H. Autrum, Munich;
F.G. Barth, Vienna;
W. Heiligenberg, La Jolla, CA;
J.G. Hildebrand, Tucson, AZ;
G. Neuweiler, Munich

Comparative aspects of metabolism and enzymology - Metabolic regulation - Respiration and gas transport - Physiology of body fluids - Circulation - Temperature relations - Endocrine regulation - Muscular physiology

Editors: H. Langer, Bochum; T. Hirano, Tokyo; W.T.W. Potts, Lancaster, UK; R.B. Reeves, Buffalo, NY

Springer
Tm.1745/MNTZ/V/1

ORDER FORM

❒ Please bill me

❒ Please charge my credit card
- ❒ Eurocard/Access/MasterCard
- ❒ American Express
- ❒ Visa/Barclaycard/BankAmericard
- ❒ Diners Club

Number

Valid until:

Please hand this order form to your bookseller or return to:
Springer-Verlag, Marketing Communication,
Postfach 10 52 80, D-69042 Heidelberg, FRG

Journal of Comparative Physiology A ISSN 0340-7594 Title No. 359

❒ Please enter my subscription beginning with 1994: Vol. 174+175 (12 issues) DM 2848,– (suggested list price) plus carriage charges: FRG DM 43,80; other countries DM 57,–
❒ Please send me a free sample copy

Journal of Comparative Physiology B ISSN 0174-1578 Title No. 360

❒ Please enter my subscription beginning with 1994: Vol. 360 (8 issues) DM 1398,– (suggested list price) plus carriage charges: FRG DM 29,20; other countries DM 38,–
❒ Please send me a free sample copy

Name / Address

Date: Signature:

Please note: I realize that I may cancel this order within ten days by writing to the address on the order form, whereby the postmark date will suffice as proof that the cancellation was made within the deadline. I confirm my understanding of this with my second signature.

2nd Signature

In EC countries the local VAT is effective. Customers in EC countries, please state your VAT-Identification-Number if applicable

A 4

Instructions to Authors

Original papers should be written in English. They should present scientific results which are essentially new and have not been submitted or published elsewhere. In order to speed up editorial scrutiny, **manuscripts and illustrations should be submitted in triplicate.**

Manuscripts should be written clearly without repetition, and carefully checked to exclude the necessity for corrections in proof. A charge will be made for changes introduced after the manuscript has been typeset.

Papers should not be divided into several parts to make them appear shorter. The title page should comprise: title of paper, first name(s) and surname of all authors, affiliations, any footnotes referring to the title, a short running title (not exceeding 72 strokes, including spaces), and the address for offprint requests.

To faciliate communication between the authors, editors and publisher, the author should furnish a telex or fax number on the title page of the manuscript.

Each manuscript should be preceded by a short **Summary** of the main results, written in clear and correct English. Detailed historical introductions should be avoided, the main problem should be outlined briefly. Continuity with earlier work on the subject should be established by reference to recent papers and reviews which need not themselves be summarized. Experimental methods must be clearly set out, but detailed descriptions of methods are of value only if they convey substantially new information.

Methods and other material of secondary importance should be marked for **small print.** This is not done to save money – it costs more to typeset – but to improve presentation. Normally a brief statement of each category of experimental results or each newly established fact is sufficient. The remaining material may be mentioned in the text or, if necessary, given in tables; lengthy tables should be avoided. The best way is to state in a footnote where the full supporting evidence may be obtained.

Footnotes to the title of the paper should be indicated by asterisks and those to the text numbered consecutively; footnotes to tables should be designated with lower-case superscript letters. All footnotes should be placed at the foot of the manuscript page on which they belong.

The **References** should contain only works referred to in the text. They should be styled as follows:

Examples:

Bresler E, McNeal BL, Carter D (1982) Saline and sodic soil. Advanced series in Agricultural Sciences 10. Springer, Berlin Heidelberg, New York

Tyree MT, Jarvis PG (1982) Water in tissues and cells. In: Lange OL, Nobel PS, Osmond CB, Ziegler H (eds) Physiological Plant Physiol 12B. Springer, Berlin Heidelberg New York, p 71

Howell TA, Hatfield JL, Rhoades JD, Meron M (1984) Response of cotton water stress indicators to soil salinity. Irrig Sci 5: 25

References should be listed at the end of the paper in alphabetical order under the last name of the first author. Works by two authors should be listed alphabetically according to the second author's surname and then chronologically; those by more than two authors should be listed chronologically.

Citations in the text should be by author and date. If there is more than one reference by the same author or team of authors in the same year, a, b, c, etc. should be added.

All **figures,** whether photographs, graphs or diagrams, should be numbered consecutively throughout and submitted on separate sheets.

Each illustration should have a concise descriptive **legend.** Legends are part of the text and should be appended to it.

The number and size of the illustrations must be kept to the minimum required to clarify the text. Explanations of figures given in legends should not be repeated extensively in the text. Data presented in tables should not duplicate those given in graphs.

Color illustrations will be accepted; however, the authors will be expected to make a contribution towards the extra costs (approx. DM 1200.– for the first and DM 600.– for each additional page). The figures together with their legends should not exceed the print area (17.6 × 23.6 cm). Several figures should be grouped into a plate on one page.

For **line drawings,** please submit good-quality prints. Lettering should be about 2 mm hight. If original drawings are submitted, they should not exceed the format of the typescript. Computer drawings are acceptable provided they are of comparable quality to line drawings. Lines and curves must be smooth. Letters and numbers should be of professional quality and proper dimensions.

Half-Tone Illustrations. Please submit well-contrasted photographic prints, trimmed at right angles and in the desired final size. Inscriptions should be about 3 mm high.

Offprints may be ordered at cost price when the page proofs are returned.

Production
Springer-Verlag
Heidi Braun
Journal Production Department III
Postfach 105 280
D-69042 Heidelberg, Germany
Tel. (0) 62 21/4 87-3 26, Telex 4-61 723,
FAX (0) 62 21/48 71 88
e-mail: braun@Springer.de

Responsible for Advertisements
Springer-Verlag
E. Lückermann
Heidelberger Platz 3
D-14197 Berlin
Germany
Tel. (0) 30/82 07-0, Telex 1-85 411,
FAX (0) 30/8 20 73 00

Printers
K. Triltsch, D-97070 Würzburg

© Springer-Verlag Berlin Heidelberg 1994
Printed in Germany
Springer-Verlag GmbH & Co KG.
D-14197 Berlin
Germany

Journals Preview Service

The number of journals covered by the Springer Journals Preview Service will increase to more than 80 in early 1994 and includes titles from the life sciences, medicine, physics, earth sciences and engineering.

This service offers

tables of contents and BiblioAbstracts via Internet from our mailserver

with

automatic delivery several weeks before you receive the new issue.

Tables of contents are free of charge; all BiblioAbstracts are available for US$ 20,- per year.
For details please send an e-mail message containing the line

help

to our mailserver
svjps@vax.ntp.springer.de

For regular e-mail, please use the address
springer@vax.ntp.springer.de

Abdominal Imaging • **Acta Neuropathologica** • Anatomy & Embryology • **Annales Geophysicae** • Applied Microbiology and Biotechnology • Archives of Environmental Contamination and Toxicology • **Archives of Gynecology and Obstetrics Archives of Microbiology • Archives of Toxicology • Behavioral Ecology and Sociobiology • Biological Cybernetics** • Bulletin of Environmental Contamination and Toxicology • **Bulletin Géodésique • Bulletin of Volcanology** • Calcified Tissue International • **Cancer Chemotherapy and Pharmacology • Cancer Immunology, Immunotherapy** • CardioVascular and Interventional Radiology • Cell and Tissue Research • Chromosoma • **Climate Dynamics** • Current Genetics • Current Microbiology • **Diabetologia • Differentiation** • Environmental Management • **European Biophysics Journal • European Journal of Applied Physiology and Occupational Physiology** • European Journal of Biochemistry • **European Journal of Cardiothoracic Surgery • European Journal of Clinical Pharmacology** • European Journal of Nuclear Medicine • **European Journal of Pediatrics** European Radiology • Experimental Brain Research • **Experientia • Fresenius' Journal of Analytical Chemistry • Der Hautarzt** • Histochemistry • Human Genetics • Immunogenetics • **Intensive Care Medicine • International Journal of Colorectal Disease** • Irrigation Science • **Journal of Cancer Research and Clinical Oncology • Journal of Comparative Physiology A** • Journal of Comparative Physiology B • The Journal of Membrane Biology • *Journal of Molecular Evolution* • **Langenbecks Archiv für Chirurgie** • Mammalian Genome • **manuscripta geodaetica • Marine Biology** • MGG Molecular & General Genetics • Microbial Ecology • **Mycorrhiza • Naturwissenschaften • Naunyn-Schmiedeberg's Archives of Pharmacology** • *Neuroradiology* • *Numerische Mathematik* • **Oecologia • Der Pathologe** • Pediatric Cardiology • Pediatric Radiology • **PerinatalMedizin** • Pflügers Archiv • **Physics and Chemistry of Minerals** • Plant Cell Reports • Planta • **Psychopharmacology** • Psychotherapeut • Radiation and Environmental Biophysics • Der Radiologe • Revue d'Imagerie Médicale • Roux's Archives of Developmental Biology • **Sexual Plant Reproduction** • Skeletal Radiology • **System Familie** • TAG Theoretical and Applied Genetics • **Transplant International • Trees - Structure and Function • Virchows Archiv** • World Journal of Surgery • **Zeitschrift für Physik A • Zeitschrift für Physik *B • Zeitschrift für Physik C• Zeitschrift für Physik D***

Springer **electronic media**
via Internet

d&p.1429.NM/V/1

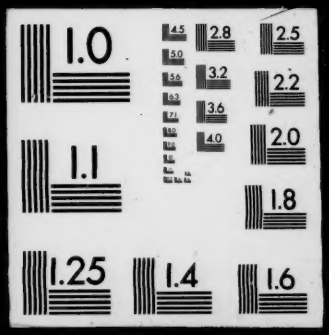
1.0
1.1
1.25
1.4
1.6
1.8
2.0
2.2
2.5
2.8
3.2
3.6
4.0
4.5
5.0
5.6
6.3
7.1
8.0
9.0